ACS OMEGA

http://pubs.acs.org/journal/acsodf

Review

Nanotherapeutic Intervention in Photodynamic Therapy for Cancer

Asif Mohd Itoo, Milan Paul, Sri Ganga Padaga, Balaram Ghosh, and Swati Biswas*[a]

Cite This: *ACS Omega* 2022, 7, 45882−45909

Read Online

ACCESS | Metrics & More | Article Recommendations

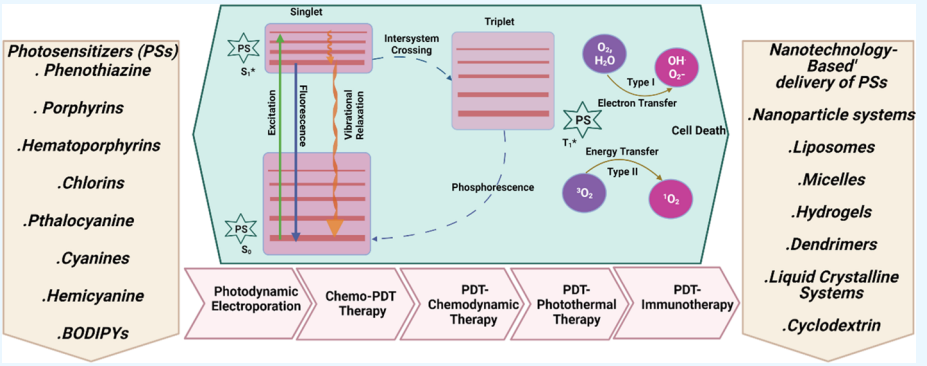

ABSTRACT: The clinical need for photodynamic therapy (PDT) has been growing for several decades. Notably, PDT is often used in oncology to treat a variety of tumors since it is a low-risk therapy with excellent selectivity, does not conflict with other therapies, and may be repeated as necessary. The mechanism of action of PDT is the photoactivation of a particular photosensitizer (PS) in a tumor microenvironment in the presence of oxygen. During PDT, cancer cells produce singlet oxygen ($^1O_2$) and reactive oxygen species (ROS) upon activation of PSs by irradiation, which efficiently kills the tumor. However, PDT's effectiveness in curing a deep-seated malignancy is constrained by three key reasons: a tumor's inadequate PS accumulation in tumor tissues, a hypoxic core with low oxygen content in solid tumors, and limited depth of light penetration. PDTs are therefore restricted to the management of thin and superficial cancers. With the development of nanotechnology, PDT's ability to penetrate deep tumor tissues and exert desired therapeutic effects has become a reality. However, further advancement in this field of research is necessary to address the challenges with PDT and ameliorate the therapeutic outcome. This review presents an overview of PSs, the mechanism of loading of PSs, nanomedicine-based solutions for enhancing PDT, and their biological applications including chemodynamic therapy, chemo-photodynamic therapy, PDT−electroporation, photodynamic−photothermal (PDT−PTT) therapy, and PDT−immunotherapy. Furthermore, the review discusses the mechanism of ROS generation in PDT advantages and challenges of PSs in PDT.

1. INTRODUCTION

Cancer is one of the most worrisome illnesses, particularly in affluent nations. Nearly 8 million people die from cancer each year, contributing significantly to the burden of cancer-related mortality and morbidity worldwide.[1−4] Chemotherapy, surgery, radiotherapy, and, more recently, small molecule-based treatments and immunotherapy, as well as a combination of these approaches, are the current clinical approaches for cancer therapy. Surgery is typically the first course of treatment; however, if metastasis has already taken place, it may not be the most appropriate treatment option. In circumstances when the tumor is situated in delicate regions, such as close to the spinal cord or other essential organs, surgical excision of the tumor is also not a practical option. In radiation therapy, the ionizing nature of radiation causes DNA damage in cells, which, if targeted specifically at the tumor, may stop tumor cells from replicating and perhaps cause the tumor to shrink. However, radiation therapy typically has long-term adverse effects such as immunosuppression, scar tissue development, and injury to healthy adjacent cells. Chemotherapeutic drugs are substances that may stop or eliminate rapidly proliferating cell lines in the body. They can either be cytostatic or cytotoxic. A chemotherapeutic agent is often administered intravenously, resulting in systemic effects. When treating metastasized cancers, this strategy may be beneficial, but it also presents a problem since it must balance the drug's therapeutic advantages with its unfavorable systemic toxic side effects.[5] In recent years, the use of nanomedicine has considerably increased the advantages of chemotherapy and other small

Received: September 9, 2022
Accepted: November 18, 2022
Published: December 6, 2022

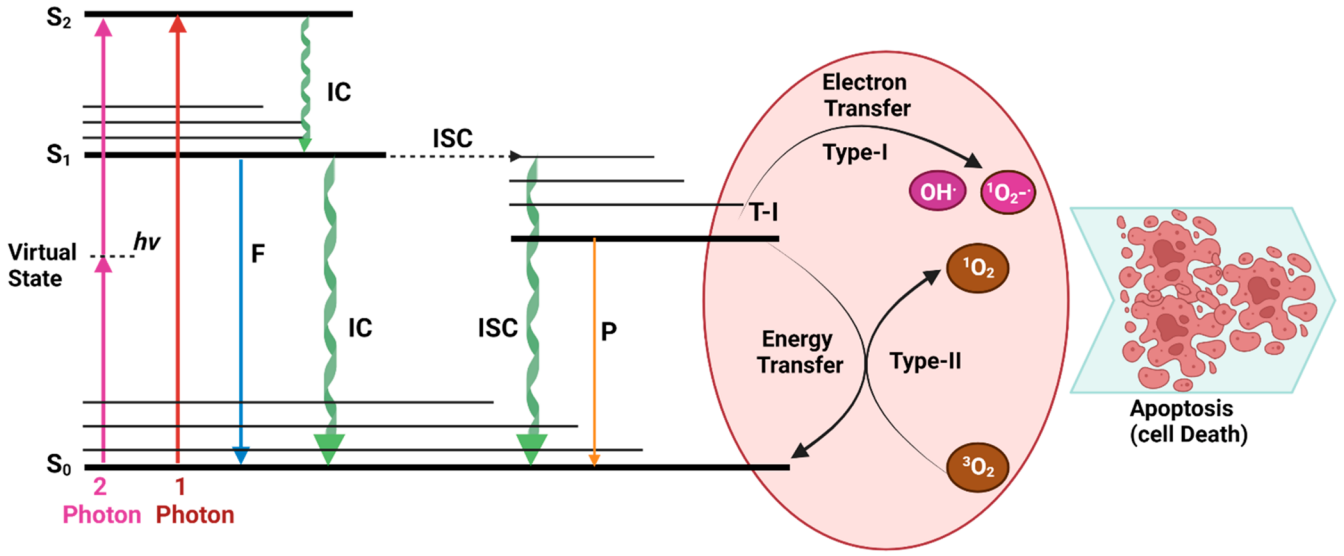

Figure 1. Jablonski energy level diagram for PDT.

molecule drugs where the therapeutic molecules are encapsulated into nanovesicles that prolong the drug's duration in circulation (by preventing nonspecific uptake and renal clearance) and enable enhanced penetration and retention (the EPR effect) to boost absorption inside the tumors by extravasation through the leaky vasculature associated with the tumor.[6−8] In order to combat cancer, immunotherapy functions by boosting the patient's own immune system or by lowering innate signaling cascade processes that encourage cancer growth and aggressiveness by employing monoclonal antibodies and cancer vaccines that are specifically directed at cancer cell receptors. The limited efficiency of highly targeted immunotherapies is due to the propensity of cancer cells to mutate. Nevertheless, immunotherapy techniques combined with radio- or chemotherapy have recently shown therapeutic effectiveness in several malignancies.[9−11]

While a large portion of contemporary cancer research is focused on improving the tumor-selectivity of the traditional cancer therapy methods previously outlined, researchers have also concentrated on finding alternative therapeutic methods that could be less risky or more effective in circumstances when significant chemotherapy, radiation, or surgery may be restricted owing to the danger of aesthetic and functional tissue damage. As a result, noninvasive photodynamic therapy (PDT) has become a promising strategy for the past few decades.[12,13] PDT consists of three basic elements: oxygen, a photosensitizer (PS) drug, and a particular wavelength of drug-activating light. When a PS is activated by light, energy transfer cascades are set off, producing cytotoxic reactive oxygen species (ROS) such as singlet oxygen, oxygen free radicals, and so on. Toxic ROS may cause necrotic and apoptotic cell death via the oxidation of DNA, RNA, protein, and cell/subcellular organelle membranes.[14−17] PDT has greater invasiveness and spatial selectivity than conventional chemotherapy because ROS are only generated in the region receiving light irradiation.[18,19] Due to this attribute, the systemic toxicity of PDT is quite low.

PDT has been the subject of in-depth research into cancer therapy since Dougherty et al. made the first contemporary demonstration of using this technique to destroy tumor cells in 1978.[20] PDT has significant advantages over traditional chemotherapy due to the PS's limited hazardous potential in the absence of light and the low systemic damage that results from its buildup in nonspecific organs. Moreover, the drug-activating light is less powerful than radiotherapy as it is nonionizing, and its impact on tissues without the PS drug is not hazardous. As a consequence, PDT may be repeated securely if necessary without incurring the risk of damaging nearby normal tissue.[21] This makes PDT particularly appealing for malignancies wherein loco-regionally recurring therapy may be required. Due to these features, PDT might potentially provide dual specificity in tumor treatment by creating innovations that ensure light irradiation of the tumor only when necessary and PS deposition in the tumor.[22] PDT has been extensively used for the local clinical therapy of several malignancies including stomach cancer, esophageal cancer, and head and neck cancers.[23,24] PDT still has poor therapeutic effectiveness despite its beneficial use. One of the key factors is that, similar to conventional chemotherapeutic drugs, PSs cannot actively concentrate in tumor tissue after *in vivo* injection.[25,26] The therapeutic effectiveness is drastically reduced by nonspecific absorption by other cells or tissues. Furthermore, enough oxygen is required for effective PDT, but tumor tissue is usually hypoxic. Even worse, PDT will result in a drop in oxygen concentration, thus jeopardizing the effectiveness of PDT.[27−29]

Developing nanoparticles (NPs) is thought to be a logical way to get over PDT's drawbacks due to the advancement of nanotechnology. Physical encapsulation or chemical conjugation are the two methods that can be used to integrate PSs into NPs. These methods alter the chemical properties of the PSs, such as their solubility, prevent them from self-quenching, and increase the effectiveness of ROS generation.[30,31] In contrast, NPs may also alter the biodistribution and pharmacokinetics of PSs *in vitro* and *in vivo*.[32,33] NPs improve PS tumor specificity by EPR effect or by altering their surface with targeted ligands.[6,34,35] Meanwhile, advancements in fiber-optic-based laser technology might offer novel strategies to transfer the drug-activating light intratumorally and interstitially. Several recent reviews have emphasized the numerous nanoparticle architectures being researched for PS's encapsulation and controlled release.[36−40] Other review studies have described

https://doi.org/10.1021/acsomega.2c05852
ACS Omega 2022, 7, 45882−45909

Table 1. PDT-Based Nanocarrier Systems to Deliver Photosensitizers

loading method	structure	size (nm)	zeta potential (mV)	laser parameters	therapy	remarks	ref
chemical conjugation	PDA-Ce6	~49	~23.4	670 nm, (50 mW/cm^2)	PDT/PTT	improved therapeutic effect and stability	47
	rGO@PDA-FA-C60	sheet		Xe lamp, (2 W/cm^2)	PDT/PTT	excited by a single light	203
	Mn_3O_4@ PDA-GQD	~100		670 nm, (4 mW/cm^2)	PDT	dual mode imaging-guided PDT	204
	PDA-A = T-ZnPc	~88	−21.5	665 nm, LED: 5 W	PDT/PTT	controlled release, DNA pairing rules	205
	$ZnFe_2O_4$−Ce6	~100	+51.5	660 nm, (50 mW/cm^2)	PDT	superior antibacterial activity	206
	RCDs−Ce6	~3.4	−32.5	671 nm, 0.05	PDT	high photostability, excellent biocompatibility,	207
	Pd−PEI−Ce6	~4.5	+10.2	660 nm, 0.05	PDT/PTT	high photostability, excellent biocompatibility,	208
	SiO_2−Ce6	80−105		normal light	PDT	biocompatibility	209
	Ce6−OC−PEI	80	+10.5	630 nm, 0.05	PDT	excellent biodegradable and biocompatible theranostic nanoagent	210
	Pd@Ce6	116		660 nm	PDT	good biocompatibility, structure stability, combination therapy effect	211
	Ac-CS/Ce6	~165.8	−29.9	660 nm	PDT	excellent singlet oxygen species generation capability	212
physical absorption	Ce6-PDA (load)	~142.8	+30.2	665 nm, 250 mW cm^{-2}	PDT/PTT	facile two-step method	49
	Ce6@CaCO3−PDA-PEG	~168		660 nm, 5 mW cm^{-2}	PDT	pH sensitivity, biomineralization	213
	PDA−PEG@IR820/Fe3+	~81	−28.3	808 nm, (1.0 W/cm^2)	PDT/PTT	dual imaging and dual therapy	214
	GNR@PDA-MB	~80	−18	671 nm, 10 min, (30 W/cm^2)	PDT/PTT	promising drug carrier, theranostic	215
	Ce6-CSNPs	~132	−35	(660−690 nm, 100 mW/cm^2)	PDT	biocompatibility	216
	IO−PG−DOX−Ce6	236.1 ± 4.62	24.73	690 nm NIR laser irradiation (0.5 W/cm^2)	Chem/PDT	dramatically improved cell uptake, photoinduced ROS generation, and cytotoxicity.	217
	ABN@HA-Sese-Ce6/CYC NPs	35 nm		650 nm laser (20 mW/cm^2)	PDT	smart drug release, excellent therapeutic efficacy	218
	MnO2@Ce6	100 nm	+38.5 mV	633 nm laser (0.8 W/cm^2)	PDT	excellent biodegradable and biocompatible theranostic nanoagent	219
encapsulation	UCNP@SiO2-MB@PDA	~38		980 nm,10 min, 1.0 W cm^{-2}	PDT/PTT	980 nm laser for PDT, mRNA target	51
	DOX@TiO2−X@PDA Cy5.5	~637		808 nm, (1.0 W/cm^2)	PDT/Chem/PTT	triple therapy, NIR/pH-triggered drug release	50
	MNPs@hy-PDA-lac	~305	0.54	LED 600 nm, (8.6 mW/cm^2)	PDT	good dispersibility, targeting ability	220
	LAP/ICG@PDA-RGD	59	−20.7	808 nm, (1.2 W/cm^2)	PDT/PTT	high encapsulation efficiency	221
	HANP/Ce6	~227.1		630 nm laser (150 mW/cm^2)	PDT	excellent biocompatibility, tumor targetability, and tumor suppression capacity	222
	Ce6/(pH)	~96.6		0.365 J/cm^2	PDT	significant suppression of tumor growth.	223

PDT's accomplishments in the clinical arena of cancer therapy. This article gives an overview of PSs, the mechanism of loading of PSs, nanomedicine-based solutions for enhancing PDT, and their biological applications, including chemodynamic therapy, chemo-photodynamic therapy, PDT−electroporation, photodynamic−photothermal (PDT−PTT) therapy, and PDT−immunotherapy. Furthermore, the review discusses the mechanism of ROS generation in PDT and the advantages and challenges of PSs in PDT.

2. MECHANISM OF REACTIVE OXYGEN SPECIES (ROS) GENERATION IN PDT

In PDT, tumors are eradicated by ROS, such as superoxide radical ($O_2^{\bullet-}$), hydroxyl radical ($OH^{\bullet}$), and singlet oxygen ($^1O_2$) species, which are formed by the interaction of oxygen (O_2) and excited PSs. This effect is very localized owing to the short duration and high reactivity of ROS.[13] Figure 1 shows a thorough breakdown of the photochemical mechanisms involved in PDT. A PS transitions from its ground state (S0) to the first singlet excited state (S1) or the second singlet excited state (S2) after absorbing a photon of the proper wavelength. Internal conversion (IC) will cause S2 to decay (≈ fs) fast to S1 (IC). S1 will either cease releasing light (fluorescence) or produce heat throughout the IC process since it is likewise unstable and has a lifespan of ns level. Intersystem crossover (ISC) of S1 may also occur in the meantime to create a more stable excited triplet state (T1). T1 has an extended lifespan (≈ μs) and is capable of undergoing a number of photochemical processes such as phosphorescent

https://doi.org/10.1021/acsomega.2c05852
ACS Omega 2022, 7, 45882−45909

emission and energy transfer to O_2 to produce $^1O_2$ (referred to as the type II PDT process). Additionally, T1 may generate radicals by reacting with intracellular substrates such as nucleic acids, proteins, and lipids via an electron transfer process. These radicals can then interact with O_2 or H_2O to generate additional ROS species like $O_2^{\bullet-}$ and $OH^{\bullet}$. This process falls under the category of type I PDT process. Under the influence of light, semiconductor nanomaterials may produce electron−hole pairs, and the subsequently separated electrons and holes can then interact with O_2 or H_2O to form $O_2^{\bullet-}$ and $OH^{\bullet}$. Heat-induced ROS production is a novel ROS generating process that has just been identified. Intense heat enhances the thermionic emission of electrons that further interact with the environment to generate ROS. Additionally, it has been shown that certain organic compounds with large π-conjugated structures may store $^1O_2$ via the production of endoperoxide at low temperatures, whereas under hot conditions, the stored $^1O_2$ can be liberated to annihilate cancer cells. It is also widely acknowledged that $^1O_2$ is mostly to blame for the photodynamic destruction of cells and biological tissues, which occurs when PSs are employed, and that the majority of PSs now in use operate predominantly via type II mechanism.[41]

The intrinsic property of PS, which serves as the cornerstone of PDT, governs the effectiveness of the treatment. However, a significant drawback of therapeutically used PSs, such as those derived from phthalocyanine (Pc) and porphyrin, is that their principal absorption band is in the ultraviolet−visible (UV−vis) region, where tissue receives a little amount of light. Due to the fact that NIR light may penetrate deeper into normal tissues than UV and visible light and has lower phototoxicity, much work has been put into designing and synthesizing PSs that are activated by NIR light. Meanwhile, the majority of organic PSs with substantial absorbance in the 700−1000 nm region of the spectral region for PDT often exhibit hydrophobic character, leading to an agglomeration state and a decrease in $^1O_2$ production and fluorescence quantum yields in aqueous solution.[42] The two-photon excitation (TPE) method, which makes use of a NIR-pulsed laser as the excitation light source, is a very attractive solution to this problem. During TPE PDT, a PS electron is stimulated from its ground state (S0) to an excited electronic state (i.e., S1 or S2) by absorption of two photons with the same frequency, which subsequently kills cancer cells through type I or type II procedure (Figure 1).[43] The energy source of ITPE should be a quick ($\approx$ 100 fs) laser pulse with high intensity in order to accomplish instantaneous absorption. The photon's energy may be lower than the energy difference between the two states, which is typically found in the NIR regime. In addition to inheriting the benefits of conventional one-photon excitation (OPE) PDT, this strategy additionally provides the following notable features. TPE PDT may eliminate deeper tumors because NIR lasers can penetrate materials more deeply than visible or UV light. Compared to OPE PDT, TPE PDT provides more precise phototherapy and greater spatial resolution in fluorescence imaging since only the sample located in the laser beam focus may be stimulated. The upconversion nanoparticles (UCNPs) also include rare-earth metals and lanthanide dopants, which may absorb numerous photons owing to the extended lifespan and actual ladder-like energy levels of lanthanide ions, producing high energy anti-Stokes fluorescence in the process. UCNPs have been used in a variety of applications including bioimaging, biosensing, and PDT.[44] Although TPE and UCNPs offer benefits in deep tumor treatment, developing PSs with the following attribute is still quite difficult: high extinction coefficient in the optical window for PDT, the proper retention period in a live organism, high ROS generation efficiency, and excellent photostability and biocompatibility.[45]

3. MECHANISM OF LOADING

PSs have been delivered via a variety of nanocarriers by many research teams. These investigations have been divided into three groups based on the multiple interactions between PSs and PDT nanocarriers including the encapsulation approach, physical absorption strategy, and chemical conjugation strategy. The summary of PDT based on various nanocarriers to deliver PSs is represented in Table 1.

3.1. Chemical Conjugation Strategy. Molecules containing groups such as dihydroxyindole, indoledione, and dopamine-like units make conjugation reactions much simpler while simultaneously furnishing high chemical reactivity to these molecules. Amine and thiol conjugations following Schiff's base reaction and Michael's addition have been used variedly throughout different studies. The presence of catechol groups increases the redox potential, posing the molecules as a candidate for PDT. Li et al. worked with one such molecule, polydopamine, and conjugated it with graphene due to their high singlet oxygen generation and high photothermal properties.[46] Furthermore, by conjugating folic acid through Schiff's base reaction, the formed, modified molecules could be tumor-targeted and simultaneously used for photodynamic and photothermal therapies against cancer cells. Another study investigated the potency of conjugation of Ce6 with these groups and observed that it increased the photostability and photodynamic effect of the formed NPs. The varied functional groups present in these structures form a much more suitable molecule for chemical conjugation. These conjugations further improve its therapeutic efficacy and the safety of the photodynamic moieties.[47]

3.2. Physical Absorption Strategy. The noncovalent interactions such as $\pi-\pi$ stacking, hydrogen bonding, and electrostatic interactions are considered easier ways to load PSs to any drug molecule. This could pertain to the fact that physical absorption does not require any activation energy and can be performed under mild conditions. Aromatic groups have a higher ability to absorb any photosensitizing agent efficiently.[48] For instance, Ce6 loaded onto polydopamine through $\pi-\pi$ stacking enhanced the photostability and improved the efficacy of the PDT as studied by Poinard et al. This noncovalent conjugation, although relatively simple, shows that the loading efficiency compared to chemical conjugation is still less efficient.[49]

3.3. Encapsulation Strategy. Encapsulation of PSs within polymers enhances their biocompatibility as well as their photodynamic and photothermal efficacy. These polymeric coatings improve the tumor tissue selectivity and penetration, prevent premature release, and hence increase the therapeutic efficacy. In a study performed by Guo et al., the PSs were encapsulated inside a silicon dioxide (SiO_2) shell, which remarkably enhanced the NIR absorbance and photodynamic effect on the cancer cells.[50] Nonetheless, these outer shell coatings might also hinder the singlet oxygen generation and, therefore, might also decrease the cytotoxic effect. Thus, tailoring the shell thickness, manipulating the shell material, and optimizing the encapsulated structure improve the ROS

https://doi.org/10.1021/acsomega.2c05852
ACS Omega 2022, 7, 45882−45909

Table 2. Methylene Blue (MB)-Based Nanocomposite Systems Used for Cancer Therapy

nanocomposites (NCs)	PS	laser parameter	size (nm)	zeta potential (mV)	cancer cell line	application	ref
methylene blue (MB) with/without gold or silver NPs	MB	NIR (660 nm; 25 W/cm^2)	21 nm, 43 nm	−48 mV	MDA-MB-468	breast cancer (PDT)	224
methylene blue-liposome	MB	NIR (660 nm; 165 mW/cm^2)	140 nm	not defined	4T1	breast cancer (PDT)	130
graphene oxide-methylene blue NCs	MB	red light LED irradiation	20 nm	not defined	MDA-MB-231	breast cancer (PDT)	225
MB and veliparib NPS (VMB-NPs)	MB	660 nm(102 J/cm^2)	90 nm	−3.7 mV	B16F10-Nex2 cells	skin cancer (PDT)	226
sulfur-doped graphene quantum dot and methylene blue preparations (GQD:MB)	MB	660 nm, 12 W	>20 nm	not defined	MCF-7 cells	breast cancer (PDT)	227
methylene blue and curcumin Ion-pair NPs	MB	(red LED 630 nm; 30 mW/cm^2); blue LED (465 nm; 34 mW/cm^2)	40−60 nm	not defined	MDA-MB-231	breast cancer (PDT)	228
methylene blue: salicylic acid (SA-MB)	MB	NIR (630 nm; 30 mW/cm^2)	not defined	not defined	MDA-MB-231	breast cancer (PDT)	229
MB-PDT	MB	660 nm	not defined	not defined	not defined	skin cancer (PDT)	230
GGH@AuNRs/MB hydrogel (Gellan Gum, Ca2+, gold nanorods (AuNRs) and methylene blue (MB)	MB	808 nm laser at 0.5 W/cm^2; 660 nm laser at 50 mW/cm^2	not defined	33.1 mV	HeLa cells, 3T3 cells and MCF-7 cells	Henrietta's cancer, breast cancer (PDT−PTT)	231
GO-MB/PF127 nanocomposite	MB	808 nm laser at 0.5 W/cm^2; 660 nm laser at 50 mW/cm^2	121.8 nm	−16.70 mV	HL-7702 cells and SiHa cells	skin cancer (PDT−PTT)	232

Table 3. Chlorin-Based Nanocomposite Systems Used for Cancer Therapy

nanocomposites (NCs)	PS	laser parameter	size (nm)	zeta potential (mV)	cancer cell line	application	ref
CM/SLN/Ce6 NPs silica NPs (SLN) with cell membrane (CM)	Ce6	680 nm laser, (1 W/cm^2)	90.4 ± 3.2 nm	+32.4 ± 1.7 mV	SGC7901 cells	gastric cancer (PDT)	233
SWCNTs-HA-Ce6 (single-walled carbon nanotubes, hyaluronic acid (HA) and chlorin e6 (Ce6)	Ce6	660 nm laser (5 and 10 J/cm^2)	203 ± 6.6 nm	−18.9 ± 1 mV	Caco-2 cells	colon cancer (PDT)	234
Ce6-Fu/AL@GG-based hydrogel (Chlorin e6 (Ce6)-fucoidan/alginates@gellam gum)	Ce6	660 nm laser (4 J/cm^2)	not defined	not defined	HT-29 cells	colon cancer (PDT)	235
Ce6-PDT	Ce6	650 nm, (4 J/cm^2)	not defined	not defined	SW620 cells	colon cancer (PDT)	236
GNPs@PEG/Ce6-human PD-L1 peptide nanoprobes gold NPS(GNPs)	Ce6	633 nm, (0.8 W/cm^2)	>100 nm	−11.38 ± 3.89 mV	HCC827 and A549 cells	lung cancer (PDT−PTT)	237
Ce6/Dox@NPs-cRGD (CDNR NPs) Cyclo(Arg-Gly-Asp-D-Phe-Cys) (c(RGDfC), cRGD)	Ce6	670 nm laser (0.25 W/cm^2)	112.6 nm	−21.5 mV	MCF-7 cells	breast cancer (PDT)	238
CNPs-Ce6, Ce6 loaded chitosan NPs (CNPs)	Ce6	635 nm laser (50 mW/cm^2)	160−200 nm	24.77 mV	A549 cells	lung cancer (PDT)	239
G-chlorin e6 (glucose-conjugated chlorin e6)	Ce6	664 nm laser (100 J/cm2) (150 mW/cm2).	not defined	not defined	MKN45 cells and HT29 cells	gastrointestinal cancer (PDT)	240
Ce6 mediated PDT	Ce6	690 nm NIR laser irradiation (0.5 w/cm^2)	not defined	not defined	Lewis cells	lung cancer (PDT)	241
Ce6 and IgG nanocomplexes (Chlorin e6 + immunoglobulin G)	Ce6	660 nm (80 mW/cm^2)	∼7 and ∼44 nm	not defined	GL261, a PD-L1 positive cell line	glioma (PDT)	242

generation along with selective delivery of the photosensitizer to the tumor microenvironment.[51]

4. PHOTOSENSITIZERS (PSS)

The selection of PS is crucial for effective PDT therapy. In order to maximize tissue penetration, light with a wavelength (600−700 nm) in the therapeutic window should ideally be used to activate the PS. It should not be harmful to cells in the dark or trigger cell death when there is no light, and it has easy solubility in the tissues of the body. Additionally, the target cells must specifically capture and/or retain it. Finally, It must also be capable of causing immunogenic cell death., which is distinguished by alterations in the structure of the cytosol and the discharge of signaling molecules that stimulates T and dendritic cells and encourages the growth of a specialized immune response that is specifically directed toward cancerous tumors.[52−54] A few PSs that typically adhere to the aforementioned requirements have been discussed in this section.

4.1. Methylene Blue (Phenothiazine Derivative). An organic dye called methylene blue (MB) has both photosensitizing and fluorescent features.[55−57] This PS efficiently destroys cancerous cells, bacteria (*in vivo*), and viruses (*in vitro*).[58−60] Human cells and bacteria interact with it more favorably due to its low molecular weight and positive charge. As a result, it is an appropriate choice for PDT of cancer and infections.[60,61] The net positive charge and hydrophilic/lipophilic balance of MB enable it to readily pass across biological membranes.[60] *Enterococcus faecalis*, *Candida albicans*, and *Escherichia coli* infections are most often treated with it as a PS in antimicrobial PDT. The application of MB as a PS in PDT for treating cancer is growing. The potential of MB in anticancer PDT is particularly intriguing because it is less expensive and more readily available than traditional PSs. As revealed by several investigations, it has shown positive outcomes. MB has been used to study a range of NPs including apoferritin nanocages, polyacrylamide, and silica.[62−65] Aerosol alginate NPs were designed by Khdair et al.

https://doi.org/10.1021/acsomega.2c05852
ACS Omega 2022, 7, 45882−45909

to administer MB and doxorubicin simultaneously as part of a PDT−chemotherapy combo treatment approach. They were able to effectively increase the cytotoxic effect in drug-resistant ovarian cancer cells while missing any active targeting domains.[66] In a study, 17 patients with basal cell carcinoma were treated with MB-PDT by Samy et al.[67] Out of the 17 patients, 11 had a full recovery with favorable aesthetic results and few adverse effects. MB-PDT is only used in clinical investigations at this time since there is no authorized clinical procedure. MB solutions are quickly removed from the body after intravenous injection despite having a significant water solubility because it is reduced into leucoMB in peripheral tissues and erythrocytes.[68] LeucoMB has no photodynamic/PS activity; hence, it is critical to safeguard MB from peripheral and blood reduction when contemplating IV delivery. NPs made from the biocompatible polymers chitosan and PLGA may be employed to increase MB stability. The other MB-based nanocomposite systems used for cancer therapy are represented in Table 2.

4.2. Porphyrins. A significant class of PSs includes compounds of porphyrin. A member of this family, photofrin or porfimer sodium, has received clinical approval in the USA for PDT treatment of a number of premalignant lesions and tumors. Although the present clinical formulation does not use a NP carrier, numerous encouraging preclinical investigations using nanoformulations of porphyrin photosensitizers have been conducted. In a study, Chen et al. delivered pheophorbides (chlorin derivatives) and 5,10,15,20-tetrakis-(m-hydroxyphenyl) porphyrin (mTHPP; a porphyrin derivative) to leukemia cells using human serum albumin NPs.[69−71] It was discovered that the NPs were shown to be absorbed via lysosomal processes and resulted in around 50% of the cell's death from apoptosis.[71] Several distinct NP systems, including gold NPs, silica, polymeric, chitosan, and metal oxide, have been used to manufacture porphyrin derivatives such as protoporphyrin IX and photofrin.[72,73] A few of the formulations have used receptor-mediated active targeting to improve cell-selective delivery, whereas the rest of them have the EPR mechanism being used to passively target solid tumors. In a study, tetrakis(1-methylpyridinium-4-yl) porphyrin (TMPyP4), which is used for multimodal imaging and subsequent PDT of breast cancer, was packaged in multifunctional iron oxide NPs by Yin et al.[74] Additional cases where porphyrin PS has been loaded in NPs that may actively or passively target cancer cells are represented in Table 3.

4.3. Photogem (Hematoporphyrin Derivative, HpD). A hematoporphyrin derivative from Russia (Moscow) is called Photogem. This first-generation PS was generated using animal blood. It has the same chemical, photophysical, diagnostic, and therapeutic properties as Photofrin. Both the Brazilian Health Surveillance Agency (ANVISA) and the Russian Federation's Pharmacology State Committee have authorized it for use in humans. It has an absorbance spectrum between 500 and 630 nm and is made up of a combination of oligomers and monomers.[75] For the first few weeks following the delivery of Photogem, which is often administered systemically, photosensitivity becomes the most frequent adverse effect. The detrimental impacts may be reduced by integrating Photogem with targeting or drug delivery systems, which enables a staggered release of PS into the system or its tailored administration to cancer. On the other hand, it has a low optical absorption within the therapeutic range of 600−700 nm, which results in protracted photosensitivity. This led to the development of second-generation PSs, such as chlorins and 5-aminolevulinic acid (ALA, Levulan), with superior absorption properties and fewer negative side effects.[76]

4.4. Chlorins. Bacteriochlorins and chlorins, present in natural substances, strongly absorb light between 640 and 700 nm. For instance, *Rhodobacter capsulatus* bacteria contain bacteriochlorins, and chlorins may be detected in chlorophyll-a (reported in certain species of Spirulina).[77] Chlorins have a fundamental structural resemblance with porphyrins since they are hydrophilic reduced porphyrins. Numerous chlorin derivatives, such as mono-L-aspartyl chlorin e6 (NPe6), have been investigated for use as PSs. It has two crucial characteristics: a powerful light absorption in the therapeutic window between 650 and 680 nm, as well as a large quantum yield of $^1O_2$ (0.70).[78] The benzoporphyrin derivative BPDMA and meso-tetrakis (m-hydroxyphenyl) chlorin are two synthetic chlorins that have interesting biological effects.[79] Photodithazine (PDZ) is the brand name of one more PS drug that originates in Russia and is part of the chlorins family. It is derived from the cyanobacterium *Spirulina platensis*, and its geometry has been amended by the inclusion of *N*-methyl-D-glucosamine (0.5%) as a stabilizing and solubilizing agent.[80] It is a second-generation PS, and it has minimal to no effect on skin photosensitivity.[81] Chlorins' ability to cure oral cancer has been well-researched.[82,83] In a study, Parihar et al.[82] conducted both *in vivo* and *in vitro* studies to investigate the efficacy of chlorin-PDT as a potential treatment for oral squamous cell carcinoma. They observed full tumor shrinkage and significant cellular damage within a week of receiving the chlorin-PDT. When it comes to the treatment of lesions in the oral cavity, aqueous solutions are not always the most effective delivery vehicle for administering a PS, despite the fact that chlorins demonstrate strong stability and water solubility. In these situations, it is preferable to include the chlorins in a mucoadhesive delivery method. It prolongs the dosage form's duration at the absorption site and enhances the end results.[84]

As an important category of PSs, chlorins have a chemical structure that is analogous to that of chlorophyll. The PS chlorin e6 (Ce6), which has been investigated for use in a variety of nanobased drug delivery systems, has the highest volume of clinical applications among the drugs in this category including hyaluronic acid, iron oxide, silica, human serum albumin, chitosan, and a variety of polymeric NPs. These chlorin-loaded NPs were mainly developed with the intention of using EPR-based passive targeting mechanisms in various cancers including those of the breast, colon, and cervical regions. Conversely, active receptor-mediated targeting has also been employed in a couple of these strategies. In a study, Benachour et al.[85] developed silica NPs loaded with a targeting peptide neuropilin-I and 5-(4-carboxyphenyl)-10,15,20-triphenylchlorin (TPC) to attack tumor angiogenic vasculature and accomplish near-complete cell killing *in vitro*. Similarly, Yoon et al. designed CD44 tumor-targeting hyaluronic acid NPs (HANPs) to deliver Ce6 and accomplish almost 100% cell killing in two distinct human colon cancer cell lines.[86] In addition, Li et al.[66] employed folate receptor targeting on pheophorbide A-loaded heparin NPs for the purpose of administration to cervical cancer. The primary emphasis of recent research using chlorin-based nanoformulations has been on the development of NPs with the dual purpose of imaging and photodynamic treatment. For instance, concurrent PDT and magnetic resonance imaging of stomach cancer was performed by Huang et al. using Ce6-

https://doi.org/10.1021/acsomega.2c05852
ACS Omega 2022, 7, 45882−45909

coupled magnetic NPs.[62] Another new nanovehicle preparation of chlorins involves a novel platform known as "upconversion NPs." This formulation of chlorins has been researched by a few different groups for the purpose of PDT for breast, cervical, and glioma malignancies.[87,88] Upconversion is a process that involves the successive absorption of numerous photons, which may then result in the emission of light at wavelengths that are shorter than the excitation wavelength.[89] Typically, the excitation occurs in the infrared range, and the resulting emission occurs in the visible range. If upconversion components, such as rare earth metals like Er^{3+}, are manufactured together with PSs inside the same vehicle, the produced light has the potential to activate the PS. As a result, this strategy has the potential to hold great promise in terms of tackling the issues associated with assuring light transmission *in vivo*. The other chlorin-based nanocomposite systems used for cancer therapy are represented in Table 4.

4.5. Phthalocyanine (Pcs). Pcs structure can be elucidated as a tetra pyrrole structure consisting of four isoindole rings, where the connecting carbon is replaced by nitrogen atoms. The C−N bonds have similar lengths due to the uniform electron density distribution that provides a stable physicochemical property to the compounds. The molecular structures of phthalocyanine derivatives and cyanine derivatives are shown in Figure 2. These compounds intensely absorb the NIR and red light while vaguely absorbing the light of 400−600 nm. Pcs have been fabricated further with diamagnetic ions, improving the tumor microenvironment's selectivity and inhibition by improvising the cytotoxic singlet oxygen quantum yields.[90] The various derivatives of PCs are described below.

4.5.1. Zinc Phthalocyanine (ZnPcs). ZnPcs provide strong photostability and shows enhanced spin−orbital coupling. Forming a part of type-II PSs, it endures oxygen dependency problems which can be overcome by introducing amine groups which in turn increases the hydrophilicity and electron-donating capability of the molecule. The tumor selectivity and target specificity can be improved by introducing folic acid, saccharides, and peptides whose receptors are overexpressed in the tumor tissues. Activatable ZnPcs also improve tumor selectivity. Exploiting the tumor microenvironment pH, which is significantly lower than the normal tissue pH, the pH-activated ZnPcs invade the tumor regions more, showing an enhanced photosensitizing effect. Taking into account the intrinsic nature of ZnPcs wherein they form π- π stacking, leading to singlet oxygen species generation, they, too, serve as precursors to the activatable form. It was reported by Xue et al. that when oligo ethylene glycol was used to connect the phthalocyanine-erlotinib. The conjugate synthesized has enhanced its binding capacity to the ATP-domain of the tyrosine kinase in EGFR, overexpressed in the tumors.[91] The study performed by Chen et al. demonstrated that conjugation of 2,4,6-tris(N,N-dimethylaminomethyl) phenoxy (TAP) with ZnPc, provided a pH-dependent activation based on the tumor microenvironment, which possesses a generally low pH than the normal tissues.[92] Albumin-dependent switchable PDT wherein ZnPc is substituted with 4-sulfonatophenoxyl, as indicated by Yoon et al., improved the effect of PDT.[93]

4.5.2. Silicon Phthalocyanine (SiPcs). SiPcs showcase sterically hindered structures that prevent the aggregation-caused quenching often observed in ZnPcs. SiPcs can be phototriggered for drug release or can be modified at multiple sites for tumor specificity due to their easily fabricable nature.

Table 4. Porphyrin-Based Nanocomposite Systems Used for Cancer Therapy

nanocomposites (NCs)	PS	laser parameter	size (nm)	zeta potential (mV)	cancer cell line	application	ref
O_2@PFOB@PGL NPs perfluorooctyl bromide (PFOB), porphyrin grafted lipid (PGL)	porphyrin	650 nm laser irradiation (200 mW/cm^2)	33 ± 2.1 nm	−18.12 ± 0.61 mV	HT-29 cells	colon cancer (PDT)	243
CM-MMNPs (MnO_2 nanosheet-coated metal−organic framework core and cancer cell membrane shell)	porphyrin	409 nm laser (1.5 W/cm^2)	59.04 ± 1.09 nm	5.28 ± 0.06 mV	HeLa cells and HepG2 cells	Henrietta's cancer (PDT)	244
porphyrin-containing metalla-assemblies	porphyrin	638 nm, 0.5 W/cm^2	30−90 nm	−46 to −5.4 mV	4T1 cells	breast cancer (PDT)	245
tumor microenvironment-responsive Fe(III)−porphyrin nanotheranostics	porphyrin	635 nm, (100 mW/cm^2)	90−160 nm	−14 to −9.85 mV	4T1 cells	breast cancer (PDT)	246
fluorinated porphyrin as oxygen nanoshuttles	porphyrin	660 nm, (100 mW/cm^2 and 785, 1 W/cm^2)	∼40 nm	not defined	4T1 cells	breast cancer (PDT)	247
lipid NPs	verteporfin	690 nm (200/J cm^2)	47.9 ± 1.0 nm	−3.7 ± 0.9 mV	SKOV-3 and OVCAR-3	ovarian cancer	248
core−shell poly methyl methacrylate NPs	nonsymmetrical diaryl-porphyrin	640, 35 mW/cm^2	>100 nm	42.11 mV and 60.95 mV	SKOV-3	ovarian cancer	249
FKR560 dye-containing poly(lactic-*co*-glycolic acid) NPs	benzoporphyrin derivative	690 nm, (100 mW/cm^2)	≈80 nm	−3.6 to −4.2 mV	OVCAR-5	ovarian cancer	250
nonporous silica core and a mesoporous silica shell	hematoporphyrin	633 nm	≈57 nm	not defined	HO-8910 PM cell	ovarian cancer	251

https://doi.org/10.1021/acsomega.2c05852
ACS Omega 2022, 7, 45882−45909

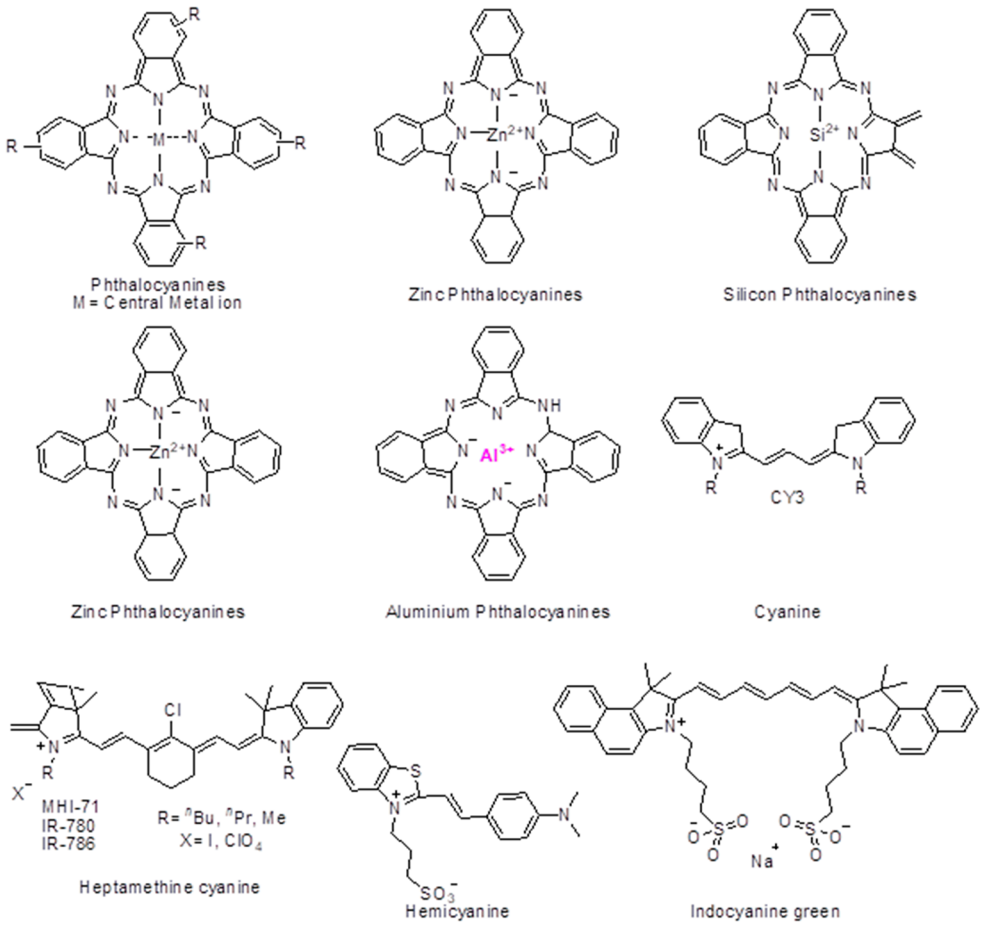

Figure 2. Molecular structures of phthalocyanine and cyanine derivatives.

These class Pcs more naturally show their effect following the PET mechanism wherein the fluorescence quenching occurs due to the electron transfer between the excited fluorophore and redox-active receptor ligand. Bai et al. reported the conjugation of IR700 (silicon derivative) with 6-TSPOmbb732 (a small targeting molecule with the molecular weight 18KDa mitochondrial translocator protein TSPO, which is present in higher quantities of multiple cancers than in normal tissue) demonstrated improved PDT efficacy.[94]

4.5.3. Aluminum Phthalocyanine (AlPcs). AlPcs supramolecular forms help to overcome the challenges observed in photodynamic therapies. As the supramolecular form is taken up by the tumor tissues, they degrade to release the monomeric units, which after accumulation into the mitochondria and lysosomes, show their cytotoxic effects. Modified AlPcs also act as tumor biomarkers which can then be further used to observe tumor specificity. For instance, the use of sulfonate-modified AlPcs and ATP resulted in higher selectivity of 4T1 tumors and more effective tumor destruction as compared to free PSs. In a study, Tang et al. reported AIE-Mito-TPP and sulfonate-modified AIPc to produce theranostic PSs for a synergistic chemo-photodynamic therapy and demonstrated that electrostatic, hydrophobic, and $\pi-\pi$ interaction could be used for mitochondrial targeting chemotherapy.[95]

4.6. Cyanine. The general structure of cyanine includes two nitrogen atoms linked by a polymethine chain. These nitrogen atoms are members of any heterocyclic molecule such as pyridine, pyrrole, indole, or imidazole. They exist in the zwitter ionic form and have both cationic and anionic moieties together. Due to the high absorption coefficients, tunable absorption of light throughout the visible and NIR regions, high biocompatibility, and comparatively low toxicity, cyanine and its derivatives have become one of the most vigorously used and studied dyes for chemo-sensors. Recent studies have demonstrated the use of cyanine compounds as PSs in photodynamic therapies. The various cyanine derivatives used in PDT are discussed below.

4.6.1. Heptamethine Cyanines (Cy7). The two nitrogen heterocycles linked to each other via a conjugated carbon chain in the Cy7 improve the cyanine solubility and the conjugation ability to various other moieties that might improve the tumor selectivity. Indocyanine green (ICG) is the FDA-approved Cy7 fluorophore with high clinical acceptance and has been used in over a hundred active clinical trials. Although it is minimally invasive and hence has been approved for clinical use, ICG shows fast clearance and low singlet oxygen generation capacity hence pertains to low cytotoxic properties. This then poses the use of higher doses of light or the drug to observe optimal cytotoxicity. To overcome these limitations, multiple researchers modified Cy7 to observe enhanced photothermal properties. For instance, Callan et al. modified Cy7 by forming monoiodinated and di-iodinated Cy7. They observed that these compounds produced significantly higher singlet oxygen than ICG and hence increased the cytotoxic property.[96] Introducing iodine, a heavy atom, enhanced the photothermal conversion capacity, as well as ROS generation, as indicated by Sun et al. Cyanines, have been providing both

https://doi.org/10.1021/acsomega.2c05852
ACS Omega 2022, 7, 45882−45909

photodynamic and photothermal efficacy, which provide an improvised anticancer effect.[97]

4.6.2. Hemicyanine. Another subclass of cyanine dyes, hemicyanines, work following the D−π−A-based ICT mechanism wherein the absorption of light occurs through the charge transfer from the donor to the acceptor through a π-bridge structure. The conjugated system could be enhanced by the activation of NIR light. Small molecule substituted hemicyanines such as bromine substituted showed less PDT effect as compared to a comparatively heavier molecule such as iodine which enhanced the effect. As the hemicyanines possess a shorter wavelength for maximum absorption as compared to Cy7 it limits its usage for deep tissue PDT. Conjugating with iodine also shifts the wavelength, thus improving the efficacy of deep-tissue penetration.

4.7. Boron Dipyrromethene (BODIPY). One of the most investigated and researched chromophores, BODIPY can be easily modified to obtain enhanced physicochemical properties with an enhanced PDT effect. They consist of multiple exemplary features, most importantly possessing a high extinction coefficient, biocompatibility, and photostability. Multiple researchers have worked on preparing BODIPY-based derivatives that could increase the maximum absorption wavelength above 600 nm. BODIPY modified at the second and sixth position using a dibromo or diiodo ensures the increase in the singlet oxygen species generation and hence impacts the cytotoxic effect. However, it has been greatly observed that the incorporation of multiple heavy moieties does not necessarily improve the singlet oxygen generation but does remarkably increase the dark toxicity. Another method investigated to improve the absorption and fluorescence wavelength was by extending the π-conjugated framework by substituting a carbazole moiety. Other modifications researched include preparing pH-activatable BODIPYs wherein, due to the tumor microenvironment, pH leads to an increased yield of singlet oxygen species. Another type of BODIPY is Aza-BODIPY, wherein a nitrogen atom is incorporated in the meso-position of the BODIPY structure, which red-shifted the maximum absorption wavelength by over 100 nm and made it therapeutically active. Another remarkable investigation showed that combining aza-BODIPY with heavy atoms such as iodine, as indicated by Huang et al. in their studies, resulted in an ultrahigh singlet oxygen yield. PDT using NIR-activated aza-BODIPY has been researched in recent years and has provided promising results. The narrow energy gap between the HOMO and LUMO allowed the nonradiative pathway of heat generation, providing positive results for photothermal tumor reductions.[98] The molecular structure of BODIPYs is shown in Figure 3.

4.8. Other Miscellaneous Photosensitizers. In addition to the primary classes of PSs that have been discussed above, numerous other interesting PS molecules have also been explored in the formulations that are based on NPs. The indocyanine green (ICG) and cyanine compounds cyanine IR-768 among them may be triggered by a longer NIR wavelength than the majority of other PSs, enabling a greater level of tissue penetration by the activating light. Pietkiewicz et al. delivered cyanine IR-768 to doxorubicin-resistant human breast cancer cell lines using oil-cored poly(*n*-butyl cyanoacrylate) nanocapsules. They were able to show an almost complete loss of cell viability *in vitro* in both cell lines., indicating the potential for employing PDT in malignancies that are immune to chemotherapy.[99] One drawback of NIR-activable PSs is that

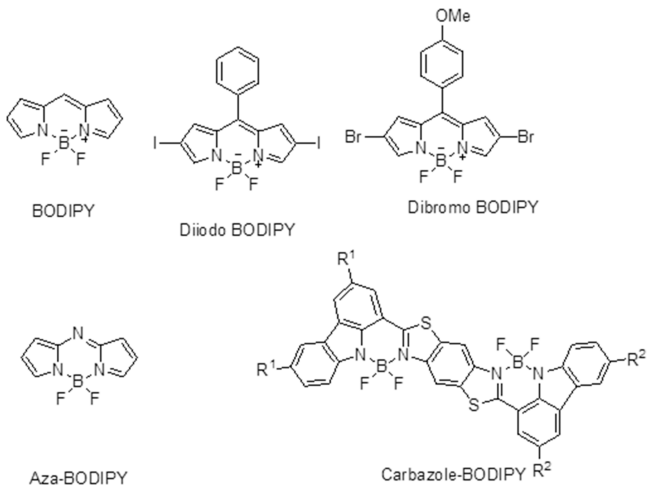

Figure 3. Molecular structures of BODIPYs.

because of their longer wavelength of activation, they transmit less energy to the PS, which results in a reduced yield of $^1O_2$. Nevertheless, a number of research teams have examined ICG-loaded NPs for the therapy of deep tissue malignancies.[100−103] *Hypericum perforatum* L., sometimes known as St. John's Wort, is a plant that contains the naturally occurring red plant pigment hypericin (HYP), which has been utilized for many years in herbal medicine. Due to its capacity to generate photosensitivity when consumed over a threshold dose, it has lately grown in favor of PDT research. The PS HYP is very hydrophobic, like many others. For example, Kleeman et al.[104] demonstrated the efficiency of HYP-PDT in the *in vitro* destruction of carcinoma cells. A relatively recent family of PSs, fullerene cages like C60 are distinguished by their closed carbon-cage polyhedron form. They may produce fluorescence and take part in the series of energy transfer events that result in the formation of $^1O_2$ owing to their abundance of π-bond electrons. They have been investigated for the therapy of prostate and cervical malignancies and have been coupled to the surfaces of cyclodextrin NPs, viral NPs, and various fullerene nanocages.[105−107]

In addition, quinones have been studied for anticancer activity in large numbers and represent one of the major classes of chemotherapeutic drugs licensed for clinical use.[108] The quinone structure is significantly represented among drugs now utilized to treat the tumor. In general, quinones with complex or reactive side chains have little anticancer action.[109] Naturally occurring quinones are classified into three groups: anthraquinones, naphthaquinones, and benzoquinones. These quinones are clinically utilized to treat a broad range of cancers. Streptonigrin and mitomycin have a heterocyclic p-benzoquinone moiety, daunomycin and adriamycin, on the other hand, have an anthraquinone component.[110] It has also been discovered that several naphthaquinone antibiotics, such as lapinone and lapachol, are effective in eliminating cancer cells. Both quinones and porphyrin are bioavailable and will not cause any adverse reactions. Porphyrin derivatives are often employed in PDT because they absorb in the PDT window area (600−900 nm). As a result, researchers developed drugs based on the structure of porphyrin. In contrast to porphyrin, benzoquinone and its simple polycyclic analogues, such as anthraquinones and naphthaquinone, absorb in a shorter wavelength range (300−400 nm). As a result, they are excluded from PDT studies. However, higher polycyclic

https://doi.org/10.1021/acsomega.2c05852
ACS Omega 2022, 7, 45882−45909

quinones may be utilized as PDT agents because of their conjugation, which allows them to absorb in the PDT window area (600−900 nm).[111] Redox cycling has been suggested as a potential mode of action for numerous quinone species.[112] Quinones participate in both the photodynamic and enzymatic production of ROS. ROS generation may be quantified using EPR, optical, and phosphorescence techniques. Many biological processes are influenced by photodynamically produced ROS. The photoinduced DNA breakage by quinones corresponds with the ROS-producing efficiency of quinones.[111,113]

5. NANOTECHNOLOGY-BASED DELIVERY OF PHOTOSENSITIZERS

Most traditional PSs have little cytotoxic effects in the dark; thus, specific light irradiation to target malignant tissue presents less intrusive techniques to treat solid tumors. However, the nonselective dissemination of PSs often causes significant complications for patients by causing hypersensitivity to regular light exposure.[114,115] One of the primary objectives of nanotechnology-based PDT is the targeted delivery of PSs to the target tissue for a better therapeutic effect. PSs may be delivered selectively using a variety of nanosized drug delivery vehicles including nanoparticle systems, liposomes, hydrogels, micelles, liquid crystalline systems, dendrimers, and cyclodextrin.

5.1. Nanoparticle Systems. NPs are particles that are less than a micrometer in size. They offer a number of benefits as a PS delivery system, including safeguarding the PS from enzymatic breakdown, the regulation of PS release makes it possible to maintain a steady and homogeneous level in a target tissue, a submicron size that allows them to enter target cells, photostability, resorb-ability and biocompatibility through natural pathways.[116]

NPs may be categorized as polymeric nanoparticles (PNPs), metallic NPs, nanostructured lipid nanocarriers (NLCs), and solid lipid NPs (SLNs), varying according to the material from which they are prepared.[117] Polymeric NPs are made from synthetic or natural polymers such as chitosan, gelatin, PCL (poly caprolactone), PLGA (poly-D,L-lactide-coglycolide), PLA (polylactic acid), and PAC (poly alkyl-cyano-acrylates), among others.[118,119] In a study, Kumari et al. developed Chlorin e6 (Ce6 conjugated polyethylene methoxy-poly(ethylene glycol)-poly(D,L-lactide) NPs for PDT. The developed NPs demonstrated particle size of 49.72 ± 3.51 nm and zeta potential of −24.82 ± 2.94 mV indicating good colloidal stability of the nanocarrier system. In comparison to free Ce6, mPEG−PLA-Ce6 NPs significantly increased the production of $^1O_2$ in water. The NPs demonstrated improved phototoxicity and cellular internalization in monolayer and 3D spheroids of human lung adenocarcinoma cells (A549). The developed NPs showed a strong attraction to tumor cells, which demonstrates that they are capable of functioning as Ce6 nanocarriers for PDT of solid tumors.[120] Ohulchanskyy et al. developed polymeric NPs for colon cancer therapy by polycondensing the organotrialkoxysilane precursors in the nonpolar core of a Tween-80/water microemulsion and then alkalinizing them. They were able to synthesize ultralow size organically modified silicon nanoparticles (SiNPs). These SiNPs were then covalently bonded with iodobenzylpyropheophorbide PS. The produced SiNPs was shown to have a strong therapeutic effect for tumor cells, demonstrating their considerable potential for PDT cancer therapy and diagnostics.[119]

In order to fabricate PNPs from dioctyl sodium sulfosuccinate and sodium alginate, Khdair et al. used a multiple emulsions cross-linking technique. They examined how well these PNPs may improve the therapeutic effectiveness of the PS methylene blue (MB) in MCF-7 and 4T1 breast cancer cell line. The anticancer photodynamic effectiveness of NP-encapsulated MB was boosted by more significant MB deposition in the nucleus and enhanced ROS generation investigated *in vitro* studies. The reported NP system had shown promise as an MB delivery strategy for anticancer PDT.[121] An innovative approach to the development of NPs is the use of photonic explorers for biomedical applications through biologically localized embedding (PEBBLE). El-Daly et al.[122] prepared NPs predicated on PEBBLE by encasing indocyanine green (ICG) PS in an organically modified silicate (ormosil) matrix. They examined the PDT effects of free ICG and ICG-loaded NPs on hepatocellular carcinoma cells (HepG2) and on human breast adenocarcinoma cells (MCF-7). They observed that the NPs strengthened ICG stability while retaining its phototoxic potential, and they anticipated that PDT with ICG-loaded NPs results in less DNA oxidative damage than PDT with free ICG.

SLNs composed of solid lipids and particles were presented as a PNP substitute in the early 1990s. The drawbacks that certain PNPs have, such as cytotoxicity and complex, large-scale manufacture, are not present with SLNs. Additionally, SLNs are less expensive than PNPs, and the solid lipids are more tolerable, but there are some drawbacks to SLNs as well, including crystallization, drug expulsion during storage, and poor encapsulation efficiency.[123] As a result, NLCs were designed to address these issues. Solid and liquid lipid phases combine to generate NLCs, which results in a disordered matrix that prevents the solid lipid from crystallizing and increases the drug payload in the NLC. Both NLCs and SLNs can be generated by cold or hot high-pressure homogenization, by precipitation, or by the microemulsion method.[123] In a study, SLNs were developed and characterized by employing the microemulsion technique to deliver hypericin by Youseef et al.[124] The compatibility of hypericin with lipids was excellent in hypericin-loaded SLNs, which forms the core of SLNs. Additionally, HYP's photostability was increased by SLN encapsulation. It is interesting to note that encapsulating HYP in SLNs reduced its phototoxicity. This might be due to the thickness and compactness of the SLN structure cause hypericin to become inactive when quenched. Furthermore, Lima et al.[125] developed hypericin-SLNs with good drug loading capacity and entrapment efficiency by employing the ultrasonication approach. They demonstrated that hypericin-loaded SLNs enhanced cytotoxicity by 26% and boosted cell uptake by 30%, in contrast to Youssef et al.[124] This enhancement was most likely brought about by the preparation method used in this investigation and the smaller size of the SLNs (153 nm), which boosted cellular uptake facilitated by the SLN vehicle and enhanced the concentration of hypericin within the cells. Moreover, metallic nanoparticles (MNPs) are a different form of NP that have shown considerable promise as a drug delivery vehicle.[126] A multifaceted C60-IONP-PEG nanomaterial was developed by Shi et al.[127] by preparing and PEGylating iron oxide NPs (IONPs) and decorating them on the surface of fullerene (C60). Next, they coupled hematoporphyrin-monomethyl-ether (HMME) PS to the C60-IONP-PEG and evaluated it against melanoma cancer

https://doi.org/10.1021/acsomega.2c05852
ACS Omega 2022, 7, 45882−45909

employing B16−F10 cells *in vitro* and in a mouse tumor model *in vivo*. The results showed that, in comparison to free HMME, C60-IONP-PEG/HMME significantly improved the PDT effect.

5.2. Liposomes. Liposomes are unilamellar or multilamellar nanometer-size spherical structures that closely match the composition of cell membranes since it is made up of one or more phospholipid bilayers. These vesicles have evolved into effective drug delivery methods owing to liposome's capacity to incorporate lipophilic or hydrophilic drugs. They are the most well-known approach for the controlled distribution of drugs used in clinical practice because of their structural adaptability, capacity to integrate a wide range of hydrophobic and hydrophilic drugs, biocompatibility, and biodegradability. Liposomes may thus be utilized to integrate both hydrophilic and lipophilic PSs for cancer PDT.[128,129]

In a study, Po-Ting Wu et al.[130] developed PDT nano agents for breast cancer cells (4T1) using methylene-blue-Encapsulated Liposomes. Methylene blue (MB) is the commonly used dye and PDT agent that generates Reactive oxygen species (ROS) and causes apoptosis when exposed to light. The results demonstrated that MB-liposomes have excellent stability, quick intracellular absorption, and the capacity to produce more ROS *in vitro* than free MB. The *in vivo* studies investigated no toxicity of MB-liposomes.[130] MB-liposome has the potential to be a powerful PDT nano agent for cancer treatment, given the characteristics discovered. In another study, Bovis et al.[131] examined the effectiveness of the intravenously administered clinical PD, m-THPC (PS) encapsulated in liposomes in tumor-bearing and normal rats. The liposomes were produced successfully by utilizing 1,2-distearoyl-*sn*-glycero-3-phosphoethanolamine-N-[amino(polyethylene glycol)-2000] and a 1:9 combination of dipalmitoylphosphatidyl glycerol and dipalmitoylphosphatidylcholine with 8% and 2% (molar equivalent ratio). As compared to the commercial formulation, the findings demonstrated that m-THPC-loaded liposomes increased tumor specificity. It was ascribed to the increased blood plasma concentrations and tumor absorption, which was thought to lessen the harmful impact to healthy cells. Additionally, it was also said that employing liposomes might lessen the cost of therapy since less m-THPC was needed when it was encapsulated into liposomes. Furthermore, Nombona et al.[132] assessed the PDT effectiveness of gold (Au) NPs or 1,6-hexanedithiol tetra-substituted zinc phthalocyanine PS-loaded liposomes on MCF-7 cells (human breast cancer cell line). The investigations revealed that PS-loaded liposomes were much more efficient than Au NPs in the destruction of breast cancer cells. This demonstrates that liposomes have the potential to be an effective formulation for cancer PDT.

5.3. Micelles (Ms). A micelle is a group of amphoteric surfactant molecules that autonomously assemble in water to form a (typically) spherical vesicle.[133] Ms may thus be utilized to integrate lipophilic PSs for cancer (PDT). Since the Ms core is hydrophobic, hydrophobic PSs may be sequestered there until a drug delivery system releases them. In order to enhance the biopharmaceutical attributes of a clinically authorized PS chlorin e6, Kumari et al.[134] developed a polylactide-based block copolymeric Ms loaded with Ce6 for PDT. Human alveolar adenocarcinoma (A549) cells and Human uterine cervical cancer (HeLa) were used to investigate the treatment efficacy of Ce6 loaded Ms upon irradiation *in vitro* in both 2D and 3D cell culture systems in monolayers and 3D spheroids, respectively. The polylactide-based Ms (Ce6-mPEG−PLA) were stable and had an effective loading of Ce6 with an encapsulation efficiency of around 75% and measuring 189.6 ± 14.32 nm in size. In comparison to free Ce6 in aqueous conditions, the Ce6-loaded Ms produced $^1O_2$ at a greater concentration, and mediated PDT showed excellent cellular uptake in both A549 and HeLa cell lines, which ultimately led to increased cytotoxic effects. On the contrary, the Ce6-loaded micelles exhibited minimal cytotoxicity when it is not subjected to radiation. In the A549 spheroidal model, the Ce6-loaded Ms penetrated deeply into the spheroids, causing phototoxicity and cellular death. According to the findings of this investigation, the newly produced nanoformulation of Ce6 might be used in PDT as a successful therapeutic strategy for solid tumors. In another study, Kumari et al.[135] developed Ce6 conjugated mPEG−PLA glutathione sensitive Ms for PDT. In comparison to free Ce6, the developed Ms system (mPEG−PLA−S−S-Ce6) enhanced $^1O_2$ production by preventing Ce6 from aggregation. In comparison to free Ce6, the Ms system prevented Ce6 from clumping, improving $^1O_2$ production. The disulfide bond was present, which caused the Ms to break down and quickly release the Ce6 that was being studied in the *in vitro* investigation.

The Ce6Ms released drugs more quickly in the presence of glutathione monoester pretreated 4T1 and A549 cells than in the absence of pretreatment. A549 and 4 T1 cells that had received 10 mM glutathione monoester before treatment for *in vitro* phototoxicity of Ms showed increased toxicity in comparison to untreated cells. As expected, 0.1 mM of buthionine sulfoximine pretreated 4T1 and A549 cells displaying decreased phototoxicity resulted in lesser drug release from Ce6 micelles. Furthermore, in contrast to free Ce6, A549 3D spheroids treated with Ce6Ms had considerable growth suppression, increased phototoxicity, and improved cellular apoptosis. The developed Ms system might be a promising formulation for cancer PDT.

5.4. Dendrimers. High-branched polymers known as dendrimers have a relatively narrow diameter range, often between 1 and 10 nm. Their key benefit is the capacity to foresee, manage, and regulate the number and size of functional groups that can be modified. This increases the predictability of drug incorporation quantity. As a result, it makes pharmacokinetics more repeatable; this enables dendrimers to a potentially useful drug delivery approach for PDT.[136] In dendrimers, PS may be conjugated in three different ways: first, PS is confined inside the gaps of a dendrimer's structure.; second, the dendrimer and PS are bonded covalently; third, PS serves as a frame for the development of a dendrimer.[137] Narsireddy et al.[138] attached nitrile tri acetic acid (NTA) group and 5,10,15,20-tetrakis(4-hydroxyphenyl)-21H,23H-porphine (PS) in a dendrimer, which is the second method for conjugating PS with a dendrimer. They linked a peptide that was unique to human epidermal growth factor 2 to the NTA group on the dendrimer so that it could work as a tumor-targeting peptide for customized *in vitro* and *in vivo* PDT. This allowed the peptide to operate as a tumor-targeting peptide. They discovered that PS-dendrimers dramatically reduced tumors in tumor-bearing mice and were effective in PDT-mediated cell killing experiments in SKOV-3 cells positive for the human epidermal growth factor receptor 2 (HER2). Similar to this, Rodriguez et al.[139] observed that the attachment of 5-aminolevulinic acid (ALA) dendrimers increases porphyrin production. Conse-

https://doi.org/10.1021/acsomega.2c05852
ACS Omega 2022, 7, 45882−45909

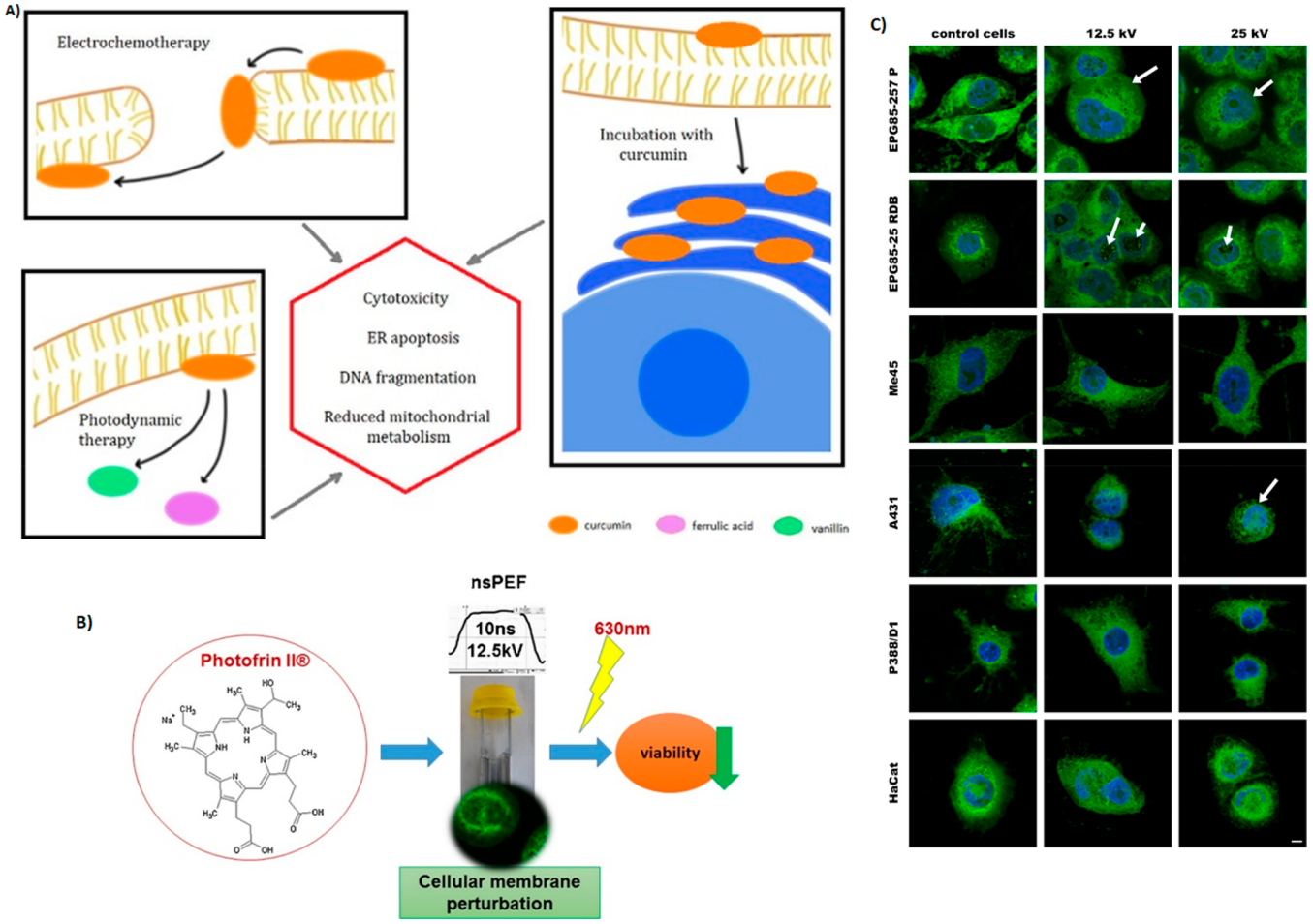

Figure 4. (A) Mechanisms of curcumin-based photodynamic therapy and its effects in combination with electroporation. Adapted with permission from ref 165. Copyright 2021 Elsevier. (B) Nanosecond pulsed electric fields (nsPEFs) impact and enhanced Photofrin II delivery in photodynamic reaction in cancer and normal cells; (C) effect of nanosecond pulsed electric field on human cancer, normal cell lines, and murine macrophages visualized by DHCC, membrane marker, and DAPI, nuclei staining, CLSM study. Reprinted with permission from ref 167. Copyright 2015 Elsevier.

quently, they tested the capacity of ALA dendrimers with 9 and 6 ALA residues to photosensitize cancer cells. They discovered that dendrimers at low doses produced more porphyrin than ALA did. However, the production of porphyrins from both substances was comparable at high doses. Additionally, ALA dendrimers applied topically did not diffuse to adjacent skin areas, suggesting a possible role of ALA macromolecules in models of superficial cancer. In another study, Nishiyama et al.[140] demonstrated that porphyrin-loaded dendrimers with ionic peripheral groups (DPs) electrostatically interacted with oppositely charged block copolymers to spontaneously produce polyion complex (PIC) micelles. Furthermore, a distinctive DP structure that resulted in a excellent *in vitro* photocytotoxicity prevented the dye molecule from self-quenching within the micellar core. The dendrimer also shown promise in the therapy of choroidal neovascularization (CNV) in rats without exhibiting any negative side effects.

5.5. Hydrogels. Hydrogels are 3D mesh structures built of polymeric materials that are able to absorb water.[141] These methods are often used in the pharmaceutical industry for the sustained release of hydrophilic drugs,[142] owing to the simplicity with which the drug may be distributed throughout the matrix. In addition to this, they are biocompatible and display physical properties that are analogous to those of real tissues.[143] Furthermore, hydrogels may be employed for the application administration of hydrophilic PSs for PDT, such as FA-PEG-PheoA, mono-L-aspartyl chlorin, aluminum(III) phthalocyanine chloride tetrasulfonic acid (Al-4), and PAD-S31, among others.[144−146] For instance, Saboktakin et al. designed biodegradable NP hydrogels packed with PS temoporfin (mTHPP) for the purpose of cancer-PDT.[147] Lyophilized conjugates of chitosan standards kept at −80 °C were used to produce chitosan hydrogels. The 0.2% chitosan hydrogel with 0.04% mTHPP dispersion in deionized water with agitation produced the mTHPP-loaded NPs. After around 3 h, the specimen was poured into a liquid nitrogen bath that had been chilled to 77 K. The sublimation method was used to dry the produced frozen droplets. The NP analysis revealed that mTHPP possesses intriguing properties that stayed constant throughout the course of the study. They concluded that these NPs are acceptable as PDT carriers.

5.6. Liquid Crystalline Systems. Lyotropic liquid crystal systems contain characteristics of both liquids and solids due to the fact that they are fluids and have a highly ordered structure. These are produced by surfactants, more specifically by the hydrates or solvates of the surfactant molecules.[148] They are succinctly described as hexagonal, lamellar, or cubic mesophases, and researchers have studied them in great

https://doi.org/10.1021/acsomega.2c05852
ACS Omega 2022, 7, 45882−45909

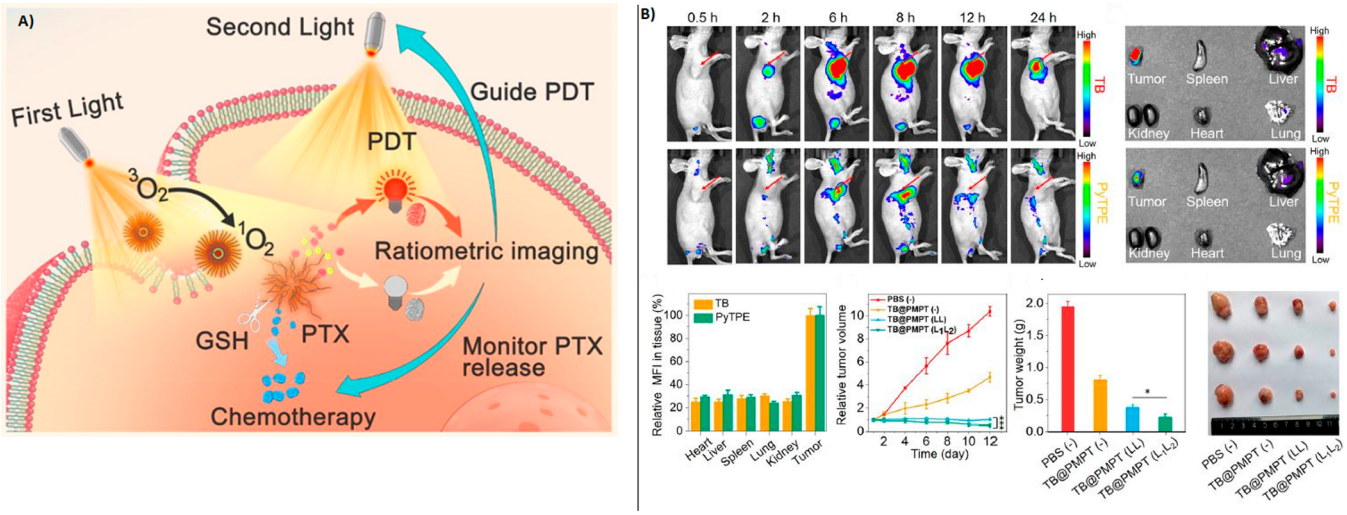

Figure 5. (A) Self-guiding polymeric prodrug micelles with two aggregation-induced emission photosensitizers for enhanced chemo-photodynamic therapy. (B) *In vivo* imaging and combinational therapy efficacy of HeLa tumor-bearing mice after the intravenous injection of TB@PMPT micelles at different time. Adapted with permission from ref 171. Copyright 2021, American Chemical Society.

detail[149] because of their bioadhesive, biodegradability, and nontoxicity qualities, which also contribute to their potential in PS drug administration.[150] Despite their low viscosities and negligible oil solubilization, there is a rather low interfacial tension between lamellar liquid crystals and oil.[151] They are generated by solvent layers sandwiched between parallel layers of surfactant bilayers.[148] Polarized light microscopy reveals that hexagonal mesophases have the appearance of long cylinders stacked in a 2D array.[142] Finally, the cubic mesophases offer more challenging structures to visualize, which typically exhibit a cubic symmetry. Moreover, several systems also showed rhombohedral and tetragonal phases.[152] A PS that is used in the PDT treatment of skin cancer loaded with a chlorine derivative was recently the subject of research into NPs of lyotropic liquid crystals. They blended poloxamer, oleic acid, monoolein, and water at a temperature of 45 °C to produce the hexagonal phase nanodispersion and observed particle size of 161 ± 4 nm with PDI 0.175 ± 0.027. After the introduction of the drug, the hexagonal liquid crystalline phase exhibited no change in its stability. The penetration investigations demonstrated that the PS packed in the hexagonal system had much greater absorption than the PS packed in PEG served as control. They revealed that the PS diffused more deeply throughout the epidermal layers in the nanodispersion of hexagonal liquid crystalline phase than in control. Finally, they came to the conclusion that the nanodispersion demonstrated promise for the transport of the PS into the skin, which is essential for effective topical PDT treatment.[153,154]

5.7. Cyclodextrin. Natural cyclodextrins (CDs) are cyclic oligosaccharides made possible by the activity of the enzyme cyclodextrin-α-glycosyl transferase (CGTase). They are made up of 6, 7, or 8 glucose units joined together by α-1,4 bonds that are designated as α-, β-, and γ-CD, respectively.[155] In order to improve the architectures of natural CDs and render them appropriate for use in applications involving drug delivery, a number of modified CDs have been generated. Due to their cone-like structure, an interior nonpolar cavity forms, which enables the development of inclusion complexes of lipophilic drugs.[156] In a study, Conte et al.[157] developed biodegradable nano assemblies based on zinc-phthalocyanine (ZnPc) and heptakis (2-oligo(ethylene oxide)-6-hexadecylthio-)-β-CD (SC16OH) and to combat phthalocyanine low water solubility. In HeLa cancer cells, they discovered potential PDT anticancer effects, indicating a potential Zn-Pc delivery method. In a similar study, Lourenço et al.[158] developed phthalocyanines functionalized with α-, β-, and γ-CDs. They demonstrated that both Pc-α-CD and Pc-γ-CD were discovered to have promising photoactivity against UM-UC-3 human bladder cancer cells.

6. APPLICATIONS OF PHOTOSENSITIZERS

PDT is an established alternative method for treating cancer. Strong specificity in tumor destruction and the feasibility of combining with other therapeutic agents are the major advantages associated with PDT.[159] A PS, which is administered in PDT, has the ability to be activated by the exposure of light of a specific wavelength and accumulate in the tumor leading to the formation of ROS in the presence of oxygen, resulting in a local inflammatory reaction.[12,160,161]

6.1. PDT−Electroporation (PDT−EP). Electroporation (EP) is a technique of reversible or irreversible breaking of cell membranes induced by electrical pulses. Electroporation provides an exterior electric field that barely exceeds the capacitance of the cell membrane and causes transient breakage of the cellular membrane, which facilitates the delivery of different compounds into cell.[162,163] The permeability of the cell membrane is facilitated by the formation of water pores, which enables the drug to enter the cytoplasm to exhibit its anticancer effect.[164]

Czapor-irabek et al. developed a combination therapy of curcumin-aided PDT with electroporation (Figure 4A). An increased cellular permeability was observed with increasing the electric field (600 and 800 V/cm electric fields) was observed with malignant (A375) and normal (HGF) cell lines.[165] Satkauskas et al. demonstrated the application of electric impulses on the efficacy of PDT (Figure 4B). Using Aluminum phthalocyanine tetra sulfonate (AlPcS4) belongs to phthalocyanines and chlorine e6 as PSs during the combination of electroporation and PDT caused an increase in the accumulation of PSs in the tumor, leading to cytotoxicity. The experiments were carried out *in vitro* in

https://doi.org/10.1021/acsomega.2c05852
ACS Omega 2022, 7, 45882−45909

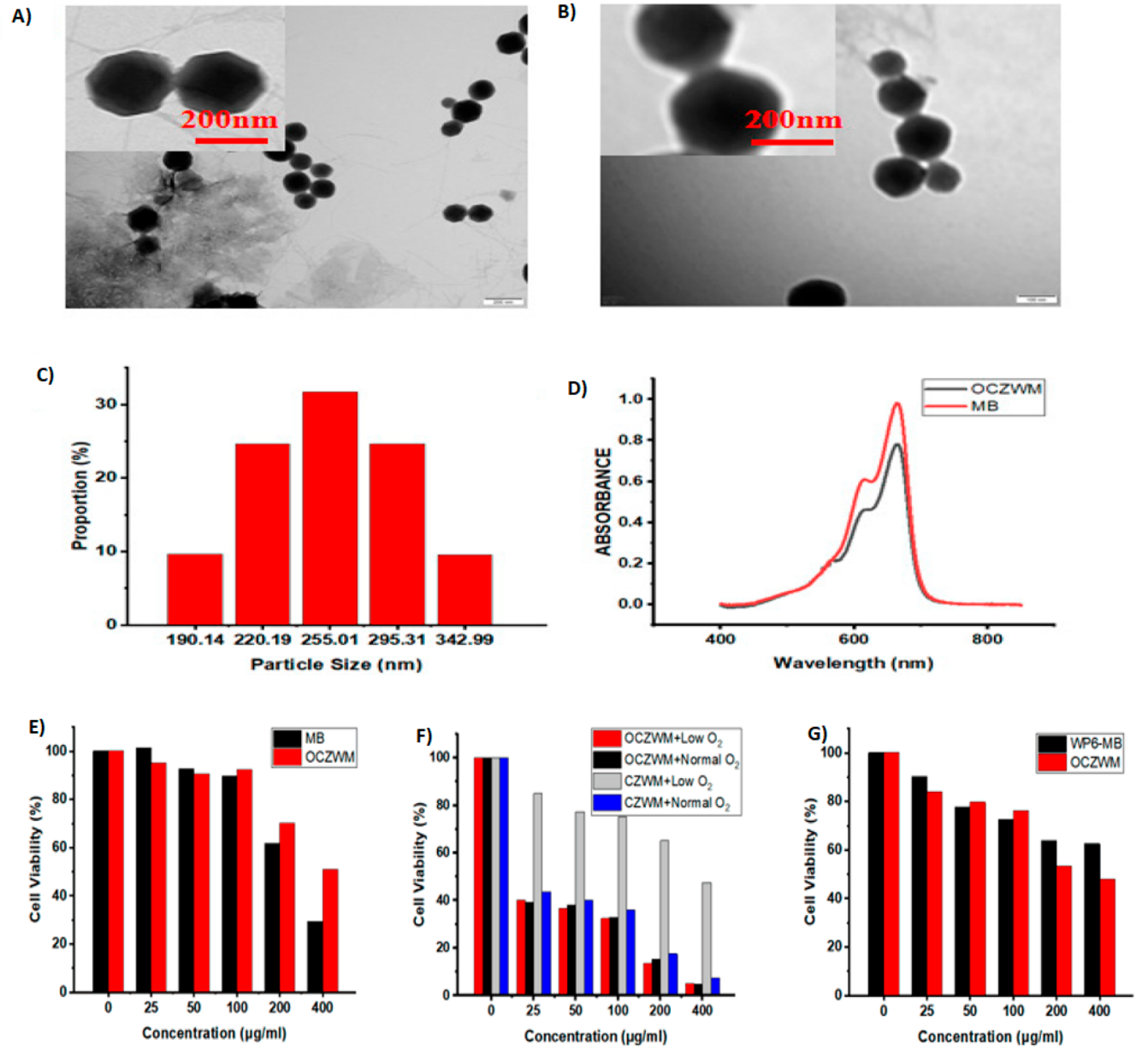

Figure 6. Supramolecular photosensitizer system based on nano-Cu/ZIF-8 capped with water-soluble pillar arene and methylene blue host−guest complexations. TEM images of (A) Cu/ZIF-8@ZIF-8 and (B) Cu/ZIF-8@ZIF-8@WP6−MB; (C) DLS data of Cu/ZIF-8@ZIF-8@WP6−MB. (D) UV−vis spectra of Cu/ZIF-8@ZIF-8@WP6−MB and MB aqueous solution at room temperature. Relative cell viability of (E) HL7702 cells and (F) HepG2 cells after treatment with OCZWM, Cu/ZIF-8@ZIF-8@WP6−MB at different concentrations. (G) Relative cell viability of HepG2 cells after treatment with OCZWM, WP6−MB at different concentrations. Adapted with permission from ref 177. Copyright 2021 MDPI.

murine hepatoma cell line MH22A (Figure 4C).[166] A study by Kulbacka et al. used PS Photofrin II for the combination of PDT and nanosecond pulsed electroporation. The results showed that the delivery of PS was improved by the electroporation and exhibited effective tumor photoactivation at low doses with a shorter incubation period.[167] We et al. studied the effect of EP-PDT on the cellular effects of drug-resistant (MCF-7/DOX) and wild-type breast cancer cell line (MCF-7/WT) by exposing the cells to PDT using photofrin and the cyanine IR-775. Due to the enhanced cellular permeability effect of electroporation and photodynamic activity, PSs exhibited a severe cytotoxic response with both cell lines.[168] A study by Todorovic et al. utilized electroporation to facilitate the transport of chemotherapeutic agents, bleomycin, and cisplatin using Murine rectum carcinoma cells CMT-93. When compared to the exposure of drugs alone, cisplatin and bleomycin resulted in 2.8- and 500-times greater increases in sensitivity, respectively, with the electroporation.[169]

6.2. Chemo-photodynamic Therapy. The PDT has the limitations of hypoxia in tumor tissues and limited light penetration. PDT must therefore be used in conjunction with other therapeutic modalities such as CDT and chemotherapy.[170] In order to improve the combination of chemo-photodynamic therapy, Yi et al. developed a dual-stage light irradiation technique by preparing a polymeric micelle system consisting of two aggregation-induced emission (AIE) photosensitizers in which one AIE photosensitizer and chemotherapeutic drug paclitaxel were conjugated to the polymer, and the other AIE photosensitizer was loaded inside the

https://doi.org/10.1021/acsomega.2c05852
ACS Omega 2022, 7, 45882−45909

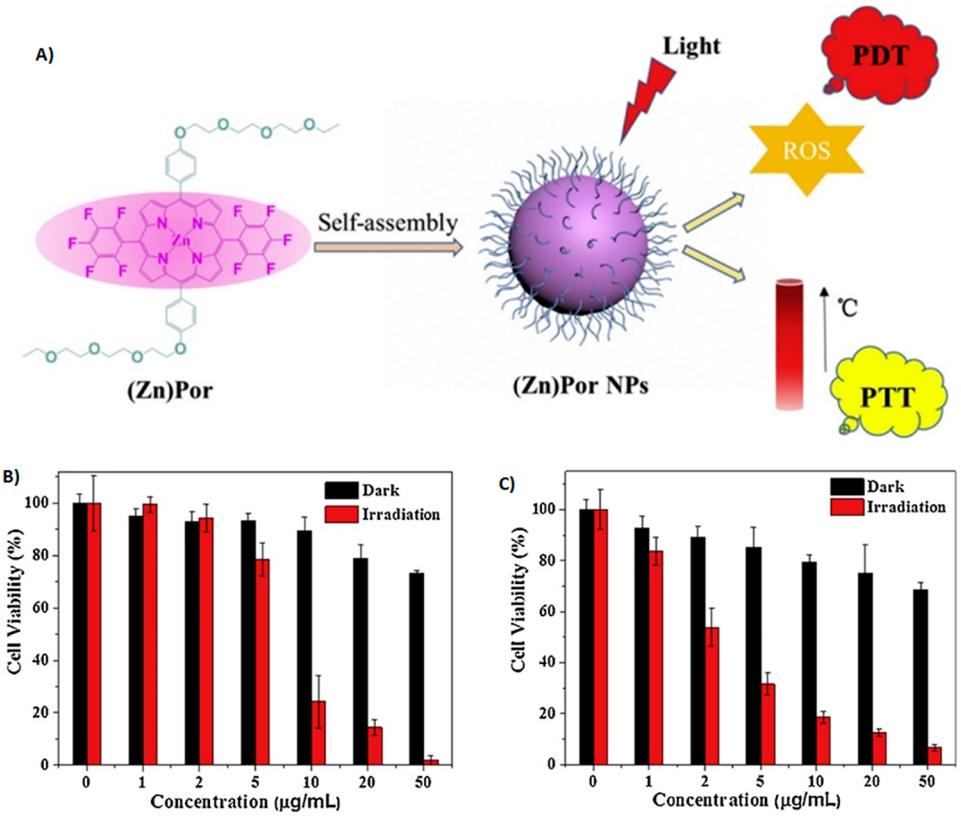

Figure 7. (A) Organic small molecular nanoparticles based on self-assembly of amphiphilic fluoroporphyrins for photodynamic and photothermal synergistic cancer therapy; concentration dependence of the cytotoxicity of (B) Por NPs and (C) ZnPor NPs against HeLa cells. Adapted with permission from ref 181. Copyright 2019 Elsevier.

hydrophobic core formed by the micelles (TB@PMPT) (Figure 5A). After reaching the tumor, the micelles caused lipid peroxidation leading to the increased permeability of the cell membrane resulting in enhanced cellular uptake of micelles.[171] TB@PMPT micelles exhibited effective inhibition of tumor cells in HeLa tumor-bearing mice due to the combination of enhanced chemotherapy and PDT (Figure 5B). A stimuli-responsive nanoparticle system was prepared by Luo et al. in which doxorubicin was conjugated with poly[*N*-(2-hydroxypropyl) methacrylamide] (poly HPMA) copolymer with disulfide bonds, and the Chlorin e6 (Ce6) was loaded. The PDT efficacy was evaluated on 4T1 murine breast cancer cells. In the physiological state, the Ce6 nanoparticle system was able to hold both chemotherapeutic drug (Doxorubicin) and photosensitizer (Ce6) and release them via intracellular cleavage of disulfide bonds in response to glutathione (GSH) present in the tumor.[172]

In one study, a homodimer was prepared by conjugating two cabazitaxel (CTX) with a single thioether bond (CTX-S-CTX). Pyropheophorbide A (PPa) allowed CTX-S-CTX to quickly assemble into homogeneous NPs in water. The phospholipid-polymer conjugate 1,2-distearoyl-*sn*-glycero-3-phosphoethanolamine-N-[amino(polyethylene glycol)-2000] (DSPE-PEG2K) was added to the NPs to prolong the blood circulation duration of NPs. The activation of CTX-S-CTX was significantly aided by the synergistic interaction of the ROS produced by PPa during laser irradiation and the endogenous ROS present inside the cell.[173] The drug delivery system composed of poly(ethylenimine) (PEI) derivatized fullerene (C60-PEI-DOX) loaded with doxorubicin, whose release is highly dependent on the environmental pH, was found to have high tumor specificity and synergistic therapeutic activity. The Dox was released into the acidic environment of the tumor. The combination therapy significantly reduced the development of tumors in mouse melanoma B16−F10 cells and *in vivo* models with few adverse effects.[174] A study by Zhao et al. utilized electrostatic interaction for the loading of anionic photosensitizer ce6 and chemotherapeutic drug Doxorubicin into a cationic polymer to achieve the combined chemotherapy and PDT. A higher loading capacity was observed for ce6 than the Dox. Due to the limited interaction with the polymer in acidic environment, Doxorubicin exhibited pH-dependent release and effective *in vitro* suppression of 4T1 breast cancer cells was observed by inducing the ROS generation.[175] Meng et al. demonstrated a host−guest approach for dual chemo-photodynamic therapy. In this study, the amphiphilic molecule formed from water-soluble pillar arene (WP5) acts as a host, and quaternary ammonium derivative integrated with boron-dipyrromethene (BODIPY) acts as both guest and photosensitizer developed supramolecular vesicles to load the doxorubicin. The system was able to encapsulate Dox effectively, and the drug was released into acidic conditions.[176]

6.3. Photodynamic Therapy−Chemodynamic Therapy (PDT−CDT). Reactive oxygen species (ROS) are generated by PSs under light irradiation. The formed ROS has the ability to oxidize the cellular components, leading to cell apoptosis. Hypoxia and increased glutathione content in the tumor can limit the therapeutic efficacy of PDT. In order to achieve a better therapeutic effect, PDT can be combined with CDT, which works by generating hydroxyl radicals in cancer cells. A study by Capped et al. utilized metal−organic

https://doi.org/10.1021/acsomega.2c05852
ACS Omega 2022, 7, 45882−45909

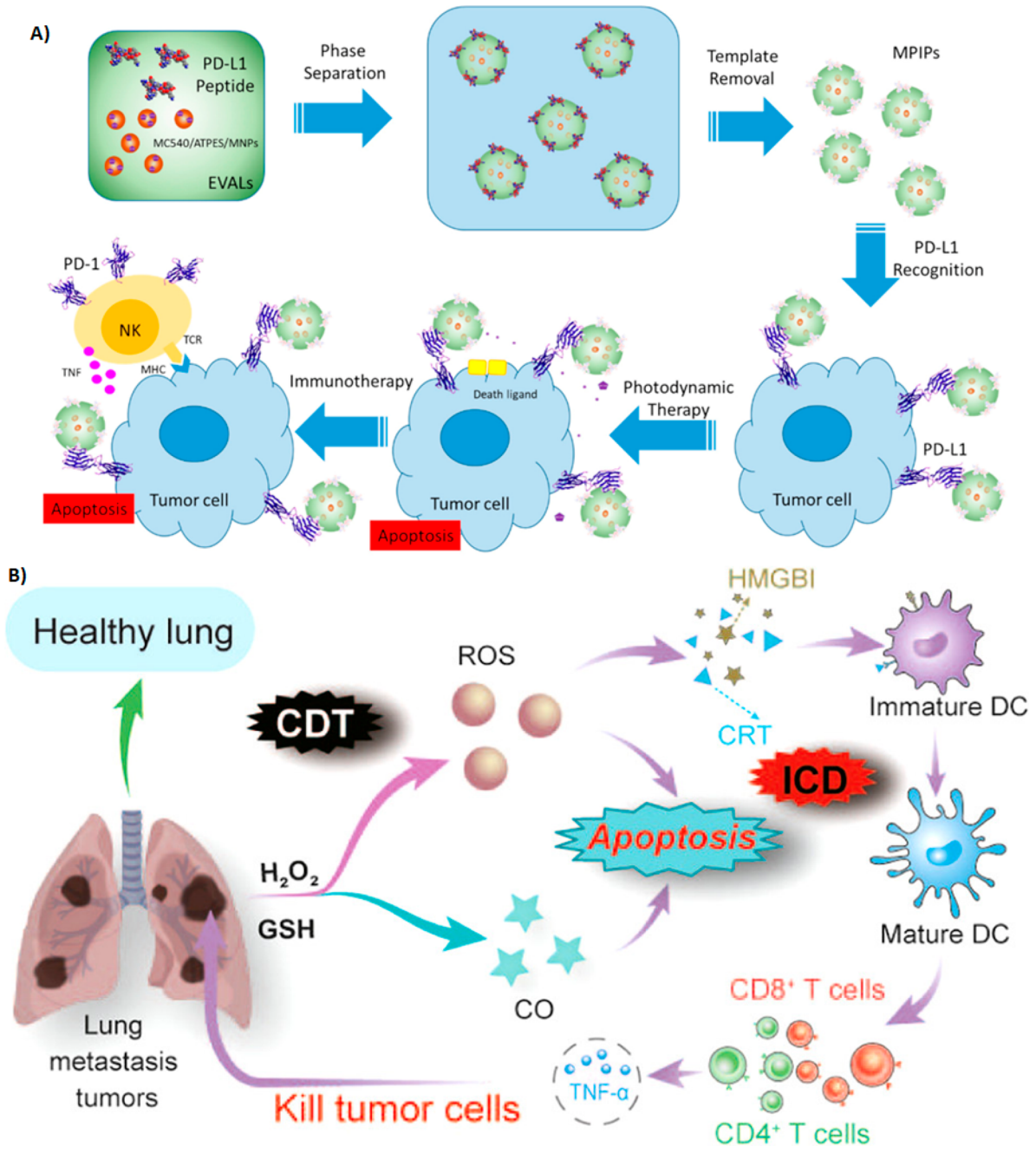

Figure 8. (A) Preparation and administration of multifunctional magnetic PD-L1 peptide-imprinted composite nanoparticles. Adapted with permission from ref 186. Copyright 2021 MDPI. (B) Tumor microenvironment-activated nanoparticles loaded with an iron−carbonyl complex for chemodynamic immunotherapy of lung metastasis of melanoma *in vivo*. Reprinted with permission from ref 187. Copyright 2021 American Chemical Society.

frameworks as carriers. In this study, the chemodynamic therapy was achieved by formulating Cu-loaded Zeolitic imidazolate frameworks-8 (ZIF-8) as nanocarriers to facilitate the adsorption of O_2 and assist in Fenton reaction with $Cu^{2+,}$ and the PDT was achieved by capping the same nanocarriers with photosensitizers through host−guest complexation of pillar arene (W6)−methylene blue (MB). The results showed the size of 190−290 nm using TEM analysis (Figure 6A,B), and TEM images demonstrated that the obtaining Cu/ZIF-8@ZIF-8@WP6−MB had an obvious fuzzy edge compared with that of the obtaining Cu/ZIF-8@ZIF-8, which can be ascribed to the assembly of WP6−MB (Figure 6C). The system exhibited good O_2 load capacity and exhibited better cytotoxicity with hepatoma cancer cells (HL7702 cells).[177] As shown in Figure 6E, without light irradiation, O_2−Cu/ZIF-8@ZIF-8@WP6−MB (OCZWM) showed reduced dark toxicity compared to free MB with HL7702 cells. As shown in Figure 6F, under the condition of normal O_2, the inhibition rates of OCZWM and Cu/ZIF-8@ZIF-8@WP6−MB on HepG2 cells were, in practical terms, the same. Moreover, it was found that, without light irradiation, the inhibition rates of OCZWM were higher than that of WP6−MB due to the CDT (Figure 6G).

https://doi.org/10.1021/acsomega.2c05852
ACS Omega 2022, 7, 45882−45909

In one study, photosensitizer porphyrin was conjugated with the chemotherapeutic agent ferrocene. Under laser irradiation, the system was able to convert oxygen into $^1O_2$ to exhibit PDT activity, and the CDT activity was achieved by the Fenton-like reaction.[178]

6.4. Photodynamic−Photothermal Therapy (PDT−PTT). With the combined effect of PDT, which causes cellular toxicity by oxidative stress,[160] and PTT, which works by inducing an increase in temperature in the local tissue environment, the limitations of PDT can be reduced.[179] In photothermal therapy, the photothermal agent can convert the light energy into thermal energy and causes the thermal destruction of tumors.[180] In a study, porphyrin-based self-assembling NPs were prepared by PSs incorporated with hydrophilic polyethylene glycol to impart the hydrophilicity and pentafluoro benzene moieties to enhance the stability and protein−ligand interactions (Figure 7A). The NPs exhibited particle size of 100 nm with better water dispersing ability, enabling the NPs to enter the lysosomes of cancer cells, leading to enhanced phototoxicity (Figure 7B, C).[181]

To overcome the hypoxic conditions of the tumor, which limits the catalytic activity of photodynamic therapeutic effect, Yang et al. developed a nanozyme approach by preparing platinum(Pt)-carbon incorporated nanozyme by immobilizing an ultrasmall platinum nanozyme inside a metal−organic framework ZIF-8 derived mesoporous carbon nanozyme. The photodynamic efficiency was improved by the catalytic activity of Pt-carbon nanozyme on the overproduced H_2O_2 caused the generation of oxygen inside the tumor (Figure 8).[182]

6.5. PDT−Immunotherapy. Immunotherapy (IMT) of cancer aims to use the immune system's capacity to vigorously and precisely attack targets based on the concept of antigen-specificity to combat and destroy tumors. PDT has been demonstrated to promote the release of antigens and immunogenic elements like damage-associated molecular patterns (DAMP) from dying tumor cells.[183,184,52] These DAMPs stimulate the dendritic cells and the growth of cytotoxic T lymphocytes (CD4+/CD8+ T cells), which in turn activates the host immune system against tumor cells.[185] Due to its immunologic effects, PDT is a favorable option for immunotherapy combinations in the treatment of cancer.

In one study, Lee et al. combined photodynamic and immunotherapy by immobilizing merocyanine as a PS onto the magnetic NPs. The tumor targeting of NPs was achieved by imprinting a single peptide sequence from programmed death-ligand one protein (PD-L1) onto the poly(ethylene-*co*-vinyl alcohol) (Figure 8A). The molecularly imprinted polymer (MIP) NPs also improved the effectiveness of natural killer (NK-92) cells by inhibiting the PD-L1 protein on human hepatoma (HepG2) cells. The NK-92 cells also assisted HepG2 cell death by promoting caspase 8 expression.[186] A study by Zhai et al. developed glutathione (GSH), and hydrogen peroxide activated nano formulation loaded with an iron−carbonyl complex, which can release CO, which causes mitochondrial damage and oxidative stress by the Fenton reaction (Figure 8B). The nanosystem caused a series of intracellular pathways that worked together to inhibit melanoma lung metastasis.[187] Additional cases where PS has been loaded in NPs that may actively or passively target cancer cells are represented in Table 5.

7. CHALLENGES

Amidst the benefits, PDT still has to tackle several challenges. The conventional organic PSs, such as phthalocyanine, chlorin, and porphyrin derivatives, have very poor water solubility and limited selectivity, difficult to synthesize and purify, and lack a cancer target domain. To boost the output of their triplets, PSs often cooperate with transition metals in the middle of their frameworks. Conversely, such transition metal complexes usually suffer from severe cytotoxic effects in the absence of light irradiation and are exorbitant in cost and complexity to synthesize.[188] However, inorganic nanoparticle-based PSs are difficult to employ in biological applications due to stimulation by a very short wavelength light source and nonbiodegradability, which causes retention in the bodily organs.[189] The wavelength of light determines how deeply it penetrates biological tissues, and these depths are often rather shallow. For instance, in bladder PDT, the depth of penetration is just 4.0 (0.1) mm (633 nm).[190] Additionally, the wavelength of the light, as well as the characteristics of the various tissue types in terms of reflection, scattering, transmission, and absorption, have a role in determining the depth of penetration. Near-infrared (NIR) light generally offers superior biosafety and a significantly longer tissue penetration depth than visible light. On the other hand, due to the high production energy needed for PDT, long wavelength light (>850 nm) has poor singlet $^1O_2$ quantum yields.[191] As a result, the light in PDT has a therapeutic window between 650 and 900 nm. ROS produced generally have short lifetimes (40 ns) and small diffusion radii (approximately 10 nm).[192,193] The PDT process consumes a lot of oxygen, but the O_2 content in solid tumors is very low, which is known as hypoxia. PDT necessitates that patients stay in the dark for an extended period of time after therapy and/or be treated with a high-powered laser. A lot of work has been put into recent years to get around PDT's limitations. This research has resulted in novel techniques to circumvent such disadvantages such as heavy atom-containing PSs with poor water solubility and aggregation-caused quenching being possibly replaced with heavy atom-free PSs with aggregation-induced emission, respectively. The poor penetration of light into PSs with short wavelength absorption may be enhanced by two-photon excitation, a FRET effect, and with red/NIR light irradiation. On the other hand, white light irradiation and ultralow/low light power light density have demonstrated promising efficacy for PDT therapy. Particularly, the molecular design of PSs toward "all-in-one", "one-for-all", and imaging-guided PDT for phototheranostics in particular illustrates a promising strategy in clinical therapy. Other tactics have been mentioned, including the introduction of targeted groups, decreased O_2 reliance, and effective triplet excited state generation, etc. However, the production of these novel PSs has not been well systematized, and it is crucial to develop organic-based photodynamic agents for PDT.

Although PDT has the potential to be used as a stand-alone method for the therapy of malignancies at various stages, currently, only flat and superficial lesions are treated with it. The critical challenge is that PDT cannot effectively treat deep-seated or solid tumors. Furthermore, whole-body irradiation is not feasible; at least with the existing technology, it cannot be utilized to treat chronic disseminated illness. It is challenging for healthcare professionals to strategize and customize the course of treatment partly because of the limitations in the attributes of the PSs that are presently accessible and in part

https://doi.org/10.1021/acsomega.2c05852
ACS Omega 2022, 7, 45882−45909

Table 5. PDT-Based Nanocomposite Systems Used for Cancer Therapy

nanocomposites (NCs)	PS	laser parameters	size (nm)	zeta potential (mV)	cancer cell line	application	ref
porphyzomes (porphyrin lipid nanovesicles)	Photofrin	PTT (135 J/cm^2 at 100 mW/cm^2) PDT (671 nm)			A549	lung cancer (PDT, PTT)	252
NAB NPs aza-boron-dipyrromethene (aza-BODIPY), dimethyl-aminophenyl units	aza-boron-dipyrromethene	PDD (20 mW/cm^2) PTT (20 mW/cm^2)	30 nm		HeLa cells	Henrietta's cancer, (PDT, PTT)	253
PDA NPs PDA-C6 NPs (polydopamine NPs)	Chlorin e6 (Ce6)	PDT-665 nm, Ce6 at (250 mW/cm^2) PTT- input energy of 28.3 J	141.3 ± 4.3 142.4 ± 4.1	−48.7 ± 1.3− 45.45 ± 1.4	T24 cells	bladder cancer (PDT, PTT)	49
Pt-ICG@PDA Pt- platinum PDA-polydopamine folate labeled liposomes	indocyanine green (ICG)	808 nm	100 nm		MCF-7 cells	breast cancer (PDT, PTT)	254
ZnPc 1,8,15,22-tera-(3-(6-hydroxyl) hexyloxy) phthalocyanine zinc(II)	pthalocyanin zinc II	650 nm (0.7 W/cm^2)	70 nm		HeLa cells L929 U14	Henrietta's cancer, (PDT, PTT)	255
Bi/MnPcE$_4$ i-bismuth	phthalocyanine manganese	808 nm (1.0 W/cm^2)	120 nm		HeLa cells	Henrietta's cancer, (PDT, PTT)	256
DPP NPs DPP+ NPs DPP2+NPs diketopyrrolopyrrole-based photosensitizer	DPP	635 nm (0.3 W/cm^2)	200 240 260	 35.5	HeLa cells MCF-7 cells L929 cells	Henrietta's cancer, breast cancer (PDT, PTT)	257
DPP-TPA NPs DPP-diketopyrrolopyrrole TPA -triphenylamine	DPP-diketopyrrolopyrrole	660 nm (1.0 W/cm^2)	∼76 nm		HeLa cells *in vivo* HCT-116 cells	Henrietta's cancer, (PDT, PTT)	258
PLL-ICG/DPEG NPs PLL- polylysine ICG- indocyanine green DPEG-polyethylene glycol	ICG-indocyanine green	808 nm (1.5 W/cm^2)	262 nm	−12	HeLa cells	Henrietta's cancer, (PDT, PTT)	259
CAM NPs chlorin Ce6, axitinib, dextro-1-methyl tryptophan, human serum albumin	chlorin e6		170 nm	∼10.5	B16F10 melano-ma cells	photodynamic immu-notherapy	260
phthalocyanines, anti-PD-L1 antibody	phthalocyanines (ZnPcs)	λ > 610 nm			B16−F10	skin cancer (PD-IMT)	261
mesoporous-silica-coated β-NaYF4: 20%Yb, 2%Er upconversion NPs (UCMSs)	merocyanine 540	980 nm	100		CT26 cells	photodynamic immu-notherapy (colon cancer)	262
Ce6/MLT@SAB boehmite nanorod Ce6-Chlorin e6MLT-melittin B-aluminum hydride	Ce6-Chlorin e6	660 nm (0.1 W/cm^2)	184.2 ± 5.4	−17.6 ± 1.5 mV	4T1 cells	breast cancer (PD-IMT)	263
P 127, (NIR-II) window type-I photosensitizers	PTS PTSe PTTe	NIRII laser 1064 nm	45.5 ± 16.8 38.3 ± 10.6 91.5 ± 13.2	−8.45, −14.70, −13.27	4T1	breast cancer (PDT, PTT)	264
NLG919/IR780 micelles NLG919- indoleamine 2,3-dioxygenase (IDO) inhibitor	IR780	808 nm (1.0 mW/cm^2)	43 ± 3.2		MCF-7 cells	breast cancer (PD-IMT)	265
verteporfin and doxorubicin(DOX) conjugated cathepsin B-cleavable peptide linker of FRRG (Phe-Arg-ArgGly) (VPF-FRRG-DOX)	verteporfin	671 nm, 40 mW	87.12 ± 3.95 nm		CT26 and H9C2	colon cancer (PDT-IMT)	266
pH-responsive DEX-HAase NPs DEX-dextran, HAaase-hyalur-onidase	Chlorin e6	660 nm (5 mW/cm^2)	≈97 nm		4T1	breast cancer (PD-IMT)	267
PEGylated HMCP NCs HMCP-hollow structured manganese carbonate (MnCO3) nanocubes	Chlorin e6	660 nm (0.1 W/cm^2)	193.0 ± 27.6 nm		HeLa cells	Henrietta's cancer (PDT−CDT)	268
lactate oxidase (LOx) and catalase (CAT) integrated Fe3O4 nanoparticle/indocyanine green (ICG) coloaded hybrid nano-gels	indocyanine green (ICG)	808 nm (0.25 W)	72.91	−22.90	not defined	PDT−CDT	269
cancer cell memebrane coated copper/manganese silicate nano-spheres (mCMSNs) a	copper silicate existing in the CMSNs acted as efficient photo-sensitizer	635 nm (0.6 W/cm^2)	∼25 nm	∼10 mV	MCF-7 NHDF	breast cancer (PDT−CDT)	270
copper/manganese silicate nanosphere (CMSN)- coated lantha-nide-doped NPs (LDNPs) (LDNPs@CMSNs)	upon NIR light excitation, the CMSNs act as photosensitizers	980 nm (0.5 W/cm^2)	45 nm		HeLa cells	Henrietta's cancer (PDT−CDT)	271

https://doi.org/10.1021/acsomega.2c05852
ACS Omega 2022, 7, 45882−45909

Table 5. continued

nanocomposites (NCs)	PS	laser parameters	size (nm)	zeta potential (mV)	cancer cell line	application	ref
tumor microenvironment (TME)-responsive (TCPP) coordination NPs (FT@HA NPs)	Fe(III)−porphyrin Fe(III)−porphyrin	635 (100 mW/cm^2)	160 ± 33 nm in length 90 ± 12 nm in width	−14.56 mV	4T1 cells and NIH-3T3 cells	breast cancer (PDT−CDT)	272
BSO-FeS_2 NPs BSO- L-buthionine-sulfoximine		808 nm	7.27 ± 1.43 nm		4T1 cell line	breast cancer (PDT−CDT)	273

because of the insufficient information about the light dose to be supplied to the tumor without adversely impacting the surrounding normal tissue. Being a localized therapy, PDT essentially needs the right amount of light to reach every part of the tumor for it to be successful in curing the tumor. Clinical PDT often fails to prevent tumor recurrence and manage residual tumor development despite sophisticated Monte Carlo calculations because the lesions are not adequately illuminated.[194] In certain additional circumstances, overillumination might result in excessive toxicity to nearby normal tissue, causing an undesirable reaction once again. In contrast to radiation treatment, where the biological reaction is well connected with the energy absorbed per mass of tissue, PDT light dosage has no generally recognized definition. This is a rather hard subject, owing to the intrinsic intricacy of the PDT process as well as a lack of acceptable clinical measurement methodologies. However, a common but primitive approach includes measuring the light fluence, the quantity of PS, and oxygen, which are then used to determine the $^1O_2$ production (explicit dosimetry).[195] The light distribution is governed by the light source parameters and the optical attributes of the tissue. However, owing to the intricacy of tissue architecture and the dearth of research on optical tissue characteristics, measuring and interpreting light fluence seems to be difficult. Despite the fact that optical spectroscopy may be used to quantify the distribution of O_2 and PS, the real distribution may differ owing to O_2 consumption during the photobleaching and photodynamic reaction, respectively. The photodynamic process thus needs more dynamic modeling. Regarding clinical PDT, the following areas need improvement, tumor selectivity, formulation of photosensitizers, and tissue penetration depth. Nanoparticles are a new technique in the realm of PDT that can overcome many of the constraints of traditional PS.[196] Generally, they are described as small particles between the size range of 1 and 100 nm. A number of synthetic or naturally occurring materials may be used to produce nanoparticles, which can be tailored to transport numerous theranostic drugs in a targeted way. Depending on the type of carrier system and the mechanism of transport, PS attachment or loading, the incorporation of nanoparticles in combination with PDT may offer some of the following advantages: they may efficiently enhance the amount of PS that can be administered to the target cells because of their high surface to volume ratios.[197,198] NPs may limit the imminent release of PS and possible drug inactivation by plasma components, avoiding its nonspecific aggregation in healthy tissues and lowering overall photosensitivity.[1] They provide PS with amphiphilicity, a quality that some potentially exceptional PS compounds lack. As a result, nanoparticles bearing the PS payload may freely circulate through the bloodstream and target the malignant cells.[199] Typically, they benefit from the EPR effect, which is a result of abnormally leaky tumor neovasculature and inadequate lymphatic drainage of the malignant cells, assisting PS carrier's diffusion into and retention inside tumor tissue.[6] Their surface may be further altered with targeting agents or functional groups to change their physical or biological characteristics, resulting in improved targeting abilities, cell uptake, pharmacokinetics, and biodistribution.[200]

8. CONCLUSION

PDT provides a number of key advantages over other conventional treatment modalities including radiotherapy,

https://doi.org/10.1021/acsomega.2c05852
ACS Omega 2022, 7, 45882−45909

chemotherapy, and surgery.[201,202] PSs are only functional after being activated or switched on by certain types of light irradiation, minimizing systemic toxicity, and have been extensively used in *in vivo* biomedical applications. PDT may be helpful by damaging the blood arteries that nourish tumor cells and by signaling the immune system to fight the tumor, and it has a broad range of potential uses since ROS affects a wide variety of cells. PDT is a minimally invasive or noninvasive technique for topical and targeted therapy. PDT may be used with radiotherapy, chemotherapy, or other anticancer medications and may be used to combat multidrug bacterial and cancer resistance. These NP drug delivery approaches provide a number of advantages for PSs such as lengthening the retention time in cancerous tissue, increasing EPR effect, and targeting only tumor tissues, which improves the drug−light interval and gives clinicians a wider window of time in which to treat patients, which they may use to irradiate the patient. Moreover, a tumor-targeted delivery method decreases the buildup of PS in healthy tissues, reducing any deleterious repercussions of photosensitivity. Tumor-targeting PS delivery devices may improve PDT by focusing on certain tumor types and more effectively accessing interior organs. PDT in the treatment of cancer is still a subject of much research. To secure a promising future for cancer therapy, more research is needed for PDT to become the widely used therapy that clinicians desire.

AUTHOR INFORMATION

Corresponding Author

Swati Biswas − *Nanomedicine Research Laboratory, Department of Pharmacy, Birla Institute of Technology & Science-Pilani, Hyderabad, Telangana 500078, India;* orcid.org/0000-0002-1575-4206; Phone: 040-6630-3630; Email: swati.biswas@hyderabad.bits-pilani.ac.in; Fax: 040-6630-3998

Authors

Asif Mohd Itoo − *Nanomedicine Research Laboratory, Department of Pharmacy, Birla Institute of Technology & Science-Pilani, Hyderabad, Telangana 500078, India*

Milan Paul − *Nanomedicine Research Laboratory, Department of Pharmacy, Birla Institute of Technology & Science-Pilani, Hyderabad, Telangana 500078, India*

Sri Ganga Padaga − *Nanomedicine Research Laboratory, Department of Pharmacy, Birla Institute of Technology & Science-Pilani, Hyderabad, Telangana 500078, India*

Balaram Ghosh − *Nanomedicine Research Laboratory, Department of Pharmacy, Birla Institute of Technology & Science-Pilani, Hyderabad, Telangana 500078, India;* orcid.org/0000-0002-3425-2439

Complete contact information is available at: https://pubs.acs.org/10.1021/acsomega.2c05852

Notes

The authors declare no competing financial interest.

ACKNOWLEDGMENTS

Prof. Swati Biswas acknowledges the Department of Science and Technology-Science and Engineering Research Board (DST-SERB) for providing research support through the core research grant (CRG/2018/001065). Asif Mohd Itoo is thankful to Lady Tata Memorial Trust for providing fellowship, and Milan Paul is thankful to ICMR for providing SRF under Grant No. 45/11/2022/NAN/BMS.

REFERENCES

(1) Master, A.; Livingston, M.; Sen Gupta, A. Photodynamic Nanomedicine in the Treatment of Solid Tumors: Perspectives and Challenges. *J. Control. release* **2013**, *168* (1), 88−102.

(2) Itoo, A. M.; Vemula, S. L.; Gupta, M. T.; Giram, M. V.; Kumar, S. A.; Ghosh, B.; Biswas, S. Multifunctional Graphene Oxide Nanoparticles for Drug Delivery in Cancer. *J. Controlled Release* **2022**, *350*, 26−59.

(3) Itoo, A. M.; Paul, M.; Ghosh, B.; Biswas, S. Oxaliplatin Delivery via Chitosan/Vitamin E Conjugate-Based Nanoassembly for Improved Efficacy and MDR-Reversal in Breast Cancer. *Carbohydr. Polym.* **2022**, *282*, 119108.

(4) Kumbham, S.; Paul, M.; Itoo, A.; Ghosh, B.; Biswas, S. Oleanolic Acid-Conjugated Human Serum Albumin Nanoparticles Encapsulating Doxorubicin as Synergistic Combination Chemotherapy in Oropharyngeal Carcinoma and Melanoma. *Int. J. Pharm.* **2022**, *614*, 121479.

(5) Darzynkiewicz, Z.; Traganos, F.; Wlodkowic, D. Impaired DNA Damage Response—an Achilles' Heel Sensitizing Cancer to Chemotherapy and Radiotherapy. *Eur. J. Pharmacol.* **2009**, *625* (1−3), 143−150.

(6) Maeda, H.; Wu, J.; Sawa, T.; Matsumura, Y.; Hori, K. Tumor Vascular Permeability and the EPR Effect in Macromolecular Therapeutics: A Review. *J. Control. release* **2000**, *65* (1−2), 271−284.

(7) Fang, J.; Nakamura, H.; Maeda, H. The EPR Effect: Unique Features of Tumor Blood Vessels for Drug Delivery, Factors Involved, and Limitations and Augmentation of the Effect. *Adv. Drug Delivery Rev.* **2011**, *63* (3), 136−151.

(8) Maeda, H. The Enhanced Permeability and Retention (EPR) Effect in Tumor Vasculature: The Key Role of Tumor-Selective Macromolecular Drug Targeting. *Adv. Enzyme Regul.* **2001**, *41*, 189.

(9) Ramakrishnan, R.; Gabrilovich, D. I. Mechanism of Synergistic Effect of Chemotherapy and Immunotherapy of Cancer. *Cancer Immunol. Immunother.* **2011**, *60* (3), 419−423.

(10) Scott, A. M.; Wolchok, J. D.; Old, L. J. Antibody Therapy of Cancer. *Nat. Rev. cancer* **2012**, *12* (4), 278−287.

(11) Kwitniewski, M.; Juzeniene, A.; Glosnicka, R.; Moan, J. Immunotherapy: A Way to Improve the Therapeutic Outcome of Photodynamic Therapy? *Photochem. Photobiol. Sci.* **2008**, *7* (9), 1011−1017.

(12) Lucky, S. S.; Soo, K. C.; Zhang, Y. Nanoparticles in Photodynamic Therapy. *Chem. Rev.* **2015**, *115* (4), 1990−2042.

(13) Li, X.; Lee, S.; Yoon, J. Supramolecular Photosensitizers Rejuvenate Photodynamic Therapy. *Chem. Soc. Rev.* **2018**, *47* (4), 1174−1188.

(14) Neginskaya, M.; Berezhnaya, E.; Uzdensky, A. B.; Abramov, A. Y. Reactive Oxygen Species Produced by a Photodynamic Effect Induced Calcium Signal in Neurons and Astrocytes. *Mol. Neurobiol.* **2018**, *55* (1), 96−102.

(15) Cozzolino, M.; Pesce, L.; Oneto, M.; Montali, C.; Bianchini, P.; Abbruzzetti, S.; Viappiani, C.; Diaspro, A. Study of Tumor Cellular Damage Induced by Photosensitizing Molecules. *Biophys. J.* **2018**, *114* (3), 535a.

(16) Dai, Y.; Yang, Z.; Cheng, S.; Wang, Z.; Zhang, R.; Zhu, G.; Wang, Z.; Yung, B. C.; Tian, R.; Jacobson, O.; et al. Toxic Reactive Oxygen Species Enhanced Synergistic Combination Therapy by Self-assembled Metal-phenolic Network Nanoparticles. *Adv. Mater.* **2018**, *30* (8), 1704877.

(17) Zhou, Z.; Song, J.; Tian, R.; Yang, Z.; Yu, G.; Lin, L.; Zhang, G.; Fan, W.; Zhang, F.; Niu, G.; et al. Activatable Singlet Oxygen Generation from Lipid Hydroperoxide Nanoparticles for Cancer Therapy. *Angew. Chem.* **2017**, *129* (23), 6592−6596.

(18) Jiang, M.; Kwok, R. T. K.; Li, X.; Gui, C.; Lam, J. W. Y.; Qu, J.; Tang, B. Z. A Simple Mitochondrial Targeting AIEgen for Image-Guided Two-Photon Excited Photodynamic Therapy. *J. Mater. Chem. B* **2018**, *6* (17), 2557−2565.

(19) Allison, R. R.; Downie, G. H.; Cuenca, R.; Hu, X.-H.; Childs, C. J. H.; Sibata, C. H. Photosensitizers in Clinical PDT. *Photodiagnosis Photodyn. Ther.* **2004**, *1* (1), 27−42.
(20) Dougherty, T. J.; Kaufman, J. E.; Goldfarb, A.; Weishaupt, K. R.; Boyle, D.; Mittleman, A. Photoradiation Therapy for the Treatment of Malignant Tumors. *Cancer Res.* **1978**, *38* (8), 2628−2635.
(21) Miller, J. D.; Baron, E. D.; Scull, H.; Hsia, A.; Berlin, J. C.; McCormick, T.; Colussi, V.; Kenney, M. E.; Cooper, K. D.; Oleinick, N. L. Photodynamic Therapy with the Phthalocyanine Photosensitizer Pc 4: The Case Experience with Preclinical Mechanistic and Early Clinical−Translational Studies. *Toxicol. Appl. Pharmacol.* **2007**, *224* (3), 290−299.
(22) Milane, L.; Duan, Z.; Amiji, M. Development of EGFR-Targeted Polymer Blend Nanocarriers for Combination Paclitaxel/Lonidamine Delivery to Treat Multi-Drug Resistance in Human Breast and Ovarian Tumor Cells. *Mol. Pharmaceutics* **2011**, *8* (1), 185−203.
(23) Civantos, F. J.; Karakullukcu, B.; Biel, M.; Silver, C. E.; Rinaldo, A.; Saba, N. F.; Takes, R. P.; Vander Poorten, V.; Ferlito, A. A Review of Photodynamic Therapy for Neoplasms of the Head and Neck. *Adv. Ther.* **2018**, *35* (3), 324−340.
(24) Ye, Z.; Liang, Y.; Ma, Y.; Lin, B.; Cao, L.; Wang, B.; Zhang, Z.; Yu, H.; Li, J.; Huang, M.; et al. Targeted Photodynamic Therapy of Cancer Using a Novel Gallium (III) Tris (Ethoxycarbonyl) Corrole Conjugated-mAb Directed against Cancer/Testis Antigens 83. *Cancer Med.* **2018**, *7* (7), 3057−3065.
(25) Mokwena, M. G.; Kruger, C. A.; Ivan, M.-T.; Heidi, A. A Review of Nanoparticle Photosensitizer Drug Delivery Uptake Systems for Photodynamic Treatment of Lung Cancer. *Photodiagnosis Photodyn. Ther.* **2018**, *22*, 147−154.
(26) Liu, Y.; Ma, K.; Jiao, T.; Xing, R.; Shen, G.; Yan, X. Water-Insoluble Photosensitizer Nanocolloids Stabilized by Supramolecular Interfacial Assembly towards Photodynamic Therapy. *Sci. Rep.* **2017**, *7* (1), 1−8.
(27) Liu, Y.; Liu, Y.; Bu, W.; Cheng, C.; Zuo, C.; Xiao, Q.; Sun, Y.; Ni, D.; Zhang, C.; Liu, J.; et al. Hypoxia Induced by Upconversion-based Photodynamic Therapy: Towards Highly Effective Synergistic Bioreductive Therapy in Tumors. *Angew. Chem.* **2015**, *127* (28), 8223−8227.
(28) Fan, W.; Bu, W.; Zhang, Z.; Shen, B.; Zhang, H.; He, Q.; Ni, D.; Cui, Z.; Zhao, K.; Bu, J.; et al. X-ray Radiation-controlled NO-release for On-demand Depth-independent Hypoxic Radiosensitization. *Angew. Chemie Int. Ed.* **2015**, *54* (47), 14026−14030.
(29) Xu, R.; Wang, Y.; Duan, X.; Lu, K.; Micheroni, D.; Hu, A.; Lin, W. Nanoscale Metal−Organic Frameworks for Ratiometric Oxygen Sensing in Live Cells. *J. Am. Chem. Soc.* **2016**, *138* (7), 2158−2161.
(30) Wu, W.; Mao, D.; Hu, F.; Xu, S.; Chen, C.; Zhang, C.; Cheng, X.; Yuan, Y.; Ding, D.; Kong, D.; et al. A Highly Efficient and Photostable Photosensitizer with Near-infrared Aggregation-induced Emission for Image-guided Photodynamic Anticancer Therapy. *Adv. Mater.* **2017**, *29* (33), 1700548.
(31) Zou, Q.; Zhao, H.; Zhao, Y.; Fang, Y.; Chen, D.; Ren, J.; Wang, X.; Wang, Y.; Gu, Y.; Wu, F. Effective Two-Photon Excited Photodynamic Therapy of Xenograft Tumors Sensitized by Water-Soluble Bis (Arylidene) Cycloalkanone Photosensitizers. *J. Med. Chem.* **2015**, *58* (20), 7949−7958.
(32) Lucky, S. S.; Idris, N. M.; Huang, K.; Kim, J.; Li, Z.; Thong, P. S. P.; Xu, R.; Soo, K. C.; Zhang, Y. Vivo Biocompatibility, Biodistribution and Therapeutic Efficiency of Titania Coated Upconversion Nanoparticles for Photodynamic Therapy of Solid Oral Cancers. *Theranostics* **2016**, *6* (11), 1844.
(33) Kang, H.; Mintri, S.; Menon, A. V.; Lee, H. Y.; Choi, H. S.; Kim, J. Pharmacokinetics, Pharmacodynamics and Toxicology of Theranostic Nanoparticles. *Nanoscale* **2015**, *7* (45), 18848−18862.
(34) Iyer, A. K.; Khaled, G.; Fang, J.; Maeda, H. Exploiting the Enhanced Permeability and Retention Effect for Tumor Targeting. *Drug Discovery Today* **2006**, *11* (17−18), 812−818.
(35) Greish, K. Enhanced Permeability and Retention (EPR) Effect for Anticancer Nanomedicine Drug Targeting. In *Cancer nanotechnology*; Springer, 2010; pp 25−37.
(36) Bechet, D.; Couleaud, P.; Frochot, C.; Viriot, M.-L.; Guillemin, F.; Barberi-Heyob, M. Nanoparticles as Vehicles for Delivery of Photodynamic Therapy Agents. *Trends Biotechnol* **2008**, *26* (11), 612−621.
(37) Chatterjee, D. K.; Fong, L. S.; Zhang, Y. Nanoparticles in Photodynamic Therapy: An Emerging Paradigm. *Adv. Drug Delivery Rev.* **2008**, *60* (15), 1627−1637.
(38) Juzenas, P.; Chen, W.; Sun, Y.-P.; Coelho, M. A. N.; Generalov, R.; Generalova, N.; Christensen, I. L. Quantum Dots and Nanoparticles for Photodynamic and Radiation Therapies of Cancer. *Adv. Drug Delivery Rev.* **2008**, *60* (15), 1600−1614.
(39) Yu, M. K.; Park, J.; Jon, S. Targeting Strategies for Multifunctional Nanoparticles in Cancer Imaging and Therapy. *Theranostics* **2012**, *2* (1), 3.
(40) Olivo, M.; Bhuvaneswari, R.; Lucky, S. S.; Dendukuri, N.; Thong, P. S.-P. Targeted Therapy of Cancer Using Photodynamic Therapy in Combination with Multi-Faceted Anti-Tumor Modalities. *Pharmaceuticals* **2010**, *3* (5), 1507−1529.
(41) Fan, W.; Huang, P.; Chen, X. Overcoming the Achilles' Heel of Photodynamic Therapy. *Chem. Soc. Rev.* **2016**, *45* (23), 6488−6519.
(42) Zhou, Z.; Song, J.; Nie, L.; Chen, X. Reactive Oxygen Species Generating Systems Meeting Challenges of Photodynamic Cancer Therapy. *Chem. Soc. Rev.* **2016**, *45* (23), 6597−6626.
(43) Shen, Y.; Shuhendler, A. J.; Ye, D.; Xu, J.-J.; Chen, H.-Y. Two-Photon Excitation Nanoparticles for Photodynamic Therapy. *Chem. Soc. Rev.* **2016**, *45* (24), 6725−6741.
(44) Hamblin, M. R. Upconversion in Photodynamic Therapy: Plumbing the Depths. *Dalt. Trans.* **2018**, *47* (26), 8571−8580.
(45) Deng, K.; Li, C.; Huang, S.; Xing, B.; Jin, D.; Zeng, Q.; Hou, Z.; Lin, J. Recent Progress in near Infrared Light Triggered Photodynamic Therapy. *Small* **2017**, *13* (44), 1702299.
(46) Park, J.; Brust, T. F.; Lee, H. J.; Lee, S. C.; Watts, V. J.; Yeo, Y. Polydopamine-Based Simple and Versatile Surface Modification of Polymeric Nano Drug Carriers. *ACS Nano* **2014**, *8* (4), 3347−3356.
(47) Zhang, D.; Wu, M.; Zeng, Y.; Wu, L.; Wang, Q.; Han, X.; Liu, X.; Liu, J. Chlorin E6 Conjugated Poly(Dopamine) Nanospheres as PDT/PTT Dual-Modal Therapeutic Agents for Enhanced Cancer Therapy. *ACS Appl. Mater. Interfaces* **2015**, *7* (15), 8176−8187.
(48) Wang, S.; Zhao, X.; Wang, S.; Qian, J.; He, S. Biologically Inspired Polydopamine Capped Gold Nanorods for Drug Delivery and Light-Mediated Cancer Therapy. *ACS Appl. Mater. Interfaces* **2016**, *8* (37), 24368−24384.
(49) Poinard, B.; Neo, S. Z. Y.; Yeo, E. L. L.; Heng, H. P. S.; Neoh, K. G.; Kah, J. C. Y. Polydopamine Nanoparticles Enhance Drug Release for Combined Photodynamic and Photothermal Therapy. *ACS Appl. Mater. Interfaces* **2018**, *10* (25), 21125−21136.
(50) Guo, W.; Wang, F.; Ding, D.; Song, C.; Guo, C.; Liu, S. TiO2-x Based Nanoplatform for Bimodal Cancer Imaging and NIR-Triggered Chem/Photodynamic/Photothermal Combination Therapy. *Chem. Mater.* **2017**, *29* (21), 9262−9274.
(51) Cen, Y.; Deng, W. J.; Yang, Y.; Yu, R. Q.; Chu, X. Core-Shell-Shell Multifunctional Nanoplatform for Intracellular Tumor-Related MRNAs Imaging and Near-Infrared Light Triggered Photodynamic-Photothermal Synergistic Therapy. *Anal. Chem.* **2017**, *89* (19), 10321−10328.
(52) Mroz, P.; Hashmi, J. T.; Huang, Y.-Y.; Lange, N.; Hamblin, M. R. Stimulation of Anti-Tumor Immunity by Photodynamic Therapy. *Expert Rev. Clin. Immunol.* **2011**, *7* (1), 75−91.
(53) Calixto, G. M. F.; Bernegossi, J.; De Freitas, L. M.; Fontana, C. R.; Chorilli, M.; Grumezescu, A. M. Nanotechnology-Based Drug Delivery Systems for Photodynamic Therapy of Cancer: A Review. *Molecules* **2016**, *21* (3), 1−18.
(54) Dougherty, T. J.; Marcus, S. L. Photodynamic Therapy: Review. *Eur. J. Cancer A* **1992**, *28*, 1734−1742.
(55) Jockusch, S.; Lee, D.; Turro, N. J.; Leonard, E. F. Photo-Induced Inactivation of Viruses: Adsorption of Methylene Blue,

https://doi.org/10.1021/acsomega.2c05852
ACS Omega 2022, 7, 45882−45909

Thionine, and Thiopyronine on Qbeta Bacteriophage. *Proc. Natl. Acad. Sci. U. S. A.* **1996**, *93* (15), 7446−7451.
(56) Phoenix, D. A.; Harris, F. Phenothiazinium-Based Photosensitizers: Antibacterials of the Future? *Trends Mol. Med.* **2003**, *9* (7), 283−285.
(57) Harris, F.; Chatfield, L. K.; Phoenix, D. A. Phenothiazinium Based Photosensitisers-Photodynamic Agents with a Multiplicity of Cellular Targets and Clinical Applications. *Curr. Drug Targets* **2005**, *6* (5), 615−627.
(58) Tuite, E. M.; Kelly, J. M. New Trends in Photobiology: Photochemical Interactions of Methylene Blue and Analogues with DNA and Other Biological Substrates. *J. Photochem. Photobiol. B Biol.* **1993**, *21* (2−3), 103−124.
(59) Millson, C. E.; Wilson, M.; Macrobert, A. J.; Bedwell, J.; Bown, S. G. The Killing of Helicobacter Pylori by Low-Power Laser Light in the Presence of a Photosensitiser. *J. Med. Microbiol.* **1996**, *44* (4), 245−252.
(60) Tardivo, J. P.; Del Giglio, A.; De Oliveira, C. S.; Gabrielli, D. S.; Junqueira, H. C.; Tada, D. B.; Severino, D.; de Fátima Turchiello, R.; Baptista, M. S. Methylene Blue in Photodynamic Therapy: From Basic Mechanisms to Clinical Applications. *Photodiagnosis Photodyn. Ther.* **2005**, *2* (3), 175−191.
(61) Soukos, N. S.; Chen, P. S.-Y.; Morris, J. T.; Ruggiero, K.; Abernethy, A. D.; Som, S.; Foschi, F.; Doucette, S.; Bammann, L. L.; Fontana, C. R.; et al. Photodynamic Therapy for Endodontic Disinfection. *J. Endod.* **2006**, *32* (10), 979−984.
(62) Huang, P.; Li, Z.; Lin, J.; Yang, D.; Gao, G.; Xu, C.; Bao, L.; Zhang, C.; Wang, K.; Song, H.; et al. Photosensitizer-Conjugated Magnetic Nanoparticles for in Vivo Simultaneous Magnetofluorescent Imaging and Targeting Therapy. *Biomaterials* **2011**, *32* (13), 3447−3458.
(63) Yan, F.; Zhang, Y.; Kim, K. S.; Yuan, H.; Vo-Dinh, T. Cellular Uptake and Photodynamic Activity of Protein Nanocages Containing Methylene Blue Photosensitizing Drug. *Photochem. Photobiol.* **2010**, *86* (3), 662−666.
(64) Kopelman, R.; Philbert, M. A.; Tang, W.; Xu, H. Photodynamic Characterization and In Vitro Application of Methylene Blue-Containing Nanoparticle Platforms. *Photochem. Photobiol.* **2005**, *81*, 242−249.
(65) He, X.; Wu, X.; Wang, K.; Shi, B.; Hai, L. Methylene Blue-Encapsulated Phosphonate-Terminated Silica Nanoparticles for Simultaneous in Vivo Imaging and Photodynamic Therapy. *Biomaterials* **2009**, *30* (29), 5601−5609.
(66) Li, L.; Bae, B.; Tran, T. H.; Yoon, K. H.; Na, K.; Huh, K. M. Self-Quenchable Biofunctional Nanoparticles of Heparin−Folate-Photosensitizer Conjugates for Photodynamic Therapy. *Carbohydr. Polym.* **2011**, *86* (2), 708−715.
(67) Samy, N. A.; Salah, M. M.; Ali, M. F.; Sadek, A. M. Effect of Methylene Blue-Mediated Photodynamic Therapy for Treatment of Basal Cell Carcinoma. *Lasers Med. Sci.* **2015**, *30* (1), 109−115.
(68) Disanto, A. R.; Wagner, J. G. Pharmacokinetics of Highly Ionized Drugs II: Methylene Blue—Absorption, Metabolism, and Excretion in Man and Dog after Oral Administration. *J. Pharm. Sci.* **1972**, *61* (7), 1086−1090.
(69) Wacker, M.; Chen, K.; Preuss, A.; Possemeyer, K.; Roeder, B.; Langer, K. Photosensitizer Loaded HSA Nanoparticles. I: Preparation and Photophysical Properties. *Int. J. Pharm.* **2010**, *393* (1−2), 254−263.
(70) Chen, K.; Wacker, M.; Hackbarth, S.; Ludwig, C.; Langer, K.; Röder, B. Photophysical Evaluation of MTHPC-Loaded HSA Nanoparticles as Novel PDT Delivery Systems. *J. Photochem. Photobiol. B Biol.* **2010**, *101* (3), 340−347.
(71) Chen, K.; Preuß, A.; Hackbarth, S.; Wacker, M.; Langer, K.; Röder, B. Novel Photosensitizer-Protein Nanoparticles for Photodynamic Therapy: Photophysical Characterization and in Vitro Investigations. *J. Photochem. Photobiol. B Biol.* **2009**, *96* (1), 66−74.
(72) Fakhar-e-Alam, M.; Ali, S. M. U.; Ibupoto, Z. H.; Kimleang, K.; Atif, M.; Kashif, M.; Loong, F. K.; Hashim, U.; Willander, M. Sensitivity of A-549 Human Lung Cancer Cells to Nanoporous Zinc Oxide Conjugated with Photofrin. *Lasers Med. Sci.* **2012**, *27* (3), 607−614.
(73) Xu, H.; Liu, C.; Mei, J.; Yao, C.; Wang, S.; Wang, J.; Li, Z.; Zhang, Z. Effects of Light Irradiation upon Photodynamic Therapy Based on 5-Aminolevulinic Acid−Gold Nanoparticle Conjugates in K562 Cells via Singlet Oxygen Generation. *Int. J. Nanomedicine* **2012**, *7*, 5029.
(74) Yin, M.; Li, Z.; Liu, Z.; Ren, J.; Yang, X.; Qu, X. Photosensitizer-Incorporated G-Quadruplex DNA-Functionalized Magnetofluorescent Nanoparticles for Targeted Magnetic Resonance/Fluorescence Multimodal Imaging and Subsequent Photodynamic Therapy of Cancer. *Chem. Commun.* **2012**, *48* (52), 6556−6558.
(75) Kessel, D.; Thompson, P. Purification and Analysis of Hematoporphyrin and Hematoporphyrin Derivative by Gel Exclusion and Reverse-phase Chromatography. *Photochem. Photobiol.* **1987**, *46* (6), 1023−1025.
(76) Machado, A. E. da H Terapia Fotodinâmica: Princípios, Potencial de Aplicação e Perspectivas. *Quim. Nova* **2000**, *23*, 237−243.
(77) Bonnett, R.; Grahn, M. F.; Salgado, A.; Turkish, M.; Valles, M. A.; Williams, N. S. Amphiphilic Chlorins Derived from Chlorophyll a for Photodynamic Therapy. *Photodyn. Ther. Biomed. Lasers* **1992**, *10*, 866−869.
(78) Taber, S. W.; Fingar, V. H.; Coots, C. T.; Wieman, T. J. Photodynamic Therapy Using Mono-L-Aspartyl Chlorin E6 (Npe6) for the Treatment of Cutaneous Disease: A Phase I Clinical Study. *Clin. Cancer Res.* **1998**, *4* (11), 2741−2746.
(79) Djelal, B.; áGeorge Truscott, T. Photophysical Properties of 5, 10, 15, 20-Tetrakis (m-Hydroxyphenyl) Porphyrin (m-THPP), 5, 10, 15, 20-Tetrakis (m-Hydroxyphenyl) Chlorin (m-THPC) and 5, 10, 15, 20-Tetrakis (m-Hydroxyphenyl) Bacteriochlorin (m-THPBC): A Comparative Study. *J. Chem. Soc. Perkin Trans. 2* **1999**, *2*, 325−328.
(80) Correa, J. C.; Bagnato, V. S.; Imasato, H.; Perussi, J. R. Previous Illumination of a Water Soluble Chlorine Photosensitizer Increases Its Cytotoxicity. *Laser Phys.* **2012**, *22* (9), 1387−1394.
(81) Ferreira, J.; Menezes, P. F. C.; Sibata, C. H.; Allison, R. R.; Zucoloto, S.; Castro e Silva, O.; Bagnato, V. S. Can. Efficiency of the Photosensitizer Be Predicted by Its Photostability in Solution? *Laser Phys.* **2009**, *19* (9), 1932−1938.
(82) Parihar, A.; Dube, A.; Gupta, P. K. Conjugation of Chlorin p 6 to Histamine Enhances Its Cellular Uptake and Phototoxicity in Oral Cancer Cells. *Cancer Chemother. Pharmacol.* **2011**, *68* (2), 359−369.
(83) Kobayashi, W.; Liu, Q.; Nakagawa, H.; Sakaki, H.; Teh, B.; Matsumiya, T.; Yoshida, H.; Imaizumi, T.; Satoh, K.; Kimura, H. Photodynamic Therapy with Mono-L-Aspartyl Chlorin E6 Can Cause Necrosis of Squamous Cell Carcinoma of Tongue: Experimental Study on an Animal Model of Nude Mouse. *Oral Oncol* **2006**, *42* (1), 45−49.
(84) Boddupalli, B. M.; Mohammed, Z. N. K.; Nath, R. A.; Banji, D. Mucoadhesive Drug Delivery System: An Overview. *J. Adv. Pharm. Technol. Res.* **2010**, *1* (4), 381.
(85) Wang, C.; Tao, H.; Cheng, L.; Liu, Z. Near-Infrared Light Induced in Vivo Photodynamic Therapy of Cancer Based on Upconversion Nanoparticles. *Biomaterials* **2011**, *32* (26), 6145−6154.
(86) Yoon, H. Y.; Koo, H.; Choi, K. Y.; Lee, S. J.; Kim, K.; Kwon, I. C.; Leary, J. F.; Park, K.; Yuk, S. H.; Park, J. H.; et al. Tumor-Targeting Hyaluronic Acid Nanoparticles for Photodynamic Imaging and Therapy. *Biomaterials* **2012**, *33* (15), 3980−3989.
(87) Castilho, M. L.; Jesus, V. P. S.; Vieira, P. F. A.; Hewitt, K. C.; Raniero, L. Chlorin E6-EGF Conjugated Gold Nanoparticles as a Nanomedicine Based Therapeutic Agent for Triple Negative Breast Cancer. *Photodiagnosis Photodyn. Ther.* **2021**, *33*, 102186.
(88) Gilyadova, A.; Ishchenko, A.; Shiryaev, A.; Alekseeva, P.; Efendiev, K.; Karpova, R.; Loshchenov, M.; Loschenov, V.; Reshetov, I. Phototheranostics of Cervical Neoplasms with Chlorin E6 Photosensitizer. *Cancers (Basel)* **2022**, *14* (1), 211.

https://doi.org/10.1021/acsomega.2c05852
ACS Omega 2022, 7, 45882−45909

(89) Ungun, B.; Prud'homme, R. K.; Budijon, S. J.; Shan, J.; Lim, S. F.; Ju, Y.; Austin, R. Nanofabricated Upconversion Nanoparticles for Photodynamic Therapy. *Opt. Express* **2009**, *17* (1), 80−86.
(90) Lo, P. C.; Rodríguez-Morgade, M. S.; Pandey, R. K.; Ng, D. K. P.; Torres, T.; Dumoulin, F. The Unique Features and Promises of Phthalocyanines as Advanced Photosensitisers for Photodynamic Therapy of Cancer. *Chem. Soc. Rev.* **2020**, *49* (4), 1041−1056.
(91) Zhang, F. L.; Huang, Q.; Zheng, K.; Li, J.; Liu, J. Y.; Xue, J. P. A Novel Strategy for Targeting Photodynamic Therapy. Molecular Combo of Photodynamic Agent Zinc(II) Phthalocyanine and Small Molecule Target-Based Anticancer Drug Erlotinib. *Chem. Commun.* **2013**, *49* (83), 9570−9572.
(92) Yan, S.; Chen, J.; Cai, L.; Xu, P.; Zhang, Y.; Li, S.; Hu, P.; Chen, X.; Huang, M.; Chen, Z. Phthalocyanine-Based Photosensitizer with Tumor-PH-Responsive Properties for Cancer Theranostics. *J. Mater. Chem. B* **2018**, *6* (38), 6080−6088.
(93) Li, X.; Yu, S.; Lee, Y.; Guo, T.; Kwon, N.; Lee, D.; Yeom, S. C.; Cho, Y.; Kim, G.; Huang, J. D.; Choi, S.; Nam, K. T.; Yoon, J. In Vivo Albumin Traps Photosensitizer Monomers from Self-Assembled Phthalocyanine Nanovesicles: A Facile and Switchable Theranostic Approach. *J. Am. Chem. Soc.* **2019**, *141* (3), 1366−1372.
(94) Yang, B.; Parsha, K.; Schaar, K.; Xi, X.; Aronowski, J.; Savitz, S. Orexin activation counteracts decreases in nonexercise activity thermogenesis (NEAT) caused by high-fat diet. *Physiol. Behav.* **2016**, *176* (1), 139−148.
(95) Chen, X.; Li, Y.; Li, S.; Gao, M.; Ren, L.; Tang, B. Z. Mitochondria- and Lysosomes-Targeted Synergistic Chemo-Photodynamic Therapy Associated with Self-Monitoring by Dual Light-Up Fluorescence. *Adv. Funct. Mater.* **2018**, *28* (44), 1−9.
(96) Atchison, J.; Kamila, S.; Nesbitt, H.; Logan, K. A.; Nicholas, D. M.; Fowley, C.; Davis, J.; Callan, B.; McHale, A. P.; Callan, J. F. Iodinated Cyanine Dyes: A New Class of Sensitisers for Use in NIR Activated Photodynamic Therapy (PDT). *Chem. Commun.* **2017**, *53* (12), 2009−2012.
(97) Cao, J.; Chi, J.; Xia, J.; Zhang, Y.; Han, S.; Sun, Y. Iodinated Cyanine Dyes for Fast Near-Infrared-Guided Deep Tissue Synergistic Phototherapy. *ACS Appl. Mater. Interfaces* **2019**, *11* (29), 25720−25729.
(98) Miao, X.; Hu, W.; He, T.; Tao, H.; Wang, Q.; Chen, R.; Jin, L.; Zhao, H.; Lu, X.; Fan, Q.; Huang, W. Deciphering the Intersystem Crossing in Near-Infrared BODIPY Photosensitizers for Highly Efficient Photodynamic Therapy. *Chem. Sci.* **2019**, *10* (10), 3096−3102.
(99) Pietkiewicz, J.; Zielińska, K.; Saczko, J.; Kulbacka, J.; Majkowski, M.; Wilk, K. A. New Approach to Hydrophobic Cyanine-Type Photosensitizer Delivery Using Polymeric Oil-Cored Nanocarriers: Hemolytic Activity, in Vitro Cytotoxicity and Localization in Cancer Cells. *Eur. J. Pharm. Sci.* **2010**, *39* (5), 322−335.
(100) Rungta, P.; Bandera, Y. P.; Roeder, R. D.; Li, Y.; Baldwin, W. S.; Sharma, D.; Sehorn, M. G.; Luzinov, I.; Foulger, S. H. Selective Imaging and Killing of Cancer Cells with Protein-Activated Near-Infrared Fluorescing Nanoparticles. *Macromol. Biosci.* **2011**, *11* (7), 927−937.
(101) Gomes, A. J.; Lunardi, L. O.; Marchetti, J. M.; Lunardi, C. N.; Tedesco, A. C. Indocyanine Green Nanoparticles Useful for Photomedicine. *Photomed. Laser Ther.* **2006**, *24* (4), 514−521.
(102) Kim, G.; Huang, S.-W.; Day, K. C.; O'Donnell, M.; Agayan, R. R.; Day, M. A.; Kopelman, R.; Ashkenazi, S. Indocyanine-Green-Embedded PEBBLEs as a Contrast Agent for Photoacoustic Imaging. *J. Biomed. Opt.* **2007**, *12* (4), 44020.
(103) Kuo, W.-S.; Chang, Y.-T.; Cho, K.-C.; Chiu, K.-C.; Lien, C.-H.; Yeh, C.-S.; Chen, S.-J. Gold Nanomaterials Conjugated with Indocyanine Green for Dual-Modality Photodynamic and Photothermal Therapy. *Biomaterials* **2012**, *33* (11), 3270−3278.
(104) Kleemann, B.; Loos, B.; Scriba, T. J.; Lang, D.; Davids, L. M. St John's Wort (Hypericum Perforatum L.) Photomedicine: Hypericin-Photodynamic Therapy Induces Metastatic Melanoma Cell Death. *PLoS One* **2014**, *9* (7), No. e103762.
(105) Wen, A. M.; Ryan, M. J.; Yang, A. C.; Breitenkamp, K.; Pokorski, J. K.; Steinmetz, N. F. Photodynamic Activity of Viral Nanoparticles Conjugated with C 60. *Chem. Commun.* **2012**, *48* (72), 9044−9046.
(106) Iohara, D.; Hiratsuka, M.; Hirayama, F.; Takeshita, K.; Motoyama, K.; Arima, H.; Uekama, K. Evaluation of Photodynamic Activity of C60/2-Hydroxypropyl-β-Cyclodextrin Nanoparticles. *J. Pharm. Sci.* **2012**, *101* (9), 3390−3397.
(107) Wang, M.; Huang, L.; Sharma, S. K.; Jeon, S.; Thota, S.; Sperandio, F. F.; Nayka, S.; Chang, J.; Hamblin, M. R.; Chiang, L. Y. Synthesis and Photodynamic Effect of New Highly Photostable Decacationically Armed [60]-and [70] Fullerene Decaiodide Monoadducts to Target Pathogenic Bacteria and Cancer Cells. *J. Med. Chem.* **2012**, *55* (9), 4274−4285.
(108) Powis, G. Free Radical Formation by Antitumor Quinones. *Free Radic. Biol. Med.* **1989**, *6* (1), 63−101.
(109) Driscoll, J. S.; Hazard, G. F., Jr; Wood, H. B., Jr; Goldin, A. Structure-Antitumor Activity Relationships among Quinone Derivatives. *Cancer Chemother. Rep. 2* **1974**, *4* (2), 1−362.
(110) Powis, G. Metabolism and Reactions of Quinoid Anticancer Agents. *Pharmacol. Ther.* **1987**, *35* (1−2), 57−162.
(111) Rajendran, M. Quinones as Photosensitizer for Photodynamic Therapy: ROS Generation, Mechanism and Detection Methods. *Photodiagnosis Photodyn. Ther.* **2016**, *13*, 175−187.
(112) Cape, J. L.; Bowman, M. K.; Kramer, D. M. Computation of the Redox and Protonation Properties of Quinones: Towards the Prediction of Redox Cycling Natural Products. *Phytochemistry* **2006**, *67* (16), 1781−1788.
(113) Polyakov, N.; Leshina, T.; Fedenok, L.; Slepneva, I.; Kirilyuk, I.; Furso, J.; Olchawa, M.; Sarna, T.; Elas, M.; Bilkis, I.; et al. Redox-Active Quinone Chelators: Properties, Mechanisms of Action, Cell Delivery, and Cell Toxicity. *Antioxid. Redox Signal.* **2018**, *28* (15), 1394−1403.
(114) MacDonald, I. J.; Dougherty, T. J. *Porphyrins Phthalocyanines* **2001**, *5*, 105−129.
(115) Orenstein, A.; Kostenich, G.; Roitman, L.; Shechtman, Y.; Kopolovic, Y.; Ehrenberg, B.; Malik, Z. A Comparative Study of Tissue Distribution and Photodynamic Therapy Selectivity of Chlorin E6, Photofrin II and ALA-Induced Protoporphyrin IX in a Colon Carcinoma Model. *Br. J. Cancer* **1996**, *73* (8), 937−944.
(116) Calixto, G.; Bernegossi, J.; Fonseca-Santos, B.; Chorilli, M. Nanotechnology-Based Drug Delivery Systems for Treatment of Oral Cancer: A Review. *Int. J. Nanomedicine* **2014**, *9*, 3719.
(117) Benergossi, J.; Calixto, G.; Fonseca-Santos, B.; Limi Aida, K.; de Cássia Negrini, T.; Duque, C.; Palmira Daflon Gremião, M.; Chorilli, M. Highlights in Peptide Nanoparticle Carriers Intended to Oral Diseases. *Curr. Top. Med. Chem.* **2015**, *15* (4), 345−355.
(118) Manmode, A. S.; Sakarkar, D. M.; Mahajan, N. M. Nanoparticles-Tremendous Therapeutic Potential: A Review. *Int. J. PharmTech Res.* **2009**, *1* (4), 1020−1027.
(119) Ohulchanskyy, T. Y.; Roy, I.; Goswami, L. N.; Chen, Y.; Bergey, E. J.; Pandey, R. K.; Oseroff, A. R.; Prasad, P. N. Organically Modified Silica Nanoparticles with Covalently Incorporated Photosensitizer for Photodynamic Therapy of Cancer. *Nano Lett.* **2007**, *7* (9), 2835−2842.
(120) Kumari, P.; Rompicharla, S. V. K.; Bhatt, H.; Ghosh, B.; Biswas, S. Development of Chlorin E6-Conjugated Poly(Ethylene Glycol)-Poly(d,l-Lactide) Nanoparticles for Photodynamic Therapy. *Nanomedicine* **2019**, *14* (7), 819−834.
(121) Khdair, A.; Gerard, B.; Handa, H.; Mao, G.; Shekhar, M. P. V.; Panyam, J. Surfactant− Polymer Nanoparticles Enhance the Effectiveness of Anticancer Photodynamic Therapy. *Mol. Pharmaceutics* **2008**, *5* (5), 795−807.
(122) El-Daly, S. M.; Gamal-Eldeen, A. M.; Abo-Zeid, M. A. M.; Borai, I. H.; Wafay, H. A.; Abdel-Ghaffar, A.-R. B. Photodynamic Therapeutic Activity of Indocyanine Green Entrapped in Polymeric Nanoparticles. *Photodiagnosis Photodyn. Ther.* **2013**, *10* (2), 173−185.

https://doi.org/10.1021/acsomega.2c05852
ACS Omega 2022, 7, 45882−45909

(123) Müller, R. H.; Mäder, K.; Gohla, S. Solid Lipid Nanoparticles (SLN) for Controlled Drug Delivery—a Review of the State of the Art. *Eur. J. Pharm. Biopharm.* **2000**, *50* (1), 161−177.
(124) Youssef, T.; Fadel, M.; Fahmy, R.; Kassab, K. Evaluation of Hypericin-Loaded Solid Lipid Nanoparticles: Physicochemical Properties, Photostability and Phototoxicity. *Pharm. Dev. Technol.* **2012**, *17* (2), 177−186.
(125) Lima, A. M.; Dal Pizzol, C.; Monteiro, F. B. F.; Creczynski-Pasa, T. B.; Andrade, G. P.; Ribeiro, A. O.; Perussi, J. R. Hypericin Encapsulated in Solid Lipid Nanoparticles: Phototoxicity and Photodynamic Efficiency. *J. Photochem. Photobiol. B Biol.* **2013**, *125*, 146−154.
(126) Duncan, B.; Kim, C.; Rotello, V. M. Gold Nanoparticle Platforms as Drug and Biomacromolecule Delivery Systems. *J. Control. release* **2010**, *148* (1), 122−127.
(127) Shi, J.; Yu, X.; Wang, L.; Liu, Y.; Gao, J.; Zhang, J.; Ma, R.; Liu, R.; Zhang, Z. PEGylated Fullerene/Iron Oxide Nanocomposites for Photodynamic Therapy, Targeted Drug Delivery and MR Imaging. *Biomaterials* **2013**, *34* (37), 9666−9677.
(128) Andrade, C. A. S.; Correia, M. T. S.; Coelho, L. C. B. B.; Nascimento, S. C.; Santos-Magalhães, N. S. Antitumor Activity of Cratylia Mollis Lectin Encapsulated into Liposomes. *Int. J. Pharm.* **2004**, *278* (2), 435−445.
(129) Chorilli, M.; Calixto, G.; Rimerio, T. C.; Scarpa, M. V. Caffeine Encapsulated in Small Unilamellar Liposomes: Characerization and in Vitro Release Profile. *J. Dispers. Sci. Technol.* **2013**, *34* (10), 1465−1470.
(130) Wu, P.-T.; Lin, C.-L.; Lin, C.-W.; Chang, N.-C.; Tsai, W.-B.; Yu, J. Methylene-Blue-Encapsulated Liposomes as Photodynamic Therapy Nano Agents for Breast Cancer Cells. *Nanomaterials* **2019**, *9* (1), 14.
(131) Bovis, M. J.; Woodhams, J. H.; Loizidou, M.; Scheglmann, D.; Bown, S. G.; MacRobert, A. J. Improved in Vivo Delivery of M-THPC via Pegylated Liposomes for Use in Photodynamic Therapy. *J. Controlled Release* **2012**, *157* (2), 196−205.
(132) Nombona, N.; Maduray, K.; Antunes, E.; Karsten, A.; Nyokong, T. Synthesis of Phthalocyanine Conjugates with Gold Nanoparticles and Liposomes for Photodynamic Therapy. *J. Photochem. Photobiol. B Biol.* **2012**, *107*, 35−44.
(133) Itoo, A. M.; Paul, M.; Ghosh, B.; Biswas, S. Oxaliplatin Delivery via Chitosan/Vitamin E Conjugate Micelles for Improved Efficacy and MDR-Reversal in Breast Cancer. *Carbohydr. Polym.* **2022**, *282*, 119108.
(134) Kumari, P.; Jain, S.; Ghosh, B.; Zorin, V.; Biswas, S. Polylactide-Based Block Copolymeric Micelles Loaded with Chlorin E6 for Photodynamic Therapy: In Vitro Evaluation in Monolayer and 3D Spheroid Models. *Mol. Pharmaceutics* **2017**, *14*, 3789−3800.
(135) Kumari, P.; Paul, M.; Bhatt, H.; Rompicharla, S. V. K.; Sarkar, D.; Ghosh, B.; Biswas, S. Chlorin E6 Conjugated Methoxy-Poly(Ethylene Glycol)-Poly(D,L-Lactide) Glutathione Sensitive Micelles for Photodynamic Therapy. *Pharm. Res.* **2020**, *37* (2), 1−17.
(136) Tomalia, D. A.; Khanna, S. N. A Systematic Framework and Nanoperiodic Concept for Unifying Nanoscience: Hard/Soft Nanoelements, Superatoms, Meta-Atoms, New Emerging Properties, Periodic Property Patterns, and Predictive Mendeleev-like Nanoperiodic Tables. *Chem. Rev.* **2016**, *116* (4), 2705−2774.
(137) Caminade, A.-M.; Turrin, C.-O.; Majoral, J.-P. Biological Properties of Water-Soluble Phosphorhydrazone Dendrimers. *Brazilian J. Pharm. Sci.* **2013**, *49*, 33−44.
(138) Rao, N.; Sunkara, M.; Amreddy, N.; Kurra, V.; Adimoolam, M. Photosensitizer and Peptide-Conjugated PAMAM Dendrimer for Targeted in Vivo Photodynamic Therapy. *Int. J. Nanomedicine* **2015**, *10*, 6865.
(139) Rodriguez, L.; Vallecorsa, P.; Battah, S.; Di Venosa, G.; Calvo, G.; Mamone, L.; Saenz, D.; Gonzalez, M. C.; Batlle, A.; MacRobert, A. J.; et al. Aminolevulinic Acid Dendrimers in Photodynamic Treatment of Cancer and Atheromatous Disease. *Photochem. Photobiol. Sci.* **2015**, *14* (9), 1617−1627.
(140) Nishiyama, N.; Jang, W.-D.; Kataoka, K. Supramolecular Nanocarriers Integrated with Dendrimers Encapsulating Photosensitizers for Effective Photodynamic Therapy and Photochemical Gene Delivery. *New J. Chem.* **2007**, *31* (7), 1074−1082.
(141) Mohy Eldin, M. S.; Kamoun, E. A.; Sofan, M. A.; Elbayomi, S. M. L-Arginine Grafted Alginate Hydrogel Beads: A Novel PH-Sensitive System for Specific Protein Delivery. *Arab. J. Chem.* **2015**, *8* (3), 355−365.
(142) DE FÁRMACOS, S. D. L. Sistemas Matriciais Hidrofílicos e Mucoadesivos Para Liberação Controlada de Fármacos. *Lat. Am. J. Pharm.* **2007**, *26* (5), 784−793.
(143) Barcellos, I. O.; Katime, I. A.; Soldi, V.; Pires, A. T. N. Influence of Comonomer and Polymerization Method on the Kinetics of Phenobarbitone Released from Hydrogels. *Polímeros* **2000**, *10*, 110−115.
(144) Mori, K.; Yoneya, S.; Anzail, K.; Kabasawa, S.; Sodeyama, T.; Peyman, G. A.; Moshfeghi, D. M. Photodynamic Therapy of Experimental Choroidal Neovascularization with a Hydrophilic Photosensitizer: Mono-L-Aspartyl Chlorin E6. *Retina* **2001**, *21* (5), 499−508.
(145) Kim, J.; Kim, K. S.; Park, S.; Na, K. Vitamin Bc-Bearing Hydrophilic Photosensitizer Conjugate for Photodynamic Cancer Theranostics. *Macromol. Biosci.* **2015**, *15* (8), 1081−1090.
(146) Noiseux, I.; Mermut, O.; Bouchard, J.-P.; Cormier, J.-F.; Desroches, P.; Fortin, M.; Gallant, P.; Leclair, S.; Vernon, M. L.; Diamond, K. R.; et al. Effect of Liposomal Confinement on Photochemical Properties of Photosensitizers with Varying Hydrophilicity. *J. Biomed. Opt.* **2008**, *13* (4), 41313.
(147) Reza Saboktakin, M.; Tabatabaie, R. M.; Maharramov, A.; Ali Ramazanov, M. Synthesis and in Vitro Studies of Biodegradable Modified Chitosan Nanoparticles for Photodynamic Treatment of Cancer. *Int. J. Biol. Macromol.* **2011**, *49* (5), 1059−1065.
(148) Gosenca, M.; Bešter-Rogač, M.; Gašperlin, M. Lecithin Based Lamellar Liquid Crystals as a Physiologically Acceptable Dermal Delivery System for Ascorbyl Palmitate. *Eur. J. Pharm. Sci.* **2013**, *50* (1), 114−122.
(149) Chorilli, M.; Prestes, P. S.; Rigon, R. B.; Leonardi, G. R.; Chiavacci, L. A.; Scarpa, M. V. Development of Liquid-Crystalline Systems Using Silicon Glycol Copolymer and Polyether Functional Siloxane. *Quim. Nova* **2009**, *32*, 1036−1040.
(150) Guo, C.; Wang, J.; Cao, F.; Lee, R. J.; Zhai, G. Lyotropic Liquid Crystal Systems in Drug Delivery. *Drug Discovery Today* **2010**, *15* (23−24), 1032−1040.
(151) Ghosh, O.; Miller, C. A. Lamellar Liquid Crystals in Equilibrium with Excess Oil in Anionic Surfactant-Oil-Brine Systems. *J. Colloid Interface Sci.* **1987**, *116* (2), 593−597.
(152) Garti, N.; Hoshen, G.; Aserin, A. Lipolysis and Structure Controlled Drug Release from Reversed Hexagonal Mesophase. *Colloids Surfaces B Biointerfaces* **2012**, *94*, 36−43.
(153) Lopes, L. B.; Ferreira, D. A.; de Paula, D.; Garcia, M. T. J.; Thomazini, J. A.; Fantini, M. C. A.; Bentley, M. Reverse Hexagonal Phase Nanodispersion of Monoolein and Oleic Acid for Topical Delivery of Peptides: In Vitro and in Vivo Skin Penetration of Cyclosporin A. *Pharm. Res.* **2006**, *23* (6), 1332−1342.
(154) Rossetti, F. C.; Depieri, L. V.; Praça, F. G.; Del Ciampo, J. O.; Fantini, M. C. A.; Pierre, M. B. R.; Tedesco, A. C.; Bentley, M. V. L. B. Optimization of Protoporphyrin IX Skin Delivery for Topical Photodynamic Therapy: Nanodispersions of Liquid-Crystalline Phase as Nanocarriers. *Eur. J. Pharm. Sci.* **2016**, *83*, 99−108.
(155) Venturini, C. de G.; Nicolini, J.; Machado, C.; Machado, V. G. Properties and Recent Applications of Cyclodextrins. *Quim. Nova* **2008**, *31*, 360−368.
(156) Saltão, R.; Veiga, F. Ciclodextrinas Em Novos Sistemas Terapêuticos. *Brazilian J. Pharm. Sci.* **2001**, *37* (1), 1−17.
(157) Conte, C.; Scala, A.; Siracusano, G.; Leone, N.; Patane, S.; Ungaro, F.; Miro, A.; Sciortino, M. T.; Quaglia, F.; Mazzaglia, A. Nanoassembly of an Amphiphilic Cyclodextrin and Zn (II)-Phthalocyanine with the Potential for Photodynamic Therapy of Cancer. *RSC Adv.* **2014**, *4* (83), 43903−43911.

https://doi.org/10.1021/acsomega.2c05852
ACS Omega 2022, 7, 45882−45909

(158) Lourenço, L. M. O.; Pereira, P. M. R.; Maciel, E.; Válega, M.; Domingues, F. M. J.; Domingues, M. R. M.; Neves, M. G.; Cavaleiro, J. A. S.; Fernandes, R.; Tomé, J. P. C. Amphiphilic Phthalocyanine−Cyclodextrin Conjugates for Cancer Photodynamic Therapy. *Chem. Commun.* **2014**, *50* (61), 8363−8366.
(159) Lan, M.; Zhao, S.; Liu, W.; Lee, C.; Zhang, W.; Wang, P. Photosensitizers for Photodynamic Therapy. *Adv. Healthcare Mater.* **2019**, *1900132*, 1−37, DOI: 10.1002/adhm.201900132.
(160) Dougherty, T. J.; Gomer, C. J.; Henderson, B. W.; Jori, G.; Kessel, D.; Korbelik, M.; Moan, J.; Peng, Q. *Photodynamic Therapy* **1998**, *90* (12), 889−905.
(161) Agostinis, P.; Berg, K.; Cengel, K. A.; Foster, T. H.; Girotti, A. W.; Gollnick, S. O.; Hahn, S. M.; Hamblin, M. R.; Juzeniene, A.; Kessel, D.; Korbelik, M.; Moan, J.; Mroz, P.; Nowis, D.; Piette, J.; Wilson, B. C.; Golab, J. Photodynamic Therapy of Cancer: An Update. *CA. Cancer J. Clin.* **2011**, *61* (4), 250−281.
(162) Gehl, J. Electroporation: Theory and Methods, Perspectives for Drug Delivery. *Gene Therapy and Research* **2003**, *177*, 437−447.
(163) Reigada, R. Biochimica et Biophysica Acta Electroporation of Heterogeneous Lipid Membranes. *BBA - Biomembr.* **2014**, *1838* (3), 814−821.
(164) Hoejholt, K. L.; Mužić, T.; Jensen, S. D.; Dalgaard, L. T.; Bilgin, M.; Nylandsted, J. Calcium Electroporation and Electrochemotherapy for Cancer Treatment: Importance of Cell Membrane Composition Investigated by Lipidomics, Calorimetry and in Vitro Efficacy. *Sci. Rep.* **2019**, *9*, 4758 DOI: 10.1038/s41598-019-41188-z.
(165) Czapor-irzabek, H.; Michel, O.; Szlasa, W.; Szewczyk, A.; Dra, M.; Kiełbik, A.; Cierluk, K.; Zalesin, A.; Saczko, J.; Kulbacka, J. Mechanisms of Curcumin-Based Photodynamic Therapy and Its Effects in Combination with Electroporation: An in Vitro and Molecular Dynamics Study. *Bioelectrochemistry* **2021**, *140*, 107806 DOI: 10.1016/j.bioelechem.2021.107806.
(166) Labanauskiene, J.; Satkauskas, S.; Kirveliene, V.; Venslauskas, M.; Atkocius, V.; Didziapetriene, J. Enhancement of Photodynamic Tumor Therapy Effectiveness by Electroporation in Vitro. *Medicina* **2009**, *45* (5), 372−377.
(167) Kulbacka, J. Photodiagnosis and Photodynamic Therapy Nanosecond Pulsed Electric Fields (NsPEFs) Impact and Enhanced Photofrin II ® Delivery in Photodynamic Reaction in Cancer and Normal Cells. *Photodiagnosis Photodyn. Ther.* **2015**, *12* (4), 621−629.
(168) We, J.; Kulbacka, J.; Saczko, J.; Rossowska, J.; Chodaczek, G. Biological Effects in Photodynamic Treatment Combined with Electropermeabilization in Wild and Drug Resistant Breast Cancer Cells. *Bioelectrochemistry* **2018**, *123*, 9−18, DOI: 10.1016/j.bioelechem.2018.04.008.
(169) Todorovic, V.; Sersa, G.; Flisar, K.; Cemazar, M. Enhanced Cytotoxicity of Bleomycin and Cisplatin after Electroporation in Murine Colorectal Carcinoma Cells. *Rad. Oncol.* **2009**, *43* (4), 264−273.
(170) Lin, H.; Chen, Y. Nanoparticle-triggered in situ catalytic chemical reactions for tumour-specific therapy. *Chem. Soc. Rev.* **2018**, *6*, 1938−1958, DOI: 10.1039/c7cs00471k.
(171) Yi, X.; Hu, J.; Dai, J.; Lou, X.; Zhao, Z.; Xia, F.; Tang, B. Z. Self-Guiding Polymeric Prodrug Micelles with Two Aggregation-Induced Emission Photosensitizers for Enhanced Chemo- Photodynamic Therapy. *ACS Nano* **2021**, *15* (2), 3026−3037, DOI: 10.1021/acsnano.0c09407.
(172) Luo, L.; Qi, Y.; Zhong, H.; Jiang, S.; Zhang, H.; et al. GSH-Sensitive Polymeric Prodrug: Synthesis and Loading with Photosensitizers as Nanoscale. *Acta Pharm. Sin. B* **2022**, *12* (1), 424−436.
(173) Zhang, S.; Wang, Z.; Kong, Z.; Wang, Y.; Zhang, X.; Sun, B. Photosensitizer-Driven Nanoassemblies of Homodimeric Prodrug for Self-Enhancing Activation and Synergistic Chemo-Photodynamic Therapy. *Theranostics* **2021**, *11* (12), 6019.
(174) Shi, J.; Liu, Y.; Wang, L.; Gao, J.; Zhang, J.; Yu, X.; Ma, R.; Liu, R.; Zhang, Z. Acta Biomaterialia A Tumoral Acidic PH-Responsive Drug Delivery System Based on a Novel Photosensitizer (Fullerene) for in Vitro and in Vivo Chemo-Photodynamic Therapy. *Acta Biomater* **2014**, *10* (3), 1280−1291.
(175) Zhao, M.; Wan, S.; Peng, X.; Zhang, B.; Pan, Q.; Li, S.; He, B.; Pu, Y. Leveraging a Polycationic Polymer to Direct Tunable Loading of an Anticancer Agent and Photosensitizer with Opposite Charges For chemo−photodynamic therapy. *J. Mater. Chem. B* **2020**, *6*, 1235−1244, DOI: 10.1039/c9tb02400j.
(176) Meng, L.; Zhang, W.; Li, D.; Li, Y.; Hu, X.; Wang, L.; Li, G. pH-Responsive Supramolecular Vesicles Assembled by Water-Soluble Pillar[5]Arene and a BODIPY Photosensitizer for Chemo-Photodynamic Dual Therapy. *Chem. Commun.* **2015**, *76*, 14381−14384, DOI: 10.1039/c5cc05785j.
(177) Hu, C.; Yu, Y.; Chao, S.; Zhu, H.; Pei, Y.; Chen, L.; Pei, Z. A Supramolecular Photosensitizer System Based on Nano-Cu/ZIF-8 Capped with Water-Soluble Pillar[6]Arene and Methylene Blue Host−Guest Complexations. *Molecules* **2021**, *26*, 3878.
(178) Lei, Z.; Zhang, X.; Zheng, X.; Liu, S.; Xie, Z. Porphyrin−ferrocene conjugates for photodynamic and chemodynamic therapy. *Org. Biomolec. Chem.* **2018**, 8613−8619, DOI: 10.1039/c8ob02391c.
(179) Fan, W.; Yung, B.; Huang, P.; Chen, X. Nanotechnology for Multimodal Synergistic Cancer Therapy. *Chem. Rev.* **2017**, 13566−13638, DOI: 10.1021/acs.chemrev.7b00258.
(180) Zhang, L.; Chen, Y.; Li, Z.; Li, L.; Saint-cricq, P.; Li, C.; Lin, J.; Wang, C.; Su, Z.; Zink, J. I. Drug Delivery Tailored Synthesis of Octopus-Type Janus Nanoparticles for Synergistic Actively-Targeted and Chemo-Photothermal Therapy. *Angewandte* **2016**, *90095*, 2118−2121.
(181) Yang, L.; Li, H.; Liu, D.; Su, H.; Wang, K.; Liu, G.; Luo, X.; et al. Colloids and Surfaces B: Biointerfaces Organic Small Molecular Nanoparticles Based on Self-Assembly of Amphiphilic Fl Uoroporphyrins for Photodynamic and Photothermal Synergistic Cancer Therapy. *Colloids Surfaces B Biointerfaces* **2019**, *182* (June), 110345.
(182) Yang, Y.; Zhu, D.; Liu, Y.; Jiang, B.; Jiang, W.; Yan, X.; Fan, K. Platinum-Carbon-Integrated Nanozymes for Enhanced Tumor Photodynamic and Photothermal Therapy. *Nanoscale* **2020**, *25*, 13548−13557, DOI: 10.1039/d0nr02800b.
(183) Garg, A. D.; Nowis, D. Photodynamic Therapy: Illuminating the Road from Cell Death towards Anti-Tumour Immunity. *Apoptosis* **2010**, *15*, 1050−1071, DOI: 10.1007/s10495-010-0479-7.
(184) Garg, A. D.; Nowis, D.; Golab, J.; Vandenabeele, P.; Krysko, D. V.; Agostinis, P. Biochimica et Biophysica Acta Immunogenic Cell Death, DAMPs and Anticancer Therapeutics: An Emerging Amalgamation. *BBA - Rev. Cancer* **2010**, *1805* (1), 53−71.
(185) Wu, C.; Guan, X.; Xu, J.; Zhang, Y.; Liu, Q.; Tian, Y. Highly Efficient Cascading Synergy of Cancer Photo-Immunotherapy Enabled by Engineered Graphene Quantum Dots/Photosensitizer/CpG Oligonucleotides Hybrid Nanotheranostics. *Biomaterials* **2019**, *205*, 106−119.
(186) Lee, M.-H.; Thomas, J.; Li, J.-A.; Chen, J.-R.; Wang, T.-L.; Lin, H.-Y. Synthesis of Multifunctional Nanoparticles for the Combination of Photodynamic Therapy and Immunotherapy. *Pharmaceuticals* **2021**, *14*, 508.
(187) Zhai, T.; Zhong, W.; Gao, Y.; Zhou, H.; Zhou, Z.; Liu, X.; Yang, S.; Yang, H. Tumor Microenvironment-Activated Nanoparticles Loaded with an Iron-Carbonyl Complex for Chemodynamic Immunotherapy of Lung Metastasis of Melanoma In Vivo. *ACS Appl. Mater. Interfaces* **2021**, *13* (33), 39100−39111, DOI: 10.1021/acsami.1c11485.
(188) Ortiz-Rodríguez, L. A.; Crespo-Hernández, C. E. Thionated Organic Compounds as Emerging Heavy-Atom-Free Photodynamic Therapy Agents. *Chem. Sci.* **2020**, *11* (41), 11113−11123.
(189) Chen, J.; Xu, Y.; Gao, Y.; Yang, D.; Wang, F.; Zhang, L.; Bao, B.; Wang, L. Nanoscale Organic−Inorganic Hybrid Photosensitizers for Highly Effective Photodynamic Cancer Therapy. *ACS Appl. Mater. Interfaces* **2018**, *10* (1), 248−255.
(190) Shackley, D. C.; Whitehurst, C.; Moore, J. V.; George, N. J. R.; Betts, C. D.; Clarke, N. W. Light Penetration in Bladder Tissue: Implications for the Intravesical Photodynamic Therapy of Bladder Tumours. *BJU Int.* **2000**, *86* (6), 638−643.
(191) Celli, J. P.; Spring, B. Q.; Rizvi, I.; Evans, C. L.; Samkoe, K. S.; Verma, S.; Pogue, B. W.; Hasan, T. Imaging and Photodynamic

Therapy: Mechanisms, Monitoring, and Optimization. *Chem. Rev.* **2010**, *110* (5), 2795−2838.
(192) Jiang, L.; Gan, C. R. R.; Gao, J.; Loh, X. J. A Perspective on the Trends and Challenges Facing Porphyrin-based Anti-microbial Materials. *Small* **2016**, *12* (27), 3609−3644.
(193) Hopper, C. Photodynamic Therapy: A Clinical Reality in the Treatment of Cancer. *Lancet Oncol* **2000**, *1* (4), 212−219.
(194) Allison, R. R. Photodynamic Therapy: Oncologic Horizons. *Futur. Oncol.* **2014**, *10* (1), 123−124.
(195) Zhu, T. C.; Finlay, J. C. The Role of Photodynamic Therapy (PDT) Physics. *Med. Phys.* **2008**, *35*, 3127−3136.
(196) Allison, R. R.; Mota, H. C.; Bagnato, V. S.; Sibata, C. H. Bio-Nanotechnology and Photodynamic Therapy—State of the Art Review. *Photodiagnosis Photodyn. Ther.* **2008**, *5* (1), 19−28.
(197) Davis, M. E.; Chen, Z.; Shin, D. M. Nanoparticle therapeutics: an emerging treatment modality for cancer. *Nat. Rev. Drug Discovery* **2008**, *7*, 771−782.
(198) Konan-Kouakou, Y. N.; Boch, R.; Gurny, R.; Allemann, E. Vitro and in Vivo Activities of Verteporfin-Loaded Nanoparticles. *J. Controlled Release* **2005**, *103* (1), 83−91.
(199) Allison, R. R.; Bagnato, V. S.; Sibata, C. H. Future of Oncologic Photodynamic Therapy. *Futur. Oncol.* **2010**, *6* (6), 929−940.
(200) Reddi, E. Role of Delivery Vehicles for Photosensitizers in the Photodynamic Therapy of Tumours. *J. Photochem. Photobiol. B Biol.* **1997**, *37* (3), 189−195.
(201) Juarranz, Á.; Jaén, P.; Sanz-Rodríguez, F.; Cuevas, J.; González, S. Photodynamic Therapy of Cancer. Basic Principles and Applications. *Clin. Transl. Oncol.* **2008**, *10* (3), 148−154.
(202) dos Santos, A. F.; De Almeida, D. R. Q.; Terra, L. F.; Baptista, M. S.; Labriola, L. Photodynamic Therapy in Cancer Treatment-an Update Review. *J. cancer metastasis Treat.* **2019**, *5*, 25.
(203) Hu, Z.; Zhao, F.; Wang, Y.; Huang, Y.; Chen, L.; Li, N.; Li, J.; Li, Z.; Yi, G. Facile Fabrication of a C60-Polydopamine-Graphene Nanohybrid for Single Light Induced Photothermal and Photodynamic Therapy. *Chem. Commun.* **2014**, *50* (74), 10815−10818.
(204) Nafiujjaman, M.; Nurunnabi, M.; Kang, S. H.; Reeck, G. R.; Khan, H. A.; Lee, Y. K. Ternary Graphene Quantum Dot-Polydopamine-Mn3O4 Nanoparticles for Optical Imaging Guided Photodynamic Therapy and T1-Weighted Magnetic Resonance Imaging. *J. Mater. Chem. B* **2015**, *3* (28), 5815−5823.
(205) Zhan, Q.; Shi, X.; Zhou, J.; Zhou, L.; Wei, S. Drug-Controlled Release Based on Complementary Base Pairing Rules for Photodynamic−Photothermal Synergistic Tumor Treatment. *Small* **2019**, *15* (3), 1−13.
(206) Thakur, D.; Thanh, Q.; Ta, H.; Noh, J. Photosensitizer-Conjugated Hollow ZnFe 2 O 4 Nanoparticles for Antibacterial Near-Infrared Photodynamic Therapy. *ACS Appl. Nano Mater.* **2022**, *5* (1), 1533−1541.
(207) Sun, S.; Chen, J.; Jiang, K.; Tang, Z.; Wang, Y.; Li, Z.; Liu, C.; Wu, A.; Lin, H. Ce6-Modified Carbon Dots for Multimodal-Imaging-Guided and Single-NIR-Laser-Triggered Photothermal/Photodynamic Synergistic Cancer Therapy by Reduced Irradiation Power. *ACS Appl. Mater. Interfaces* **2019**, *11* (6), 5791−5803.
(208) Zhao, Z.; Shi, S.; Huang, Y.; Tang, S.; Chen, X. Simultaneous Photodynamic and Photothermal Therapy Using Photosensitizer-Functionalized Pd Nanosheets by Single Continuous Wave Laser. *ACS Appl. Mater. Interfaces* **2014**, *6* (11), 8878−8885.
(209) Lin, J. F.; Li, J.; Gopal, A.; Munshi, T.; Chu, Y. W.; Wang, J. X.; Liu, T. T.; Shi, B.; Chen, X.; Yan, L. Synthesis of Photo-Excited Chlorin E6 Conjugated Silica Nanoparticles for Enhanced Anti-Bacterial Efficiency to Overcome Methicillin-Resistant: Staphylococcus Aureus. *Chem. Commun.* **2019**, *55* (18), 2656−2659.
(210) Wang, Q.; Zhang, D.; Feng, J.; Sun, T.; Li, C.; Xie, X.; Shi, Q. Enhanced Photodynamic Inactivation for Gram-Negative Bacteria by Branched Polyethylenimine-Containing Nanoparticles under Visible Light Irradiation. *J. Colloid Interface Sci.* **2021**, *584*, 539−550.
(211) Liu, Y.; Ding, L.; Wang, D.; Lin, M.; Sun, H.; Zhang, H.; Sun, H.; Yang, B. Hollow Pd Nanospheres Conjugated with Ce6 to Simultaneously Realize Photodynamic and Photothermal Therapy. *ACS Appl. Bio Mater.* **2018**, *1* (4), 1102−1108.
(212) Li, F.; Na, K. Self-Assembled Chlorin E6 Conjugated Chondroitin Sulfate Nanodrug for Photodynamic Therapy. *Biomacromolecules* **2011**, *12* (5), 1724−1730.
(213) Dong, Z.; Feng, L.; Hao, Y.; Chen, M.; Gao, M.; Chao, Y.; Zhao, H.; Zhu, W.; Liu, J.; Liang, C.; Zhang, Q.; Liu, Z. Synthesis of Hollow Biomineralized CaCO3-Polydopamine Nanoparticles for Multimodal Imaging-Guided Cancer Photodynamic Therapy with Reduced Skin Photosensitivity. *J. Am. Chem. Soc.* **2018**, *140* (6), 2165−2178.
(214) Wang, J.; Guo, Y.; Hu, J.; Li, W.; Kang, Y.; Cao, Y.; Liu, H. Development of Multifunctional Polydopamine Nanoparticles As a Theranostic Nanoplatform against Cancer Cells. *Langmuir* **2018**, *34* (32), 9516−9524.
(215) Bhatta, A.; Krishnamoorthy, G.; Marimuthu, N.; Dihingia, A.; Manna, P.; Biswal, H. T.; Das, M.; Krishnamoorthy, G. Chlorin E6 Decorated Doxorubicin Encapsulated Chitosan Nanoparticles for Photo-Controlled Cancer Drug Delivery. *Int. J. Biol. Macromol.* **2019**, *136*, 951−961.
(216) Wang, C.; Cheng, L.; Liu, Y.; Wang, X.; Ma, X.; Deng, Z.; Li, Y.; Liu, Z. Imaging-Guided PH-Sensitive Photodynamic Therapy Using Charge Reversible Upconversion Nanoparticles under near-Infrared Light. *Adv. Funct. Mater.* **2013**, *23* (24), 3077−3086.
(217) Li, T. F.; Xu, H. Z.; Xu, Y. H.; Yu, T. T.; Tang, J. M.; Li, K.; Wang, C.; Peng, X. C.; Li, Q. R.; Sang, X. Y.; Zheng, M. Y.; Liu, Y.; Zhao, L.; Chen, X. Efficient Delivery of Chlorin E6 by Polyglycerol-Coated Iron Oxide Nanoparticles with Conjugated Doxorubicin for Enhanced Photodynamic Therapy of Melanoma. *Mol. Pharmaceutics* **2021**, *18* (9), 3601−3615.
(218) Feng, C.; Chen, L.; Lu, Y.; Liu, J.; Liang, S.; Lin, Y.; Li, Y.; Dong, C. Programmable Ce6 Delivery via Cyclopamine Based Tumor Microenvironment Modulating Nano-System for Enhanced Photodynamic Therapy in Breast Cancer. *Front. Chem.* **2019**, *7*, 1−11.
(219) Cao, W.; Liu, B.; Xia, F.; Duan, M.; Hong, Y.; Niu, J.; Wang, L.; Liu, Y.; Li, C.; Cui, D. MnO2@Ce6-Loaded Mesenchymal Stem Cells as an "Oxygen-Laden Guided-Missile" for the Enhanced Photodynamic Therapy on Lung Cancer. *Nanoscale* **2020**, *12* (5), 3090−3102.
(220) Shao, C.; Shang, K.; Xu, H.; Zhang, Y.; Pei, Z.; Pei, Y. Facile Fabrication of Hypericin-Entrapped Glyconanoparticles for Targeted Photodynamic Therapy. *Int. J. Nanomedicine* **2018**, *13*, 4319−4331.
(221) Xu, F.; Liu, M.; Li, X.; Xiong, Z.; Cao, X.; Shi, X.; Guo, R. Loading of Indocyanine Green within Polydopamine-Coated Laponite Nanodisks for Targeted Cancer Photothermal and Photodynamic Therapy. *Nanomaterials* **2018**, *8* (5), 1−16.
(222) Gao, S.; Wang, J.; Tian, R.; Wang, G.; Zhang, L.; Li, Y.; Li, L.; Ma, Q.; Zhu, L. Construction and Evaluation of a Targeted Hyaluronic Acid Nanoparticle/Photosensitizer Complex for Cancer Photodynamic Therapy. *ACS Appl. Mater. Interfaces* **2017**, *9* (38), 32509−32519.
(223) Chu, W. Y.; Tsai, M. H.; Peng, C. L.; Shih, Y. H.; Luo, T. Y.; Yang, S. J.; Shieh, M. J. PH-Responsive Nanophotosensitizer for an Enhanced Photodynamic Therapy of Colorectal Cancer Over-expressing EGFR. *Mol. Pharmaceutics* **2018**, *15* (4), 1432−1444.
(224) Jesus, V.P.S.; Raniero, L.; Lemes, G.M.; Bhattacharjee, T.T.; Caetano Junior, P.C.; Castilho, M.L. Nanoparticles of Methylene Blue Enhance Photodynamic Therapy. *Photodiagnosis Photodyn. Ther.* **2018**, *23*, 212−217.
(225) Hosseinzadeh, R.; Khorsandi, K.; Hosseinzadeh, G. Graphene Oxide-Methylene Blue Nanocomposite in Photodynamic Therapy of Human Breast Cancer. *J. Biomol. Struct. Dyn.* **2018**, *36* (9), 2216−2223.
(226) Magalhães, J. A.; Arruda, D. C.; Baptista, M. S.; Tada, D. B. Co-Encapsulation of Methylene Blue and PARP-Inhibitor into Poly (Lactic-Co-Glycolic Acid) Nanoparticles for Enhanced PDT of Cancer. *Nanomaterials* **2021**, *11* (6), 1514.
(227) Monroe, J. D.; Belekov, E.; Er, A. O.; Smith, M. E. Anticancer Photodynamic Therapy Properties of Sulfur-Doped Graphene

https://doi.org/10.1021/acsomega.2c05852
ACS Omega 2022, 7, 45882−45909

Quantum Dot and Methylene Blue Preparations in MCF-7 Breast Cancer Cell Culture. *Photochem. Photobiol.* **2019**, *95* (6), 1473−1481.
(228) Hosseinzadeh, R.; Khorsandi, K. Methylene Blue, Curcumin and Ion Pairing Nanoparticles Effects on Photodynamic Therapy of MDA-MB-231 Breast Cancer Cell. *Photodiagnosis Photodyn. Ther.* **2017**, *18*, 284−294.
(229) Hosseinzadeh, R.; Khorsandi, K.; Jahanshiri, M. Combination Photodynamic Therapy of Human Breast Cancer Using Salicylic Acid and Methylene Blue. *Spectrochim. Acta Part A Mol. Biomol. Spectrosc.* **2017**, *184*, 198−203.
(230) Wulf, H. C.; Al-Chaer, R. N.; Glud, M.; Philipsen, P. A.; Lerche, C. M. A Skin Cancer Prophylaxis Study in Hairless Mice Using Methylene Blue, Riboflavin, and Methyl Aminolevulinate as Photosensitizing Agents in Photodynamic Therapy. *Pharmaceuticals* **2021**, *14* (5), 433.
(231) Jin, X.; Yao, S.; Qiu, F.; Mao, Z.; Wang, B. A Multifunctional Hydrogel Containing Gold Nanorods and Methylene Blue for Synergistic Cancer Phototherapy. *Colloids Surfaces A Physicochem. Eng. Asp.* **2021**, *614*, 126154.
(232) Ma, M.; Cheng, L.; Zhao, A.; Zhang, H.; Zhang, A. Pluronic-Based Graphene Oxide-Methylene Blue Nanocomposite for Photodynamic/Photothermal Combined Therapy of Cancer Cells. *Photodiagnosis Photodyn. Ther.* **2020**, *29*, 101640.
(233) Yang, J.; Teng, Y.; Fu, Y.; Zhang, C. 68. *Int. J. Nanomedicine* **2019**, *14*, 5061.
(234) Sundaram, P.; Abrahamse, H. Effective Photodynamic Therapy for Colon Cancer Cells Using Chlorin E6 Coated Hyaluronic Acid-Based Carbon Nanotubes. *Int. J. Mol. Sci.* **2020**, *21* (13), 4745.
(235) Karuppusamy, S.; Hyejin, K.; Kang, H. W. Nanoengineered Chlorin E6 Conjugated with Hydrogel for Photodynamic Therapy on Cancer. *Colloids Surfaces B Biointerfaces* **2019**, *181*, 778−788.
(236) Yang, K.; Niu, T.; Luo, M.; Tang, L.; Kang, L. Enhanced Cytotoxicity and Apoptosis through Inhibiting Autophagy in Metastatic Potential Colon Cancer SW620 Cells Treated with Chlorin E6 Photodynamic Therapy. *Photodiagnosis Photodyn. Ther.* **2018**, *24*, 332−341.
(237) Liu, B.; Qiao, G.; Han, Y.; Shen, E.; Alfranca, G.; Tan, H.; Wang, L.; Pan, S.; Ma, L.; Xiong, W.; et al. Targeted Theranostics of Lung Cancer: PD-L1-Guided Delivery of Gold Nanoprisms with Chlorin E6 for Enhanced Imaging and Photothermal/Photodynamic Therapy. *Acta Biomater* **2020**, *117*, 361−373.
(238) He, Z.; Jiang, H.; Zhang, X.; Zhang, H.; Cui, Z.; Sun, L.; Li, H.; Qian, J.; Ma, J.; Huang, J. Nano-Delivery Vehicle Based on Chlorin E6, Photodynamic Therapy, Doxorubicin Chemotherapy Provides Targeted Treatment of HER-2 Negative, A$\nu\beta$3-Positive Breast Cancer. *Pharmacol. Res.* **2020**, *160*, 105184.
(239) Ding, Y.-F.; Li, S.; Liang, L.; Huang, Q.; Yuwen, L.; Yang, W.; Wang, R.; Wang, L.-H. Highly Biocompatible Chlorin E6-Loaded Chitosan Nanoparticles for Improved Photodynamic Cancer Therapy. *ACS Appl. Mater. Interfaces* **2018**, *10* (12), 9980−9987.
(240) Nishie, H.; Kataoka, H.; Yano, S.; Yamaguchi, H.; Nomoto, A.; Tanaka, M.; Kato, A.; Shimura, T.; Mizoshita, T.; Kubota, E.; et al. Excellent Antitumor Effects for Gastrointestinal Cancers Using Photodynamic Therapy with a Novel Glucose Conjugated Chlorin E6. *Biochem. Biophys. Res. Commun.* **2018**, *496* (4), 1204−1209.
(241) Ma, Q.-L.; Shen, M.-O.; Han, N.; Xu, H.-Z.; Peng, X.-C.; Li, Q.-R.; Yu, T.-T.; Li, L.-G.; Xu, X.; Liu, B.; et al. Chlorin E6Mediated Photodynamic Therapy Triggers Resistance through ATM-Related DNA Damage Response in Lung Cancer Cells. *Photodiagnosis Photodyn. Ther.* **2022**, *37*, 102645.
(242) Xu, J.; Yu, S.; Wang, X.; Qian, Y.; Wu, W.; Zhang, S.; Zheng, B.; Wei, G.; Gao, S.; Cao, Z.; Fu, W.; Xiao, Z.; Lu, W. High Affinity of Chlorin E6 to Immunoglobulin G for Intraoperative Fluorescence Image-Guided Cancer Photodynamic and Checkpoint Blockade Therapy. *ACS Nano* **2019**, *13* (9), 10242−10260.
(243) Liang, X.; Chen, M.; Bhattarai, P.; Hameed, S.; Dai, Z. Perfluorocarbon@ Porphyrin Nanoparticles for Tumor Hypoxia Relief to Enhance Photodynamic Therapy against Liver Metastasis of Colon Cancer. *ACS Nano* **2020**, *14* (10), 13569−13583.
(244) Zhang, D.; Ye, Z.; Wei, L.; Luo, H.; Xiao, L. Cell Membrane-Coated Porphyrin Metal − Organic Frameworks for Cancer Cell Targeting and O 2 - Evolving Photodynamic Therapy. *ACS Appl. Mater. Interfaces* **2019**, *11* (43), 39594−39602, DOI: 10.1021/acsami.9b14084.
(245) Jiang, X.; Zhou, Z.; Yang, H.; Shan, C.; Yu, H.; Wojtas, L.; Zhang, M.; Mao, Z.; Wang, M.; Stang, P. J. Self-Assembly of Porphyrin-Containing Metalla-Assemblies and Cancer Photodynamic Therapy. *Inorg. Chem.* **2020**, *59* (11), 7380−7388.
(246) Wang, B.; Dai, Y.; Kong, Y.; Du, W.; Ni, H.; Zhao, H.; Sun, Z.; Shen, Q.; Li, M.; Fan, Q. Tumor Microenvironment-Responsive Fe(III)−Porphyrin Nanotheranostics for Tumor Imaging and Targeted Chemodynamic−Photodynamic Therapy. *Cite This ACS Appl. Mater. Interfaces* **2020**, *12*, 53634−53645.
(247) Tao, D.; Feng, L.; Chao, Y.; Liang, C.; Song, X.; Wang, H.; Yang, K.; Liu, Z. Covalent Organic Polymers Based on Fluorinated Porphyrin as Oxygen Nanoshuttles for Tumor Hypoxia Relief and Enhanced Photodynamic Therapy. *Adv. Funct. Mater.* **2018**, *28* (43), 1804901.
(248) Michy, T.; Massias, T.; Bernard, C.; Vanwonterghem, L.; Henry, M.; Guidetti, M.; Royal, G.; Coll, J.-L.; Texier, I.; Josserand, V.; et al. Verteporfin-Loaded Lipid Nanoparticles Improve Ovarian Cancer Photodynamic Therapy in Vitro and in Vivo. *Cancers (Basel)* **2019**, *11* (11), 1760.
(249) Ballestri, M.; Caruso, E.; Guerrini, A.; Ferroni, C.; Banfi, S.; Gariboldi, M.; Monti, E.; Sotgiu, G.; Varchi, G. Core−Shell Poly-Methyl Methacrylate Nanoparticles Covalently Functionalized with a Non-Symmetric Porphyrin for Anticancer Photodynamic Therapy. *J. Photochem. Photobiol. B Biol.* **2018**, *186*, 169−177.
(250) Huang, H. C.; Pigula, M.; Fang, Y.; Hasan, T. Immobilization of Photo-Immunoconjugates on Nanoparticles Leads to Enhanced Light-Activated Biological Effects. *Small* **2018**, *14* (31), 1−11.
(251) Zhang, R.; Wu, C.; Tong, L.; Tang, B.; Xu, Q. H. Multifunctional Core-Shell Nanoparticles as Highly Efficient Imaging and Photosensitizing Agents. *Langmuir* **2009**, *25* (17), 10153−10158.
(252) Guidolin, K.; Ding, L.; Chen, J.; Wilson, B. C.; Zheng, G. Porphyrin-Lipid Nanovesicles (Porphysomes) Are Effective Photosensitizers for Photodynamic Therapy. *Nanophotonics* **2021**, *10* (12), 3161−3168.
(253) Tang, Q.; Xiao, W.; Huang, C.; Si, W.; Shao, J.; Huang, W.; Chen, P.; Zhang, Q.; Dong, X. pH-Triggered and Enhanced Simultaneous Photodynamic and Photothermal Therapy Guided by Photoacoustic and Photothermal Imaging. *Chem. Mater.* **2017**, *29* (12), 5216−5224, DOI: 10.1021/acs.chemmater.7b01075.
(254) Cao, H.; Yang, Y.; Liang, M.; Ma, Y.; Sun, N.; Gao, X.; Li, J. Pt@polydopamine nanoparticles as nanozymes for enhanced photodynamic and photothermal therapy. *Chem. Commun.* **2021**, *2*, 255−258, DOI: 10.1039/d0cc07355e.
(255) Wang, Z.; Gai, S.; Wang, C.; Yang, G.; Zhong, C.; Dai, Y.; et al. Self-Assembled Zinc Phthalocyanine Nanoparticles as Excellent Photothermal/Photodynamic Synergistic Agent for Antitumor Treatment. *Chem. Eng. J.* **2019**, *361*, 117−128.
(256) Wang, Z.; Jia, T.; Sun, Q.; Kuang, Y.; Liu, B.; Xu, M.; Zhu, H.; He, F.; Gai, S.; Yang, P. Biomaterials Construction of Bi/Phthalocyanine Manganese Nanocomposite for Trimodal Imaging Directed Photodynamic and Photothermal Therapy Mediated by 808 Nm Light. *Biomaterials* **2020**, *228*, 119569.
(257) Li, C.; Zhang, W.; Liu, S.; Hu, X.; Xie, Z. Mitochondria-Targeting Organic Nanoparticles for Enhanced Photodynamic/Photothermal Therapy. *ACS Appl. Mater. Interfaces* **2020**, *12* (27), 30077−30084, DOI: 10.1021/acsami.0c06144.
(258) Cai, Y.; Liang, P.; Tang, Q.; Yang, X.; Si, W.; Huang, W.; Zhang, Q.; Dong, X. Diketopyrrolopyrrole−Triphenylamine Organic Nanoparticles as Multifunctional Reagents for Photoacoustic Imaging-Guided Photodynamic/Photothermal Synergistic Tumor Therapy. *ACS Nano* **2017**, *11*, 1054.
(259) Zhang, P.; Gao, Z.; Cui, J.; Hao, J. Dual-Stimuli-Responsive Polypeptide Nanoparticles for Photothermal and Photodynamic

https://doi.org/10.1021/acsomega.2c05852
ACS Omega 2022, 7, 45882−45909

Therapy. *ACS Appl. Bio Mater.* **2020**, *569*, 561−569, DOI: 10.1021/acsabm.9b00964.

(260) Zhou, Y.; Ren, X.; Hou, Z.; Wang, N.; Jiang, Y.; Luan, Y. Engineering a Photosensitizer Nanoplatform for Amplified Photodynamic Immunotherapy via Tumor Microenvironment Modulation. *Nanoscale Horizons* **2021**, *2*, 120−131, DOI: 10.1039/d0nh00480d.

(261) Zheng, B.; Li, S.; Zheng, B.; Ying, J.; Hu, Q.; Peng, X.; Li, X.; Ke, M.; Huang, J. Dyes and Pigments Phthalocyanine-Based Photosensitizers Combined with Anti-PD-L1 for Highly Efficient Photodynamic Immunotherapy. *Dye. Pigment.* **2021**, *185* (PA), 108907.

(262) Ding, B.; Shao, S.; Yu, C.; Teng, B.; Wang, M.; Cheng, Z. Large-Pore Mesoporous-Silica-Coated Upconversion Nanoparticles as Multifunctional Immunoadjuvants with Ultrahigh Photosensitizer and Antigen Loading Efficiency for Improved Cancer Photodynamic Immunotherapy. *Adv. Mater.* **2018**, *1802479*, 1−10, DOI: 10.1002/adma.201802479.

(263) Liu, H.; Hu, Y.; Sun, Y.; Wan, C.; Zhang, Z.; Dai, X.; Lin, Z.; He, Q.; Yang, Z.; Huang, P.; Xiong, Y.; Cao, J.; Chen, X.; Chen, Q.; Lovell, J. F.; Xu, Z.; Jin, H.; Yang, K. Co-Delivery of Bee Venom Melittin and a Photosensitizer with an Organic − Inorganic Hybrid Nanocarrier for Photodynamic Therapy and Immunotherapy. *ACS Nano* **2019**, *13* (11), 12638−12652, DOI: 10.1021/acsnano.9b04181.

(264) Wen, K.; Tan, H.; Peng, Q.; Chen, H.; Ma, H.; Wang, L.; Peng, A.; Shi, Q.; Cai, X.; Huang, H. Achieving Efficient NIR-II Type-I Photosensitizers for Photodynamic/Photothermal Therapy upon Regulating Chalcogen Elements. *Adv. Biomater.***2022**, *2108146*, 1−12.
.

(265) Peng, J.; Xiao, Y.; Li, W.; Yang, Q.; Tan, L.; Jia, Y.; Qu, Y. Photosensitizer Micelles Together with IDO Inhibitor Enhance Cancer Photothermal Therapy and Immunotherapy. *Adv. Sci.* **2018**, *5* (5), 1700891 DOI: 10.1002/advs.201700891.

(266) Choi, J.; Shim, M. K.; Yang, S.; Hwang, H. S.; Cho, H.; Kim, J.; Yun, W. S.; Moon, Y.; Kim, J.; Yoon, H. Y.; Kim, K. Visible-Light-Triggered Prodrug Nanoparticles Combine Chemotherapy and Photodynamic Therapy to Potentiate Checkpoint Blockade Cancer Immunotherapy. *ACS Nano* **2021**, *15* (7), 12086−12098, DOI: 10.1021/acsnano.1c03416.

(267) Wang, H.; Han, X.; Dong, Z.; Xu, J.; Wang, J.; Liu, Z. Hyaluronidase with PH-Responsive Dextran Modification as an Adjuvant Nanomedicine for Enhanced Photodynamic- Immunotherapy of Cancer. *Adv. Funct. Mater.* **2019**, *29* (29), 1902440 DOI: 10.1002/adfm.201902440.

(268) Dong, X. Manganese-Based Nanoplatform As Metal Ion-Enhanced ROS Generator for Combined Chemodynamic/Photodynamic Therapy. *ACS Appl. Mater. Interfaces* **2019**, *11* (44), 41140−41147, DOI: 10.1021/acsami.9b16617.

(269) Qin, X.; Wu, C.; Niu, D.; Qin, L.; Wang, X.; Wang, Q.; Li, Y. Chemodynamic and Photodynamic Therapy. *Nat. Commun.* **2021**, *12*, 1−15.

(270) Liu, C.; Wang, D.; Zhang, S.; Cheng, Y.; Yang, F.; Xing, Y.; Xu, T.; Dong, H.; Zhang, X. Biodegradable Biomimic Copper/Manganese Silicate Nanospheres for Chemodynamic/Photodynamic Synergistic Therapy with Simultaneous Glutathione Depletion and Hypoxia Relief. *ACS Nano* **2019**, *13*, 4267.

(271) Xu, J.; Shi, R.; Chen, G.; Dong, S.; Yang, P.; Zhang, Z.; Niu, N. All-in-One Theranostic Nanomedicine with Ultrabright Second Near-Infrared Emission for Tumor-Modulated Bioimaging and Chemodynamic/Photodynamic Therapy. *ACS Nano* **2020**, *14* (8), 9613−9625, DOI: 10.1021/acsnano.0c00082.

(272) Wang, B.; Dai, Y.; Kong, Y.; Du, W.; Ni, H.; Zhao, H.; Sun, Z.; Shen, Q.; Li, M.; Fan, Q. Tumor Microenvironment-Responsive Fe(III) − Porphyrin Nanotheranostics for Tumor Imaging and Targeted Chemodynamic − Photodynamic Therapy. *ACS Appl. Mater. Interfaces* **2020**, *12* (48), 53634−53645, DOI: 10.1021/acsami.0c14046.

(273) Li, X.; Wang, Y.; Shi, Q.; Zhen, N.; Xue, J.; Liu, J.; Zhou, D.; Zhang, H. Zein-Based Nanomedicines for Synergistic Chemodynamic/ Photodynamic Therapy. *ACS Omega* **2022**, *7* (33), 29256−29265, DOI: 10.1021/acsomega.2c03404.

https://doi.org/10.1021/acsomega.2c05852
ACS Omega 2022, 7, 45882−45909